LICENTIATE THESIS

Stability of Tailings Dams

Focus on Numerical Modelling

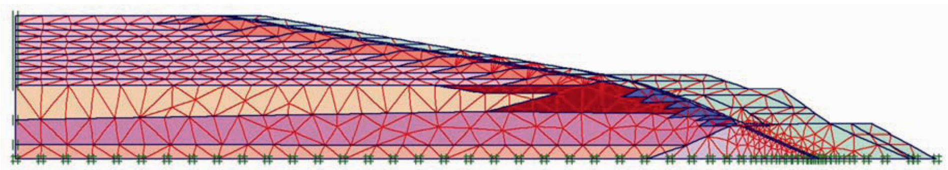

Muhammad Auchar Zardari

LULEÅ UNIVERSITY OF TECHNOLOGY

Stability of Tailings Dams

Focus on Numerical Modelling

Muhammad Auchar Zardari

Department of Civil, Environmental and Natural Resources Engineering

Division of Mining and Geotechnical Engineering

Luleå University of Technology

SE-97187 Luleå, Sweden

Cover illustration: Finite Element Model of Aitik Tailings Dam, Sweden.

Printed by Universitetstryckeriet, Luleå 2011

ISSN: 1402-1757
ISBN 978-91-7439-245-6

Luleå 2011

www.ltu.se

PREFACE

I am grateful to the Quaid-e-Awam University of Engineering, Science and Technology, Nawabshah Pakistan for providing me the financial support to pursue Ph.D studies. The financial assistance (in research related costs) from the Luleå University of Technology, Luleå, Sweden is also acknowledged.

I am deeply indebted to my Supervisor Prof. Sven Knutsson and Co-supervisor Dr. Hans Mattsson for their scientific guidance in the research work.

I would also like to thank my co-authors of the two papers, Linda Ormann and Annika Bjelkevik for their assistance in numerical modelling.

I also wish to express thanks to Kerstin Pousette, Dr. Bo Westerberg and Martin Lindmark for their help in different ways.

The help of Hassan Raza Bhatti (MSc student) in preparation of figures is also acknowledged.

I would like to express gratitude to my wife Hussan Bano and my two sons Zakir Hussain and Khadim Hussain for their joyful company with me.

Finally, I wish to thank my teacher from Pakistan Prof. Nazir Ahmed Khokhar for his moral support and well wishes for completion of my studies.

Luleå, March 2011

Muhammad Auchar Zardari

ABSTRACT

Upstream tailings dams may experience slope stability problems when the rate of raising is too fast. Tailings consolidate slowly due to low hydraulic conductivity. The excess pore pressures can build up due to accelerated rate of raising. The cumulative increase in excess pore pressures due to successive raisings can endanger slope stability of a tailings dam. The stability of a tailings dam is closely related to the consolidation process.

The consolidation process and associated stability of an upstream tailings dam during staged construction was modelled with the finite element program PLAXIS. The analysis indicated that the stability of the dam reduced during raising due to increase of excess pore pressures. The safety of the dam was improved by adding rockfill banks on the downstream side. The volume of the rockfill banks was minimized with an optimization technique. This technique involves (*i*) construction of a rockfill bank on the downstream side when the factor of safety is less than a permissible limit, (*ii*) utilization of a minimum volume of the rockfill that is necessary to stabilize the slope. This technique can be practicable when the rate of raising is moderate, and partial consolidation occurs between consecutive raisings.

Numerical analysis was also performed on a curved embankment of an upstream tailings dam in order to investigate the possible risk of hydraulic fracturing and internal erosion in a corner of the dam. The analysis showed that low compressive stresses occurred above the phreatic level, near the zones of filter and rockfill banks. These zones contain coarse material, and are, therefore, not susceptible to hydraulic fracturing and internal erosion. An increase in the radius of the corner is suggested in order to prevent large reductions in compressive stresses that may occur due to future

raisings. Presently the curved dam section is stable. However, an additional rockfill bank on the downstream side will be required for future raisings.

Static liquefaction is considered as a common cause of disastrous flow failures of tailings dams. These flow failures can be predicted with numerical modelling using suitable constitutive models. In this context, some constitutive models capable of simulating static liquefaction behaviour of loose saturated sands are reviewed.

It is generally concluded that the finite element method can be a helpful tool for modelling stability of tailings dams.

TABLE OF CONTENTS

Appended Research Report and Papers

1 INTRODUCTION

Tailings are a by-product from the mining industry when the minerals are extracted from the ore. The particle size of tailings may vary between medium sand to silt or clay size. Tailings slurries are normally transported to the disposal area by a pipeline. The slurries can be distributed by different techniques such as sub aerial discharge (with spigots), sub aqueous discharge (slurry is injected below the water surface) and thickened discharge (slurry with low water content) (Jewell, 1998). The coarse particles of tailings (i.e. sand) settle close to the point of discharge, and the fine particles (i.e. silt and clay, generally termed as slimes) run down the beach into the pond and settle there (Vick, 1990).

Tailings are produced in huge quantities annually, and may contain some toxic chemicals that are harmful to the environment. Therefore, it is necessary to store tailings in an environmentally safe and economical way. Tailings are generally stored in surface impoundments, which commonly consist of raised embankments (Vick, 1990). The raised embankments are generally constructed with either of the following raising methods: upstream, downstream, or centre line (Vick, 1990).

The tailings dams raised with upstream construction method require less volume of mechanically placed fill material (beach sand tailings) for raising of perimeter dikes, and are therefore economical in cost as compared to the tailings dams raised with the downstream and centreline construction methods (Vick, 1990). Therefore, many tailings dams are raised with the upstream construction method (Martin and McRoberts, 1999; WISE, 2011). However, in an upstream tailings dam, stability problems may occur due to (*i*) quick rate of raising, (*ii*) hydraulic fracturing and internal erosion, (*iii*) static/seismic liquefaction of tailings, and (*iv*) excessive settlements and horizontal deformations etc.

Tailings consolidate slowly due to low hydraulic conductivity. Therefore, excess pore pressures may continuously increase in the dam (particularly in the zones of slimes) due to successive raisings of the dam. The increase in excess pore pressures results in reduction of effective stresses and shear strength of tailings. Hence, during staged construction of a tailings dam, a potential dangerous stability situation can arise in which an embankment slope may become unstable.

An unstable slope of an upstream tailings dam can be stabilized by using rockfill supports at the downstream toe. The weight of the rockfill provides resistance to sliding, this in turn increases slope stability. As the use of rockfill is directly related to the cost, therefore, it is necessary to minimize the volume of the rockfill without compromising the required slope stability. Thus, an optimization technique is required to utilize a minimum volume of the rockfill to maintain desired slope stability.

The layout of a tailings impoundment depends on the topography of a site, and may consist of a curve or corner between two straight sections of the dam. In a curved embankment, lateral earth pressure of the stored tailings acts on the inner side of the curve, and as a result, low compressive stresses (and even tensile stresses) may develop on the outer side of the embankment. In this situation, the zones of low compressive stresses in the corner may be sensitive to hydraulic fracturing and internal erosion. The hydraulic fracturing can cause a concentrated leak in the embankment, through which internal erosion may initiate. As the erosion progresses, the concentrated leak will enlarge, which may lead to failure of the embankment (Fell *et al.*, 2005).

An upstream tailings dam, under undrained conditions, may be sensitive to liquefaction-induced failures due to seismic shaking or static loading. If a tailings dam is located in a non-seismic zone, still it may be susceptible to flow failure due to static liquefaction. The loose and contractant tailings may liquefy due to rapid rate of raising, changes in pore pressures, overtopping and erosion of an outer embankment. The flow failures due to static liquefaction can be predicted with numerical analyses by using a constitutive model that can simulate the static liquefaction behaviour of tailings material. It is therefore, relevant to identify presently available constitutive models that are capable to capture static liquefaction behaviour of tailings. A constitutive model can be practically used for a numerical analysis when it is available in a finite element/ finite difference program.

This thesis is an attempt to address the issues like strengthening of unstable slope with rockfill banks by utilizing minimum volume of the rockfill, potential risk of hydraulic fracturing and internal erosion in a curved embankment, and selection of a constitutive model for predicting static liquefaction related flow failures in tailings dams.

It is appropriate to perform numerical analyses of upstream tailings dams with advanced numerical software, based on e.g. the finite element method due to a number of reasons: (*i*) the stability of a tailings dam is closely related to the consolidation process, which is complex due to variations in material properties in a deposit, (*ii*) minimization of volume of the rockfill banks used for slope stablization, (*iii*) identification of zones of low compressive stresses (which may be sensitive to hydraulic fracturing and internal erosion) in an embankment.

1.1 Objectives of the Research

The main objectives of the research presented in this thesis are:

1. To examine the consolidation process and associated stability of an upstream tailings dam during staged construction
2. To analyze the strengthening of an unstable slope of tailings embankment with the assistance of rockfill banks by utilizing an optimum volume of rockfill
3. To investigate the potential risk of hydraulic fracturing and internal erosion in a curved embankment of an upstream tailings dam
4. To review liquefaction behaviour of tailings material under static loading conditions and identify some of the available strain softening constitutive models

1.2 Research Methodology

In order to accomplish the above mentioned objectives, the following approach was adopted:

1. A literature review (Zardari, 2010) was carried out to understand the relevant aspects like: mechanical properties of tailings material, behaviour of tailings dams during raising, failure modes of tailings dams, pore pressures that develop during construction of a tailings embankment, conditions of analysis for tailings embankments, choice of a numerical tool and review of available constitutive soil models.
2. The commercial finite element program PLAXIS 2D (Brinkgreve *et al.*, 2008) was chosen as a numerical tool for modelling staged construction of a tailings dam.

3. The Aitik tailings dam (located close to Gällivare in the north part of Sweden) is selected as a case study; because of availability of laboratory and field tests so that realistic material parameters can be used in numerical analyses.
4. The consolidation analyses were performed for staged construction of the dam in order to (*i*) take into account strength gain due to dissipation of excess pore pressures, and (*ii*) observe the development of excess pore pressures in the dam body during raising phase and reduction of excess pore pressures during consolidation phase.
5. The slope stability of the dam was assessed with factors of safety, which were computed with safety analyses. As per recommendations of Swedish tailings dams' safety guidelines document GruvRIDAS (2007), a safety factor of approximately 1.5 was required to be maintained during each raising of the dam. Therefore, the safety factors were computed for every raise. If safety factor was less than 1.5 during a raise; the slope was stabilized by adding a rockfill bank on the downstream side. The volume of rockfill bank was optimized by gradually changing the width and height of the bank until the required safety factor was achieved.
6. Hydraulic fracturing in an embankment dam may proceed through the zones of low compressive stresses, i.e. along the plane of minor effective principal stress (Kjaernsli *et al.*, 1992). The zones of low compressive stresses in a curved embankment were identified by locating the minor effective principal stress, which was computed from the results of consolidation analyses.
7. Results have been discussed and conclusions have been drawn in the appended papers. Ideas for future research have been proposed.

1.3 Layout of the Thesis

This thesis consists of the following appended parts:

Research Report	Mechanical properties of fine grained, sulphur rich, silty soils
Paper I	Numerical analysis of strengthening by rockfill embankments on an upstream tailings dam (*To be submitted to Canadian Geotechnical Journal*)
Paper II	Numerical analysis of curved embankment of an upstream tailings dam (*To be submitted to Electronic Journal of Geotechnical Engineering*)
Paper III	Static liquefaction of tailings: A review of constitutive models (*Manuscript*)

Research Report

The following topics are reviewed in the Research Report:

- engineering properties of tailings such as: density, hydraulic conductivity, compressibility, consolidation, drained and undrained shear strength
- methods of construction of tailings dams, design considerations for long time stability of tailings dams, failure modes of tailings dams
- effect of phreatic surface on stability of tailings dam, measures for lowering of phreatic surface, control of seepage
- pore pressures in tailings embankments, conditions for analysis for tailings dams

- effect of anisotropy on shear strength of clay and sand
- undrained behaviour of tailings in cyclic loading
- general features of creep in clay and sand
- constitutive soil models in PLAXIS.

Paper I

The staged construction of an upstream tailings dam was modelled with the finite element program PLAXIS. In the numerical model, it was assumed that (*i*) the stored tailings and the dam were raised three meters per year, and (*ii*) the dam was raised in eleven stages, each stage comprised of a raising phase and a consolidation phase. The consolidation and safety analyses were performed for the eleven raises of the dam. The analyses indicated that the slope stability of the dam reduced due to increase of excess pore pressures during the raising phase. The safety of the dam was enhanced by adding rockfill banks on the downstream side. In this paper, an optimization technique is described to minimize the volume of rockfill banks by gradually increasing the width and height of the bank until desired stability is achieved.

This finite element based optimization technique can be helpful for minimizing the volume of rockfill without compromising the stability of a dam. Thus, a significant cost can be saved by reducing the volume of the rockfill banks.

Paper II

A curved embankment of an upstream tailings dam may be subjected to low compressive stresses near the surface along the outer side of the embankment, when the horizontal pressure of stored tailings acts at the inner side of the embankment.

The zones of low compressive stresses may be sensitive to hydraulic fracturing and internal erosion.

In this paper, a curved embankment of upstream tailings was analyzed with the finite element method in order to find the zones of low compressive stresses. An axisymmetric model was assumed for the numerical analysis of the curved embankment. In order to compare the compressive stresses in the curved embankment and the straight section of the dam, the same curved embankment was also analyzed with the plane strain model.

The numerical analyses showed that in comparison to straight section of the dam, low compressive stresses occurred in the curved embankment above the phreatic level, in the rockfill and the filter zones. These zones contain coarse materials, which are not sensitive to the hydraulic fracturing and internal erosion.

It is proposed to increase the radius of the curved embankment in order to prevent too low compressive stresses that may occur due to future raisings.

The slope stability analysis indicated that the curved embankment is presently stable, but an additional rockfill bank on the downstream toe is needed for future raisings.

The finite element based approach described in this paper can be helpful in identifying the zones of low compressive stresses in a curved embankment of a tailings dam. In this way, this approach can be applied for predicting potential risk of the hydraulic fracturing and internal erosion in a curved embankment of a dam.

Paper III

The static liquefaction process is reviewed about (*i*) strain softening behaviour of tailings, and (*ii*) constitutive models for the static liquefaction of loose saturated sands.

Static liquefaction is considered a most common cause of flow failures of tailings dams, for example: Stava (ICOLD, 2001; Sammarco, 2004), Sullivan Mine (WISE, 2010; Davies *et al.*, 2002), Merriespruit (Fourie *et al.*, 2001), and Aznalcóllar (Davies *et al.*, 2002).

In this paper, it is inferred that the factors, which can contribute to static liquefaction of a tailings dam, are contractive behaviour of tailings material, overloading, changes in pore pressures, high phreatic level, improper drainage, overtopping and erosion of an outer embankment.

From the previous studies on static liquefaction in saturated sands/silty sands (Kramer and Seed, 1988; Lade and Yamamuro, 1997; Yamamuro and Lade, 1997), it is deduced that static liquefaction resistance of tailings may (*i*) increase with increase of relative density and confining pressure, (*ii*) decrease with increase of shear stress and fines content.

Some of the presently available constitutive models (implemented in commercial finite element/finite difference programs) that can simulate static liquefaction behaviour of loose saturated sands are: UBCSAND model (Byrne *et al.*, 1995; Puebla *et al.*, 1997; Beaty and Byrne, 1998), Hypoplastic model for sand (Wolffersdorff, 1996; Niemunis and Herle, 1997), NorSand (Jefferies, 1993; Jefferies and Shuttle, 2002), and CASM – a unified state parameter model for clay and sand (Yu, 1998; Yu *et al.*, 2006).

It is believed that catastrophic flow slides of tailings dams can be predicted with finite element analyses using such constitutive model(s).

2 IDEAS FOR FUTURE RESEARCH

The research regarding numerical modelling of tailings dams can be extended on the following aspects; the order, in which suggestions are listed, does not show any priority.

1. **Comparison with field measurements**

   For more confidence, the predictions from the numerical analyses should be compared with field measurements e.g. settlements, horizontal displacements, and excess pore pressures.

   In order to get representative values of field measurements, it is important that the instrumentation for such measurements should be installed at right locations. In this connection, the results of numerical analyses on a tailings dam can be utilized to point out the best locations for the instrumentation.

2. **Use of advanced constitutive models for simulating strain hardening /softening behaviour of tailings material**

   Tailings may be characterized as a complex material, which shows both strain hardening and strain softening behaviour in triaxial tests on reconstituted samples (Fourie and Papageorgiou, 2001; Chang, 2009). This difference in behaviour may be attributed to method of sample preparation (Ishihara 1996;

Fourie and Papageorgiou, 2001; Chang, 2009). It is also generally perceived that in a tailings dam, the exterior (perimeter dikes) material is dilative, and the interior (slimes) material is contractive.

The simple elastic- perfectly plastic Mohr-Coulomb model cannot capture the strain hardening/softening behaviour of tailings material. It is relevant to choose a constitutive model, which can simulate both the strain hardening/softening features of tailings material. In this regard, a possible choice is to apply the UBCSAND model (Byrne *et al.*, 1995; Puebla *et al.*, 1997; Beaty and Byrne, 1998), which is capable to deal with both the strain hardening/softening response of tailings.

Some of the parameters of the UBCSAND model can be evaluated from Triaxial / Direct shear tests, and the rest of the parameters can be determined from empirical relations (Puebla, 1999; Tsegae, 2010). It is necessary to evaluate the model parameters carefully, because the response of a constitutive model is directly associated with the input given by the model parameters. It is also relevant that the model predictions should be compared with the laboratory tests, e.g. Triaxial / Direct shear tests. These suggestions also apply to the next recommendations presented below.

3. Numerical modelling of static liquefaction of tailings dams

Numerical analyses of static liquefaction of tailings dams should be carried out using any of the constitutive models, e.g. UBCSAND model, Hypoplastic sand model, NorSand, and CASM. By performing such numerical analyses, the material zones susceptible to static liquefaction can be identified and the effect of liquefied zones on the overall stability of the dam can be determined.

4. Dynamic analyses of tailings dams

A tailings dam may be subjected to dynamic loads such as: vibrations from blasting at a mine, movement of heavy machinery on the dam crest, and nearby road/railway traffic.

Moreover, an earthquake may occur during the staged construction of a tailings dam or during the long time abandoned state (say 1000 years). It is therefore appropriate to perform dynamic analyses for tailings dams in order to take into account the effect of above-mentioned dynamic loads on the stability of tailings dams. In this connection, the UBCSAND model can be applied for dynamic analyses of tailings dams.

5. Tests for creep behaviour

The tailings dams contain high embankments. The loads due to weight of embankments can break the angular particles of underlying tailings. The large particles can crush into fine particles. The presence of fine particles may increase the creep rate in tailings material. The creep tests (Oedometer and Triaxial) can give valuable information for understanding of the creep behaviour of tailings (slimes and sands).

When the creep behaviour of tailings material is known, the available constitutive models containing creep effects can be identified. Such constitutive models can be used for numerical analyses of tailings dams if the creep effects are of much concern.

6. **Formulation of long time stability criteria based on numerical analyses**

   Presently the environmental policies dictate that the tailings dams should be stable for a long time, i.e. 1000 years. Currently there are no criteria to assess the stability of tailings dams for such a long time. Long time stability criteria might be formulated with the help of numerical analyses by considering probable worst conditions of rainstorm, snowmelt, dynamic loads, and creep effects.

3 REFERENCES

Beaty, M., and Byrne, P.M. (1998), An effective stress model for predicting liquefaction behaviour of sand. *ASCE, Geotechnical Special Publication,* 75, pp.766-777.

Brinkgreve, R.B.J., Broere, W., and Waterman, D. (2008), PLAXIS user's manual – version 9. PLAXIS bv, the Netherlands.

Byrne, P.M., Roy, D., Campanella, R.G., and Hughes, J. (1995), Predicting liquefaction response of granular soils from pressuremeter tests. *ASCE, Geotechnical Special Publication,* **56**, pp. 122-135.

Chang, H.N. (2009), *The effect of fabric on the behaviour of gold tailings. Doctoral Thesis.* Department of Civil Engineering, Built Environment and Information Technology, University of Pretoria.

Davies, M., McRoberts, E., and Martin, T. (2002), Static liquefaction of tailings – fundamentals and case histories. *In Proceedings of Tailings Dams 2002, ASDSO/USCOLD, Las Vegas.*
Web http://www.infomine.com/publications/docs/Davies2002c.pdf. Accessed 18 December 2010.

Fell, R., MacGregor, P., Stapledon, D., and Bell, G. (2005), *Geotechnical Engineering of Dams.* Balkema, Leiden, ISBN 041536440x.

Fourie, A.B., and Papageorgiou, G. (2001), Defining an appropriate steady state line for Merriespruit gold tailings. *Canadian Geotechnical Journal*, **38**(4):695-706.

Fourie, A.B., Blight, G.E., and Papageorgiou, G. (2001), Static liquefaction as a possible explanation for the Merriespruit tailings dam failure. *Canadian Geotechnical Journal*, **38**(4):707–719.

GruvRIDAS. (2007), *Gruvindustrins riktlinjer för dammsäkerhet*, Svensk Energi AB/ SveMin, Stockholm (in Swedish).

ICOLD. (2001), Tailings dams - Risk of dangerous occurrences. *Bulletin 121*. Commission Internationale des Grands Barrages – 151, bd Haussmann, 75008 Paris.

Ishihara, K. (1996), *Soil Behaviour in Earthquake Geotechnics*. Oxford University Press. ISBN 0-19-856224-1.

Jefferies, M.G. (1993), NorSand: a simple critical state model for sand. *Geotechnique*, **43**(1):91-103.

Jefferies, M.G., and Shuttle, D.A. (2002), Dilatancy in general Cambridge-type models. *Geotechnique*, **52**(9):625-638.

Jewell, J. R. (1998), An Introduction to Tailings. *Case Studies on Tailings Management.* International Council on Metals and the Environment, United Nations Environment Programme, ISBN 1-895720-29-X.

Kjærnsli, B., Valstad, T., and Höeg, K. (1992), Rockfill Dams, *In the series Hydropower Development*, Vol. 10, Norwegian Institute of Technology, Trondheim, ISBN 82-7598-014-3.

Kramer, S.L., and Seed, H.B. (1988), Initiation of soil liquefaction under static loading conditions. *Journal of Geotechnical Engineering*. **114**(4):412-430.

Lade, P.V., and Yamamuro, J.A. (1997), Effects of nonplastic fines on static liquefaction of sands. *Canadian Geotechnical Journal*, **34**(6):918–928.

Martin, T.E., and McRoberts, E.C. (1999), Some considerations in the stability analysis of upstream tailings dams. *In proceedings of sixth International Conference on Tailings and Mine Waste '99, Fort Collins, Colorado, 24-27 January 1999*. A.A Balkema Rotterdam, pp 1-17.

Niemunis, A., and Herle, I. (1997), Hypoplastic model for cohesionless soils with elastic strain range. *Mechanics of Cohesive-Frictional Materials*, **2**(4):279-299.

Puebla, H., Byrne, P.M., and Phillips, R. (1997), Analysis of CANLEX liquefaction embankments: prototype and centrifuge models. *Canadian Geotechnical Journal*, **34**(5):641-657.

Puebla, H. (1999), *A constitutive model for sand and the analysis of CANLEX embankments*. *Ph.D Thesis*, Department of Civil Engineering, the University of British Coulombia, Canada.

Sammarco, O. (2004), A tragic disaster caused by the failure of tailings dams leads to the formation of the Stava 1985 Foundation. *Mine Water and the Environment*, **23**(2):91–95.

Tsegaye, A.B. (2010), *PLAXIS liquefaction model (UBC3D)*. *Report No.1*. Plaxis, b.v, Delft, The Netherlands.

Vick, S.G. (1990), *Planning, design, and analysis of tailings dams*. BiTech Publishers Ltd, Canada.

Wolffersdorff, V.P-A. (1996), A hypoplastic relation for granular materials with a pre-defined limit state surface. *Mechanics of Cohesive-Frictional Materials*, **1**(4):251-271.

WISE. (2010), Chronology of major tailings dam failures. Web http://www.wise-uranium.org/mdaf.html. Accessed 15 January 2010.

WISE. (2011), Safety of tailings dams. Web http://www.wise-uranium.org/mdas.html. Accessed 31st March 2011.

Yamamuro, J.A., and Lade, P.V. (1997), Static liquefaction of very loose sands. *Canadian Geotechnical Journal*. **34**(6):905-917.

Yu, H.S. (1998), CASM - A unified state parameter model for clay and sand. *International Journal of Numerical and Analytical Methods in Geomechanics,* **22**(8):621-653.

Yu, H.S., Khong, C., and Wang, J. (2006), A unified plasticity model for cyclic behaviour of clay and sand. *Mechanics Research communications*, 34(2): 97-114.

Zardari, M.A. (2010), *Mechanical properties of fine grained, sulphur rich, silty soils. Research report.* Department of Civil, Mining, and Environmental Engineering, Luleå University of Technology, Luleå, Sweden.

Research Report

MECHANICAL PROPERTIES OF FINE GRAINED, SULPHUR RICH, SILTY SOILS

M.A. Zardari

Luleå University of Technology 2010

RESEARCH REPORT

MECHANICAL PROPERTIES OF FINE GRAINED, SULPHUR RICH, SILTY SOILS

Muhammad Auchar Zardari

LULEÅ UNIVERSITY OF TECHNOLOGY

MECHANICAL PROPERTIES OF FINE GRAINED, SULPHUR RICH, SILTY SOILS

Muhammad Auchar Zardari

Luleå University of Technology
Department of Civil, Mining and Environmental Engineering
Division of Mining and Geotechnical Engineering

Cover illustration: Embankment raising work in progress at Aitik tailings dam, Sweden.

Tryck: Universitetstryckeriet, Luleå, 2010

ISSN: 1402-1528
ISBN 978-91-7439-119-0

Luleå 2010

www.ltu.se

Preface

The purpose of the literature survey presented is to gain insights into the mechanical properties of tailings in order to use reliable constitutive models for prediction of long time behaviour of tailings dams and impoundments.

In this regard, I am grateful to the Luleå University of Technology (LTU) Sweden for supporting research related costs for my doctoral studies and to the Higher Education Commission (HEC), government of Pakistan for providing me the financial assistance for living expenses under the faculty development programme of Quaid-e-Awam University of Engineering Science and Technology (QUEST), Nawabshah, Pakistan.

I am deeply indebted to my supervisor Prof. Sven Knutsson and co-supervisor Dr. Hans Mattsson for their valuable comments and suggestions in preparation of this research report.

Luleå, May 2010

Muhammad Auchar Zardari

Abstract

Tailings are the waste products produced during extraction of minerals from the ore. The particle size of tailings varies from medium sand to silt or clay size. Tailings are used as a construction material for raising of embankments called tailings dams. During spigotting, the coarse particles (sands) lie close to the embankment, while the fine particles (slimes) move downwards to the impoundment. The rate of failure in tailings dams is higher than that for the conventional water dams. In the past, tailings dams have failed due to various causes such as meteorological incidents, slope instability, piping/seepage, weak foundations, and seismic liquefaction etc. The statistics shows that the tailings dams are not safe even in their construction stages. The closure and reclamation measures require that the tailings dams and impoundments should be stable for a long time (more than 1000 years). Hence, the proper understanding of the mechanical properties (i.e., permeability, stiffness and strength) of tailings is essential in order to make reliable predictions for the long time stability of tailings dams and impoundments.

The purpose of the literature survey carried out is: (a) to understand the mechanical properties of tailings material regarding anisotropy, cyclic loading, particle crushing and creep effects; (b) to know the current design practice and identify the factors that may have strong influence on the long time stability of tailings dams and impoundments, and (c) to find from literature, an appropriate constitutive model that can predict realistic behaviour of tailings material.

There is similarity in properties of coarse tailings and loose to medium dense natural sands. Slimes are complex material and may show resemblance to natural sands, clays, or a combination of both. The hydraulic conductivity of tailings varies from point to point in a deposit. Tailings are more compressible than the natural soils. The coefficient of consolidation of slimes is in the range shown by natural clays. Due to high particle angularity, the sands and slimes show higher drained shear strength than that for similar natural soils. Undrained strength of sands is important in evaluation of liquefaction behaviour.

The embankments can be raised with upstream, downstream or centreline construction methods. The upstream method is susceptible to liquefaction, whereas the downstream and centreline methods are relatively seismic resistant. The stability

of the tailings embankments can be enhanced by keeping the phreatic surface low within the embankment body. The phreatic surface can be lowered with the application of cores, drainage zones, and the use of sand tailings in the embankment construction. Cut-off trenches, slurry walls, grout curtains, and liners can control seepage in tailings dams.

The pore water pressures develop during construction of tailings embankments. These pore pressures are described as initial static pore pressure, initial excess pore pressure, and pore pressure due to shearing. The stability analyses conditions for conventional water dams (such as end of construction, staged construction, and long term) are also applicable to the tailings dams. The end of construction condition, and staged construction condition of a tailings dam can be analysed with undrained strength analysis. The drained analysis can be used for the long-term condition of a tailings dam (when an embankment attains maximum height and is constructed slowly).

The aim of reclamation measures for tailings dams and impoundments is to achieve long time mass stability, environmental safety, and productive land use. Tailings impoundments can be stabilized with ripraps, chemicals, vegetation, and dry/wet covers etc.

Most natural soils show anisotropy in strength due to their depositional history. Due to low density and high degree of saturation, tailings show large cyclic strains in a few cycles of stress reversal. The cyclic strength of tailings can increase with decreasing void ratio. Creep occurs in all soils. Clays show more creep than sands. Loose sands creep more than dense sands. The loads due to high tailings embankments may cause particle crushing and creep.

The long time stability of tailings dams and impoundments can be predicted with finite element analysis with suitable constitutive models. The numerical analysis needs to be carried out for severe conditions of rainfalls, floods, and earthquakes.

TABLE OF CONTENTS

1. INTRODUCTION

The waste products obtained during the extraction of the minerals from ore are called tailings. The ore is crushed to less than 0.1 mm particle size. The grain size distribution of tailings depends upon the characteristics of ore and the milling process used. The grain size may range from medium sand to silt or clay size. The tailings are transported to the disposal area in a wet form.

Tailings slurries with solid content of 40 - 50 % can be pumped in a pipeline to the tailings impoundment. The slurry is distributed with different discharge methods such as sub aerial discharge (with spigots), sub aqueous discharge (slurry injected below the water surface) and thickened discharge (slurry with low water content). The discharge method influences the rate of settlement of solid particles in the slurry. In sub aerial disposal method, a sloping beach is formed from the point of deposition. Normally, the coarse tailings settle near the point of deposition, while fine tailings settle towards the beach. The water in slurry forms a pool on the sloped beach. The upper surface of tailings may become dry and partially unsaturated, but the lower portion of tailings remains saturated. Tailings deposited at dry areas with high evaporation rates, may have water contents of 20% or more (Jewell, 1998).

Tailings behaviour can be predicted by applying principles of Soil Mechanics with respect to consolidation, drainage conditions and slurry flows. However, tailings are different from most natural soils (Jewell, 1998).

The mining industry produces waste (in both solid and fluid forms) in large quantities due to mining of low-grade ore. In order to minimize environmental impacts, new disposal techniques such as underground hydraulic backfilling, paste backfilling or in-pit waste disposal have been developed. However, the mine waste is widely disposed on surface as waste dumps, waste piles, or impoundments. Due to the increased waste production, the available land is either not enough or more expensive; hence, surface disposal results in higher dumps (Priscu, 1999).

The surface impoundments for the disposal of wet tailings are called Tailings Dams. The raised embankment type of dam is common in mining industry. The raised embankments are constructed in stages over the life of impoundment with tailings and/or mined waste rock as construction material. Tailings dams are important hydraulic structures that store billions of tons of tailings. Failure of such structure might cause loss of lives, environmental and economic damages (Priscu, 1999).

Rico *et al.* (2008) made a comprehensive review of the tailings dams' failures worldwide. Various causes of failures of tailings dams are shown in Figure 1. It was concluded that:

- Meteorological events (rainfall 26% and snow 3%) were the major cause of failure. This accounted for 25% failures worldwide and 35% in Europe. There were 14% incidents due to seismic liquefaction.
- Poor management (poor beach management, improper maintenance of the dam drainage structures, quick rate of raising, and use of heavy machinery in unstable dams) is the second most important cause of tailings dams failures in Europe.
- Other causes of failures in Europe included: foundations, seepage/piping, overtopping and mine subsidence.
- All the failures in European tailings dams occurred when they reached a height of less than 45 m, and one third of such failed dams were 20-30 m high.
- Throughout the world, more than 85% of the incidents happened in active tailings dams, and only 15% of the incidents occurred in abandoned dams.
- In Europe, failure incidents were found in upstream and downstream dams (44% each), whereas 66% of the failures occurred in upstream dams worldwide.

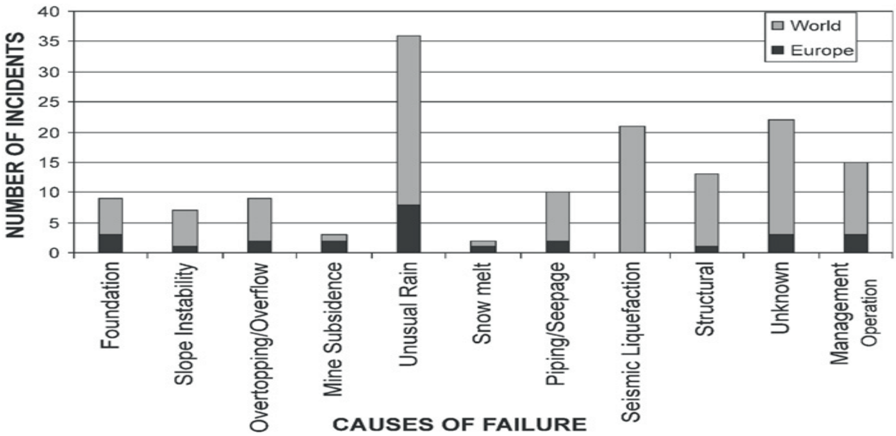

Figure 1. Causes of failures of tailings dams in the world and in Europe (Rico *et al.*, 2008).

It is estimated that there are more than 3500 tailings dams worldwide. The data shows that there have been approximately 2-5 major tailings dam failure incidents per year. The probability of rate of failure in tailings dams is 1 in 700 to 1 in 1750. While the probability of rate of failure for conventional water dams is 1 in 10000 (Witt *et al.*, 2004).

The present statistics shows that there have been failures of tailings dams in operation and abandoned state. This indicates that the tailings dams are not safe even in the present state. Further, the closure and reclamation measures of the tailings dams necessitate that the tailings dams and impoundments should be stable for a long time, i.e., more than 1000 years without maintenance. It is also anticipated that in the future long time, the occurrence of natural events such as floods, rainfalls, and earthquakes may be high (Robertson and Skermer, 1988). Bjelkevik (2005) mentions that in the long time the filters and drainage zones may not function properly. Hence, in order to be on safe side, the function of filters and drains should not be considered in the long time stability analysis. Presently there are not enough criteria to judge the stability of the tailings dams for such a long time. Therefore, there is need for development of criteria for estimating the long time stability of tailings dams and impoundments.

Finite Element Analysis (FEA) is a powerful tool for computation of stresses and strains in the embankments and foundations. FEA takes into consideration the staged construction, variation of material properties in different zones and foundation. Although, the finite element program involves various approximations in formulation of nonlinear finite element method, solution of nonlinear global equations, and integration of the constitutive equations. Still, it is the best resource for prediction of the soil behaviour in different geotechnical applications.

Currently, various constitutive models for soils have been developed. These models cover a wide range of features of soils such as anisotropy, cyclic loading, destructuration, creep etc. The selection of a constitutive model for a geotechnical application depends on the mechanical properties of the soil, previous history of the soil and the stress changes that will occur in future (Wood, 1990).

Previously Mohr-Coulomb model (Ollala and Cuellar, 2001; Gens and Alonso, 2006; Psarropoulos and Tsompanakis, 2008) and Modified Cam Clay model (Priscu, 1999) have been used for the numerical analysis of tailings dams. These models were used by assuming that they were applicable to the tailings material. It was also suggested to examine the suitability of Modified Cam Clay model for the tailings (Priscu, 1999). Hence, there is need for understanding of the mechanical properties of tailings in order to find an appropriate constitutive model for tailings for predicting the behaviour of tailings dams and impoundments with some degree of confidence.

The topics reviewed in this literature survey are: mechanical properties of tailings, construction methods, measures for control of phreatic surface and seepage, stability analysis of tailings embankments, reclamation of tailings impoundments, anisotropy, cyclic loading, creep, and constitutive models used in finite element code PLAXIS 2D (Brinkgreve *et al.*, 2008).

2. MECHANICAL PROPERTIES OF TAILINGS

A tailings impoundment consists of several layers of sediment formed by the processes of deposition, sedimentation, and consolidation. The knowledge of the properties such as density, hydraulic conductivity, compressibility, consolidation, drained and undrained shear strength is important in order to know the behaviour of tailings material. These properties are described below.

2.1 In-place density

In place-density is expressed in terms of either dry density γ_d or void ratio *e*. The thicker the layer depth, the higher is the dry density and lower the void ratio. In-place dry density depends mainly on three factors: specific gravity, type of tailings (sands or slimes), and clay content. Within an impoundment, there is variation in specific gravity, type of tailings, and clay content. Hence, the dry density of a tailings deposit shows a wide range of values (Vick, 1990). The typical values of dry density, void ratio, and water content for Swedish tailings are shown in Table 1.

Table 1. Dry density, void ratio, and water content of Swedish tailings (Bjelkevik and Knutsson, 2005).

Name of tailings dam	Distance (m) from discharge	Dry density Kg/m^3	Void ratio	Water content %
Kiruna	0	1700	0.72	22.4
	300	1770	0.60	20.5
Svappavaara	0	1760	1.09	22.7
	300	1740	0.81	24.1
Malmberget	0	2110	0.61	14.9
	300	1900	0.70	20.1
Aitik	0	1640	0.73	23.3
	1500	1550	0.82	27.5
	3000	1270	1.21	39.3
Boliden	0	1970	1.15	16.0
	300	1750	1.24	12.1
Garpenberg	0	1610	0.84	25.4
	300	1310	1.30	36.9
Zinkgruvan	0	1590	0.75	25.6
	200	1480	0.90	15.3

2.2 Relative density

The void ratio of coarse soils (sands and gravels) varies with the state of compaction between the loosest and the densest states. The relative density (or density index I_D) is defined (Craig, 2004) as:

$$I_D = \frac{e_{\max} - e}{e_{\max} - e_{\min}} \quad (1)$$

where e is the in-situ void ratio, $e_{\max}$ is the void ratio in loosest state and $e_{\min}$ is the void ratio in densest state.

Relative density is not uniform within a tailings deposit. Many beach sand tailings deposits can attain average relative densities in the range of 30-50% (loose state of compaction). The risk of liquefaction is higher in the sand tailings with low relative density (Vick, 1990). The state of compaction of granular soil deposits with respect to their relative densities is shown in Table 2.

Table 2. Description of granular soil deposits (Das, 1998).

Relative density %	Description of soil deposit
0-15%	very loose
15-50%	loose
50-70%	medium
70-85%	dense
85-100	very dense

2.3 Hydraulic conductivity

Hydraulic conductivity of a tailings deposit depends on grain size, plasticity, depositional mode, and depth within the deposit (Vick, 1990). The average hydraulic conductivity for sand tailings can be best calculated by Hazen's formula (Mittal and Morgenstern, 1975).

$$k = d^2_{10} \qquad (2)$$

where k is the average hydraulic conductivity (cm/s), d_{10} is the grain size in millimetres for which 10% of the particles pass by weight.

However, Bjelkevik and Knutsson (2005) are of the opinion that hydraulic conductivity of tailings cannot be calculated very well neither by Hazen's formula nor by the Chapuis equation (Chapuis, 2004).

Hydraulic conductivity in horizontal and vertical directions is different due to the layered nature of a tailings deposit. The ratio of horizontal to vertical hydraulic conductivity is generally in the range of 2-10 for uniform beach sand deposits and for underwater-deposited slime zones. The uncontrolled discharge of tailings can cause sand-slime interlayering, and the ratio of horizontal to vertical hydraulic conductivity can be 100 or more (Vick, 1990). The hydraulic conductivity values of Swedish tailings are shown in Table 3.

Table 3. Hydraulic conductivity values of Swedish tailings (Bjelkevik and Knutsson, 2005).

Name of tailings dam	Distance (m) from Discharge	Hydraulic conductivity m/s
Kiruna	300	14.7×10^{-6}
Svappavaara	0	6.08×10^{-6}
	300	5.67×10^{-6}
Malmberget	0	16.3×10^{-6}
	300	18.7×10^{-6}
Aitik	0	2.54×10^{-6}
	1500	1.41×10^{-6}
	3000	1.01×10^{-6}
Boliden	0	2.56×10^{-6}
	300	2.78×10^{-6}
Garpenberg	0	2.68×10^{-6}
	300	1.70×10^{-6}
Zinkgruvan	0	18.1×10^{-6}
	200	5.41×10^{-6}

2.4 Compressibility

The sands and slimes tailings are more compressible than most natural soils of similar type, due to loose depositional state and high angularity (Vick, 1990). Generally, the most slimes deposits are normally consolidated. The compressibility of a soil can be expressed by the compression index, or the coefficient of volume compressibility (Craig, 2004) as mentioned below.

(a) The compression index

The slope of the normal consolidation line in a plot of void ratio versus logarithm of vertical effective stress is denoted by compression index C_c. It is expressed (Craig, 2004) as:

$$C_c = \frac{e_0 - e_1}{\log(\sigma_1'/\sigma_0')} \tag{3}$$

where σ' is an effective stress, and the subscripts 1 and 2 represent two arbitrary points on the normal consolidation line.

The compression index C_c values of tailings usually range from 0.05 to 0.10 and 0.20 to 0.30 for sand tailings and low plasticity slimes respectively (Vick, 1990).

(b) The coefficient of volume compressibility

The coefficient of volume compressibility m_v is defined as the volume change per unit volume per unit change in effective stress. It is described (Craig, 2004) as:

$$m_v = \frac{1}{1+e_0}\left(\frac{e_0 - e_1}{\sigma_1' - \sigma_0'}\right) \tag{4}$$

where subscripts 0 and 1 represent two arbitrary points on the normal consolidation line.

2.5 Consolidation

Budhu (2007) describes the consolidation of soil as "the time dependent settlement of soils resulting from the expulsion of water from the soil pores. The consolidation settlement consists of primary consolidation and secondary compression or creep. Primary consolidation is the change in volume of a fine-grained soil caused by the expulsion of water from the voids and the transfer of load from the excess pore water pressure to the soil particles. Secondary compression is the change in volume of a fine-grained soil caused by the adjustment of the soil fabric (internal structure) after primary consolidation has been completed.”

The coefficient of consolidation C_v is defined (Craig, 2004) as:

$$C_v = \frac{k}{m_v \gamma_w} \tag{5}$$

where k is the coefficient of hydraulic conductivity of soil, m_v is the coefficient of volume compressibility and γ_w is the unit weight of water.

Vick (1990) states “coefficient of consolidation C_v varies from about 5 x 10^{-1} to 10^2 cm^2/sec for beach sand deposits. For slimes tailings, C_v is generally about 10^{-2} to 10^{-4} cm^2/sec, in the same range as typically shown by natural clays.” The typical values of coefficient of consolidation of copper tailings are shown in Table 4.

Terzaghi’s theory of one-dimensional consolidation (Terzaghi, 1925) is unsuitable for analysing the consolidation of mine tailings (Senevirante *et al.*, 1996) due to the following assumptions: (i) thin layer, (ii) no self-weight consolidation of soil, (iii) infinitesimal strains and (iv) constant permeability and compressibility under a particular load increment.

Alternatively, the nonlinear one-dimensional consolidation equation given by Gibson *et al*. (1967 and 1981) is considered more suitable for self-weight consolidation, variable void ratio and coefficient of permeability (Priscu, 1999). The consolidation behaviour of fine tailings is reported to be modelled satisfactorily using one-dimensional nonlinear finite strain code- FS-Consol (Barnekow *et al*., 1999).

Table 4. Typical values of coefficient of consolidation of copper tailings.

Material type	C_v (cm^2/sec)	Source
Copper beach sands	3.7 x 10^{-1}	Volpe, 1979
Copper slimes	1.5 x 10^{-1}	Volpe, 1979
Copper slimes	10^{-3} - 10^{-1}	Mittal and Morgenstern, 1976
Gold slimes	6.3 x 10^{-2}	Blight and Steffen, 1979
Copper tailings (Atik, Sweden)	4.3 x 10^{-2}- 6.6 x 10^{-1}	Pousette, 2007

2.6 Drained shear strength

The drained condition occurs when the excess pore water pressure dissipates. Tailings have high drained shear strength due to their high degree of particle angularity. Generally, tailings show an effective friction angle of 3-5^0 higher than that for similar natural soils at the same density and stress level (Vick, 1990). Normally, tailings are cohesionless. The slow rate of strain and full saturation of the tailings sample in direct shear test, can avoid increase in pore pressure, otherwise the test results will be incorrect showing cohesion intercept. The sample can be fully saturated with backpressure in triaxial tests (Vick, 1990). The values of drained friction angle ϕ' for sand tailings rarely vary more than 3-5^0 for a range of densities commonly shown in tailings deposits (Vick, 1990). The typical values of the drained friction angle are shown in Table 5. The drained friction angle values (evaluated at maximum deviatoric stress) from triaxial tests (Pousette, 2007) are shown in Table 6.

Table 5. Typical values of drained friction angle ϕ' of tailings.

Material	ϕ' (degrees)	Effective stress range (kpa)	Source
Copper Sands	34	0-816	Mittal and Morgenstern, 1975
Copper sands	33-37	0-672	Volpe, 1975
Copper slimes	33-37	0-672	Volpe, 1975
Gold slimes	28-40.5	960	Blight and Steffen, 1979

The stress range affects the values of friction angle ϕ' of tailings. Even a low applied effective stress can cause very high stresses at the point-to-point contacts of the angular grains, and produce particle crushing. Hence, the strength envelope is curved at low applied effective stress (Vick, 1990). Figure 2 shows that the angle of internal friction ϕ' for loose tailings sand decreases with increasing the applied effective normal stress. Figure 3 illustrates the variation of the friction angle ϕ' for dense sand tailings with effective stress level. Both particle crushing and dilatancy are noticeable at effective stress levels up to 276 kPa; the friction angle ϕ' becomes relatively constant at higher effective stresses (Vick, 1990).

Table 6. Drained friction angle ϕ' values of Swedish tailings (Pousette, 2007).

Sample	Test condition	Isotropic consolidation pressure (kPa)	ϕ' (degrees)
Consolidated	drained	140	40
Consolidated	drained	200	37
Consolidated	drained	300	39
Consolidated	undrained	150	40
Loose	drained	40	42
Loose	drained	170	40
Loose	undrained	90	43
Loose	undrained	170	41
Loose fabricated	drained	40	40
Loose fabricated	drained	100	38

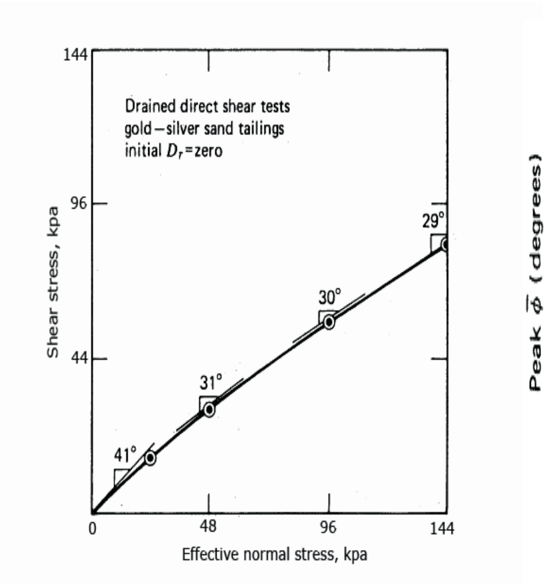

Figure 2. Strength envelope curvature at low stress levels (Vick, 1990).

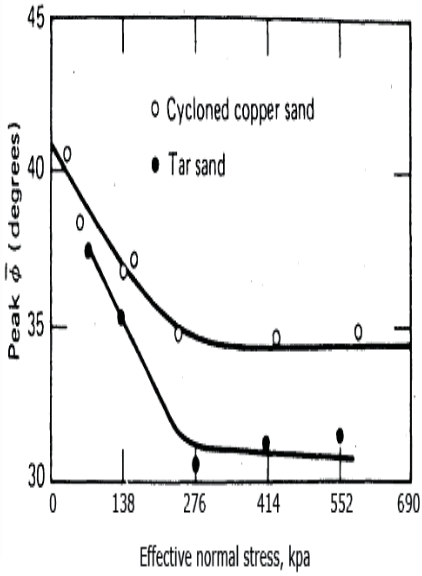

Figure 3. Variation in ϕ' with stress level (Vick, 1990).

2.7 Undrained shear strength

Undrained condition occurs when the excess pore water pressure cannot drain rapidly from the soil. If the rate of loading is faster than rate of dissipation of excess pore water pressure, there will be no change in volume of a saturated soil. For fine-grained soils the excess pore water pressure does not dissipate during construction or shortly after (short-term condition), and hence, undrained condition applies. The coarse-grained soils are highly permeable and under static loading conditions the excess pore water pressure dissipates very rapidly and, therefore, the undrained condition does not apply. However, dynamic loading such as earthquake can occur so quickly that the excess pore water pressure does not dissipate even in coarse-grained soils and undrained condition is applicable.

In the laboratory, undrained shear strength is commonly determined by consolidated undrained triaxial tests. For most tailings deposits the total stress friction angle ϕ_T is in the range of 14-24^0, roughly 15^0 less than the effective friction angle ϕ' for similar materials (Vick, 1990). Total cohesion C_T observed in some tailings is realistic (Vick, 1990). The typical values of ϕ_T and C_T for tailings are shown in Table 7.

Table 7. Typical total stress-strength parameters.

Material	Initial void ratio e_0	Total friction angle ϕ_T (degrees)	Total cohesion C_T (kpa)	Source
Copper tailings, all types	-	13-18	0-96	Volpe, 1979
Copper beach sands	0.7	19-20	34-43	Wahler, 1974
Copper slimes	0.6	14	62	Wahler, 1974
Copper slimes	0.9-1.3	14-24	0-19	Wahler, 1974

2.8 Characteristics of Swedish tailings

Bjelkevik (2005) studied the mechanical properties of seven Swedish tailings dams in operation (Kiruna, Svappavaara, Malmberget, Aitik, Boliden, Garpenberg and Zinkgruvan). The Swedish tailings are characterized as the angular particles less than 0.01-0.1 mm size (medium silt to fine sand). The Swedish tailings have high water content, low to moderate hydraulic conductivity, low plasticity, low to moderate shear strength, and high to moderate compressibility (Bjelkevik, 2005).

Bjelkevik and Knutsson (2005) made the following conclusions while comparing Swedish tailings with natural materials:

- Grain densities of tailings are 2.79 - 4.23 t/m^3 which are approximately 60% higher than grain densities of normal geological material, i.e. 2.6 – 2.8 t/m^3
- Generally the bulk density decreases with increasing distance from the discharge point
- The dry densities vary between 1.27-2.11 t/m^3
- The water content varies between 9-39% and the degree of saturation is almost 100%
- Modified Proctor Compaction tests of tailings show maximum dry density of approximately 1.7-2.7 t/m^3 at optimum water content of 10-17%, where as moraine and sand normally have dry density values of 2.0-2.2 t/m^3 and 1.7-2.0 t/m^3 respectively and optimum water content values of 5-9 % and 10-18 % respectively
- The degree of compaction of a tailings deposit (the ratio of measured dry density and the proctor maximum dry density), is in the range of 71-96%
- Tailings can be compacted to a void ratio of 0.6, which is similar to natural silty materials
- The hydraulic conductivity of tailings, from laboratory tests was found to vary between (1.0-18.7) x 10^{-6} m/s, this range of hydraulic conductivity relates to fine sand and silt (Budhu, 2007).

3. TAILINGS DAMS AND IMPOUNDMENTS

Tailings are retained on the surface with the help of dams and embankments. There are two general types of surface impoundments: water retention type of dams and raised embankments. The surface impoundments are discussed below.

3.1 Water retention type of dams

For water retention type of dams, the tailings are discharged after the embankments reach their maximum height. There is a small difference in appearance, design or construction between the water retention type tailings dams and conventional water dams. The local borrow soils are used as construction material. The design principles of conventional water dams can be applied to water retention type of dams. The condition of rapid drawdown is not applicable to water retention type of dams; hence, their upstream slopes can be steeper than the conventional water dams. Water retention types of dams are feasible for impoundments with large storm run off (Vick, 1990).

3.2 Raised embankments

In order to retain the mill tailings for initial 2-3 years production, a starter dike is constructed from natural borrow soil. Then the embankments are raised in stages until the closure of mining operation. The embankments may be constructed of natural borrow soils, pit mine waste, and tailings. Generally, the raised embankments are constructed using the upstream, downstream or centreline method.

3.2.1 Upstream method

In the upstream method (Figure 4), the tailings are discharged on the crest of the initial starter dike to form a beach. The perimeter dike is constructed on the previous beach and this process is repeated for subsequent raising. This method is simple in construction and economical in cost, but is vulnerable to phreatic surface control, water storage capacity and seismic liquefaction.

The stability of a tailings embankment depends on the location of the phreatic surface. The phreatic surface location is affected by factors such as: the permeability of the foundation, the degree of grain-size segregation and lateral permeability variation within the deposit, and the location of the ponded water relative to the embankment top (Vick, 1990). The influence of these factors on the phreatic surface location is shown in Figure 5.

Figure 5(a) shows that the phreatic level increases with increase of pond level. The increase in phreatic level can damage embankment stability, in severe cases, it may cause overtopping and breach of embankment. Figure 5(b) illustrates that phreatic level decreases with increasing degree of segregation of tailings (coarse tailings near the embankment and fine tailings towards the beach). Figure 5(c) depicts that phreatic level reduces by increasing foundation permeability.

During operation the ponded water can be pushed back from the embankment by proper tailings spigotting and decant procedures. The pond water level can be lowered and the wide separation distance between pond and crest can be achieved by increasing the decanting rates. A wide beach can be obtained by spigotting. However, the increase in phreatic surface due to floods and runoff inflows cannot be controlled by spigotting and decanting (Vick, 1990).

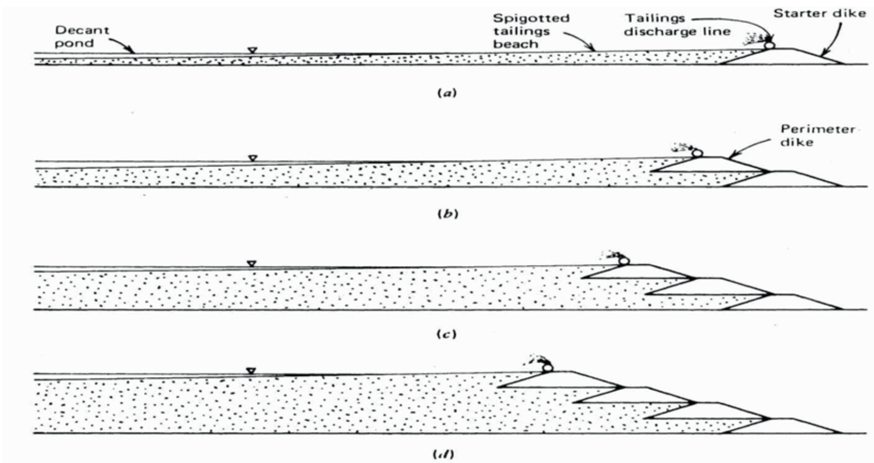

Figure 4. Upstream construction method (Vick, 1990).

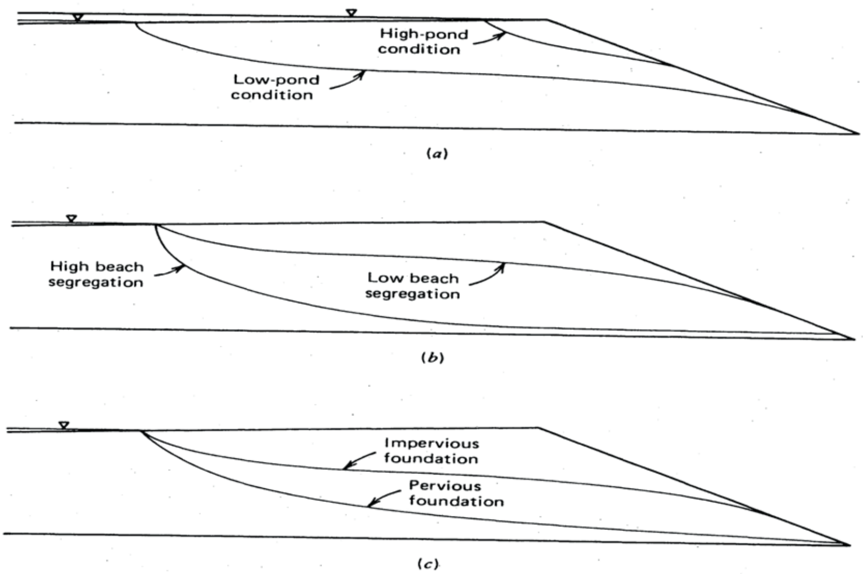

Figure 5. Factors influencing phreatic surface location for upstream embankments. (a) Effect of pond water location, (b) Effect of beach grain size segregation and lateral permeability variation, (c) Effect of foundation permeability (Vick, 1990).

The upstream method is not suitable for the conditions such as build up of water due to flood, seasonal run off and high rate mill water. The upstream method is not feasible for seismic areas due to lower relative density and high saturation within the tailings deposit (Vick, 1990). The upstream tailings dams can be constructed with a limited rate of raising. When raising rate exceeds 4.5-9 m/year, excess pore pressures can develop in slime zones (Mittal and Morgenstern, 1976).

3.2.2 Downstream method

In the downstream method (Figure 6), initially tailings are discharged towards the back of the starter dike. The fill is placed on the downstream slope of the previous raise. The structural measures within the embankment such as impervious cores and internal drains for control of phreatic surface can be incorporated. These measures help in storing large volumes of water. Due to low phreatic surface level and ease of compaction, this method provides more resistance to liquefaction. There is no restriction on raising rate because the downstream raises are structurally independent of the spigotted tailings deposit. However, this method is costly due to large volumes of embankment fill (Vick, 1990).

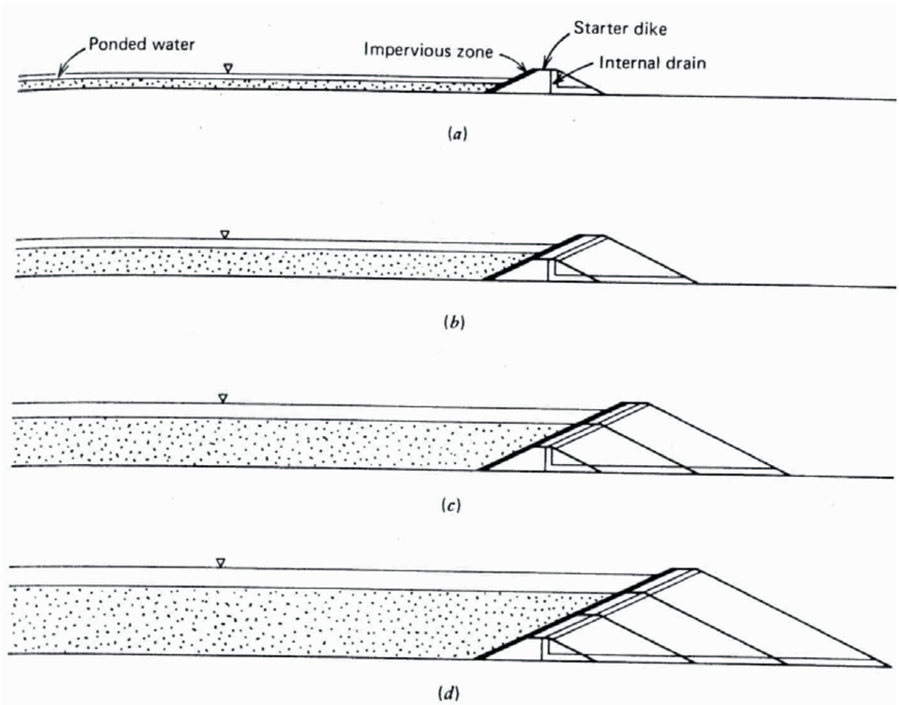

Figure 6. Downstream construction method (Vick, 1990).

3.2.3 Centreline method

In the centreline method (Figure 7), tailings are spigotted from the initial starter dike. The fill is placed continuously on the beach and the downstream slope of the previous raise. The centreline remains the same as the embankments are raised (Vick, 1990).

With proper internal drainage zones, the phreatic surface can be controlled and the temporary rise of water due to floods will not affect the stability of the structure. This method has generally good seismic resistance, due to the ease of compaction of the main body of the dam and the control of saturation level by internal drainage. Failure due to liquefaction can occur to the limited portion of upstream fill placed on the beach; however, the central and downstream portions of the embankment remain safe (Vick, 1990).

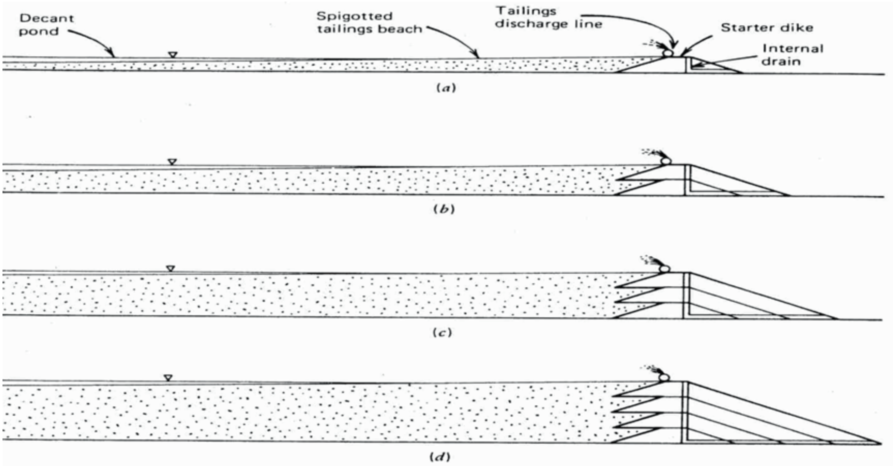

Figure 7. Centreline construction method (Vick, 1990).

3.3 Design considerations for long time stability of tailings impoundments

The actions due to the natural events (floods, earthquakes, wind and water erosion, frost, weathering and decomposition, and chemical reaction) may cause failure of tailings dams and impoundments (Robertson and Skermer, 1988). The extreme climatic events may occur in the future long time. Floods may occur from snowmelt and rainfall. The global warming may occur, causing melting of polar ice caps and flooding of low-lying regions. Dynamic loads, due to earthquakes, may result in the liquefaction of low density saturated tailings or un-compacted saturated portions of granular embankments or embankment foundation material. Hence, the long time design criteria for rains, floods, and earthquakes need careful attention (Robertson and Skermer, 1988).

Erosion is a major long time concern for tailings impoundments. Erosion may occur due to wind or water action. Both are severe causes of instability of tailings surfaces and embankments. Wind erosion can be controlled by wind erosion resistant cover, such as vegetation, waste rock etc (Robertson and Skermer, 1988).

The diversion structures or outlet works may block due to build up of ice. Freezing of drains may increase pore pressures in the embankments and may cause slope failure. Accumulation of frozen tailings prevents drainage, dissipation of pore pressures and the consolidation of the tailings (Robertson and Skermer, 1988).

In non-permafrost areas, thawing of the ice may cause seepage and high pore pressures in the tailings. Large consolidation settlements and cracking of covers may occur in tailings impoundments (Robertson and Skermer, 1988).

Frost heave is the uplift and deformation of ground surface due to freezing of saturated soil. Frost heave causes cracks in pavements and damages foundations of buildings etc. In the embankments, soil particles can move upward on freezing and move downward on thawing. Therefore, the freezing and thawing of the embankments may cause mass movement of the embankments. When the temperature falls below 0^0C, the freezing of pore water occurs in saturated soils. Although soil temperature increases with depth but due to continuous subzero temperature the zone of freezing can increase downwards. Initially, water freezes in larger pores. When the temperature drops below zero, higher soil suction develops and water moves towards the ice in the larger voids and freezes there. As this process continues, the formation of ice lenses and rise of ground surface occurs (Craig, 2004).

The magnitude of frost heave reduces with decrease of degree of saturation of the soil. When thawing occurs, the soil becomes soft and shows low strength. During freezing, the volume of water expands approximately 9%, therefore, in a saturated soil the volume of voids above the freezing level will increase by the same amount. This expansion in volume of voids can cause 2.5-5% increase in overall volume of the soil (Craig, 2004).

The long time stability of tailings dams and impoundments can be achieved by the design considerations such as decreasing the height of embankments, slope flattening, avoiding weak foundations at the toe of embankment, controlling pore pressure by drainage, construction methods, appropriate freeboard and spillway capacity to manage maximum flood conditions, erosion resistant diversion ditches and flow control structures, and maintenance to some acceptable low level (Robertson and Skermer, 1988).

Bjelkevik (2005) believes that long time stable tailings dams can be constructed by enhancing our present knowledge of tailings dams further in the following aspects "internal and external erosion, long term material behaviour, the effect of hydraulic gradient on slope stability, interaction between tailings material and foundation, and seepage through the tailings dam and impoundment."

The tailings dams must be designed to resist the extreme static, dynamic, and hydraulic loads due to floods, rainfalls and earthquakes which may occur in the future long term. The finite element analyses should be based on simple reliable constitutive models and the results should be verified by field measurements (Witt *et al.,* 2005).

3.4 Failure modes of tailings dams

The failure of tailings dams may occur due to various factors such as overtopping, slope instability, internal erosion, external erosion, seismic action and damage to decant systems etc. The causes of failures in tailings dams and their remedies (ICOLD Bulletin 106) are given in Table 8.

Table 8. Failure modes of tailings dams, their causes and remedial measures (ICOLD Bulletin 106).

Failure mode	Cause	Remedy
Overtopping	• Inadequate hydrological or hydraulic design • Loss of freeboard due to crest settlement	• Gabions, mine pit waste or surrounding borrow material may be quickly imported to aid the strength of embankment • Opening of emergency pumps and spillways
Slope instability	• Overstressing of foundation soil and dam fill • Inadequate control of pore pressure	• Soil reinforcement and strengthening measures • Installing a drainage trench at the toe of downstream face and/or horizontal bore drains. Filters can prevent the entry of fill material into the drain.
Internal erosion	• Inadequate control of seepage • Bad filter and drain design • Poor design or construction control resulting in cracks or leakage through conduits	• Raising downstream embankments with drainage blanket • Installation of horizontal bores to relieve pressure • Installation of deep trenches towards downstream face
External erosion	• Inadequate slope and toe protection	• Vegetation of the downstream face • Placing crushed mine waste on the downstream embankment face • Construction of berms on downstream face • Placing rock fill such as mine pit waste adjacent to the toe
Earthquake action	• Steep slopes • Liquefaction of embankment and foundation soil	• Filling of cracks with a suitable material
Damage to decant system	• Excessive settlement • Chemical attack on concrete/steel	• Opening of emergency pumps or spillways

4. CONTROL OF PHREATIC SURFACE AND SEEPAGE

The measures to control phreatic surface and seepage in tailings dams are discussed below.

4.1 Control of phreatic surface

The overall stability of a tailings embankment under both static and seismic loading conditions depends on the low phreatic surface or internal water level in the embankment. It is necessary to keep the phreatic surface as low as possible near the embankment face. A general rule is that permeability of various internal zones should increase in the direction of seepage flow. The phreatic surface decreases due to increase in permeability of the material, and hence, the embankments should be constructed with the most pervious available material (Vick, 1990).

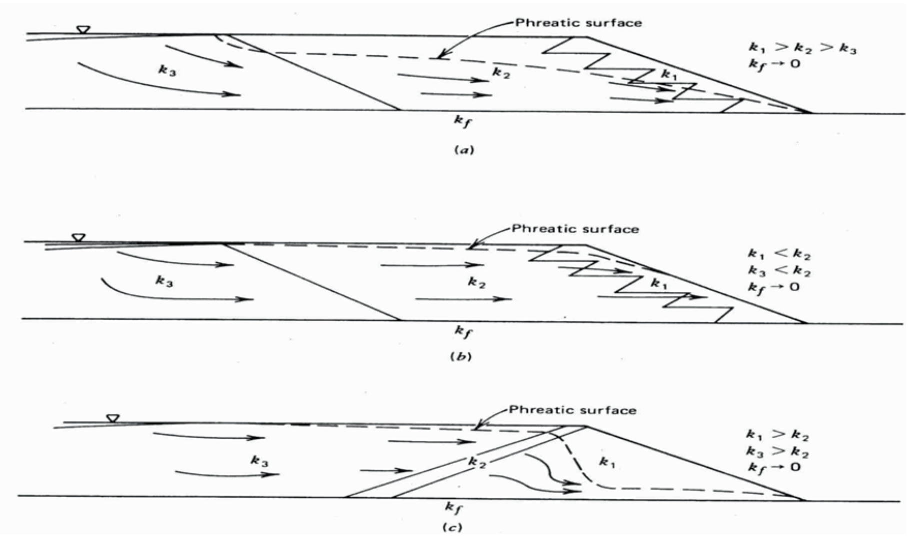

Figure 8. Effect of internal zoning on phreatic surface. (a) Proper internal permeability configuration for control of phreatic surface, (b) Seepage blocked by low permeability material at embankment face, producing high phreatic surface, (c) Seepage restricted by upstream core and drained by downstream pervious zone to produce good phreatic surface control (Vick, 1990).

Figure 8(a) shows an idealized upstream embankment in which low permeability slimes are near the pond and high permeability sands are at the embankment face. The phreatic surface is fairly lower near the embankment face due to highly permeable sands. Figure 8(b) shows that the low permeability zone at the embankment face prevents drainage and results in high phreatic surface, and may cause mass instability, piping and erosion. Figure 8(c) shows a downstream or water retention type of embankment with an upstream core and a pervious downstream shell. The location of the phreatic surface can be controlled by the use of cores, drainage zones, and tailings material, as mentioned below.

4.1.1 Cores

The core is an impervious zone constructed within an embankment dam to reduce the quantity of seepage. For conventional embankment dams, a zoned section with an impermeable core is considered better than a homogeneous section of impervious material (Singh and Varshney, 1995).

While selecting the core material for a conventional embankment dam, the properties such as permeability, compacted density, shear strength, compressibility, flexibility, and erosion resistance are considered. High compacted density of core is desired as it increases shear strength and erosion resistance, and reduces permeability. In highly compressible soils extreme settlements, cracking, and high pore pressures can occur during construction (Singh and Varshney, 1995).

Inclined cores are suitable for downstream raises, while central cores are appropriate for centreline method (Figure 9). The phreatic surface can be controlled by making use of either inclined core or vertical core, if the downstream shell materials are sufficiently pervious with respect to the core (Vick, 1990).

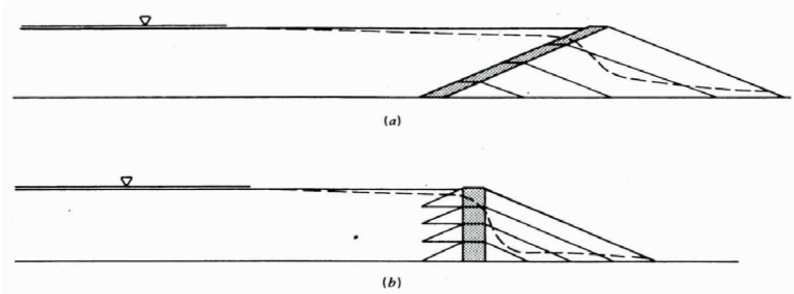

Figure 9. Use of low permeability cores in raised embankments. (a) Downstream embankment. Phreatic surface indicated by dashed line, (b) Centreline embankment (Vick, 1990).

4.1.2 Drainage zones

Drainage of an embankment reduces pore pressures in the dam body. The phreatic surface can also be controlled by provision of internal drainage zones as a supplement to the cores, or as an alternative when only permeable soils are available at site (Vick, 1990). Internal drainage zones may be of either chimney or blanket type. The chimney drains rise upward within the embankment, either vertically or inclined, and prevent lateral seepage. Horizontal blanket drains are used to drain the embankment and downstream foundation, and may be used alone at the base of the structure or in combination with chimney drains (Vick, 1990).

Figure 10(a) shows that the phreatic surface reduces due to the presence of a blanket drain that extends upstream from the starter dike. For upstream embankments, the starter dike should be more pervious than the tailings in order to avoid the increase in phreatic surface level at or above the starter dike crest. Figures 10(b) and (c) show the use of chimney-blanket drains in the downstream and centreline-type embankments. The use of combined chimney-blanket drain arrangements can prevent seepage along the base of structure and saturation of downstream shell, and does not put restriction on permeability of remaining fill zone in the downstream shell. Hence, the downstream shell can be constructed with any easily available material that satisfies strength requirements (Vick, 1990).

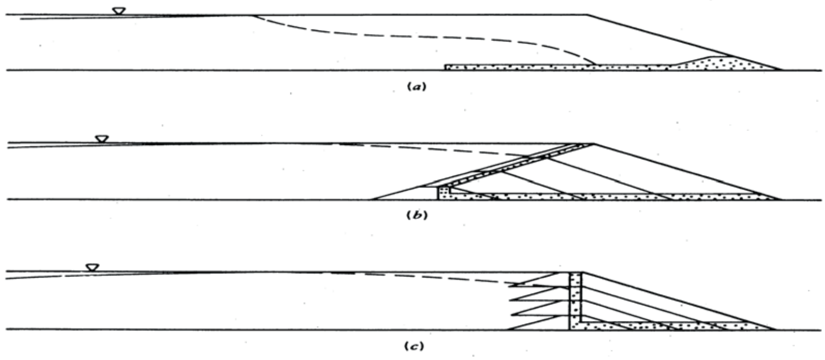

Figure 10. Use of internal drainage zones in raised embankments. (a) Upstream embankment using pervious starter dike with upstream blanket drain, (b) (b) Downstream embankment using inclined chimney drain and blanket drain, (c) Centreline embankment with vertical chimney drain and blanket drain (Vick, 1990).

4.1.3 Use of tailings

In case of shortage of locally available material (less permeable for cores and high permeable for drainage zones), tailings themselves can be used as a measure of phreatic surface control. The phreatic surface reduces, when the permeability difference between adjacent zones is of about two orders of magnitude. This difference is achieved by separating sands and slimes through cycloning (Vick, 1990). During cycloning of tailings on the embankment, sands are placed near the embankment and the slimes are discharged through pipes away from the embankment. Figure 11 shows that the use of slimes and sands can lower the phreatic surface.

The use of tailings as a measure of phreatic surface control can be effective by keeping wide beach and minimum runoff. The cycloned sand (due to high effective strength and permeability) is a suitable material for drainage (Vick, 1990).

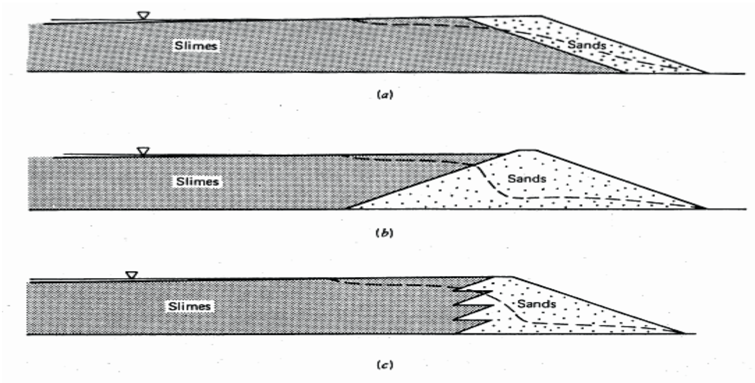

Figure 11. Use of tailings for internal drainage. (a) Upstream embankment, (b) Downstream Embankment, (c) Centreline embankment (Vick, 1990).

In downstream embankments with cores, the phreatic surface reduces when the material in the downstream shell is more permeable than the core. In general, a shell-core permeability ratio of 100 or more results in low phreatic surfaces both in downstream and centreline embankments (Vick, 1990).

4.2 Control of seepage

Fell *et al.* (2005) describes, "Seepage occurs through all embankment dams and their foundations. The permeability of most compacted earth fill core materials is less than 10^{-8} or 10^{-9} m/sec." Most of the seepage occurs through foundations (Fell *et al.,* 2005).

The preventive and curative measures are taken in order to control seepage through the embankment and the foundation. The preventive measures include, use of core in the embankment, cut-off trenches, grout curtains, slurry trench, concrete diaphragm wall, sheet pile wall for foundation. The curative measures consist of a drainage system as mentioned earlier. Some preventive measures are discussed below.

4.2.1 Cut-off trenches

The seepage through a permeable foundation can be minimized by constructing a low permeability cut-off through the permeable material. The degree of effectiveness of cut-offs depends on their permeability and depth. The cut-offs may include cut-off trenches, slurry wall and grout curtains etc, as shown in Figure 12.

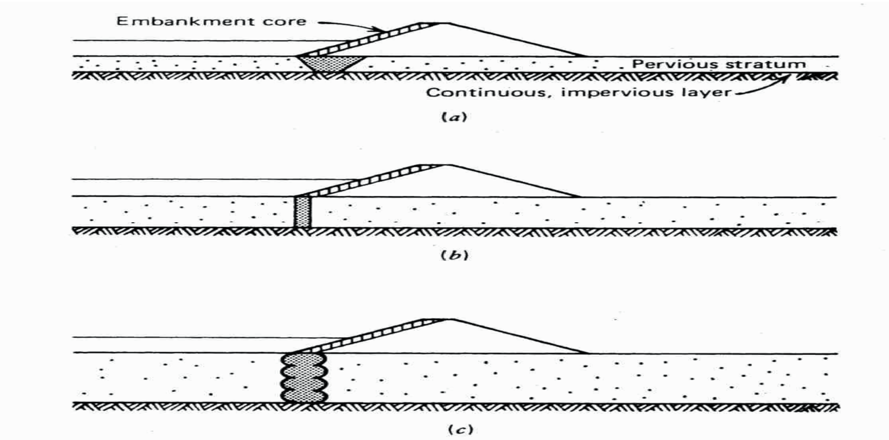

Figure 12. Seepage barriers. (a) Cut-off trench, (b) Slurry wall, (c) Grout curtain (Vick, 1990).

Cut-off trench is commonly used to control seepage in tailings dams. In this method, the trench is filled with compacted soil having low hydraulic conductivity. Cut-off trenches can function effectively when they are installed down to the impervious layer (Fell *et al.,* 2005).

4.2.2 Slurry walls

Slurry walls have been used for tailings dams and conventional water retention dams. The trench is backfilled either with slurry of soil and bentonite or bentonite containing cement additives. The properties of sodium bentonite include high swelling capacity, good plasticity, high shear strength, low hydraulic conductivity and compressibility that are desirable for tailings dams (Mylona *et al.*, 2004). The slurry walls can be constructed in saturated foundations where cut-off trenches are impractical to excavate. However, slurry walls are relatively costly and cannot easily penetrate the fractured bedrock (Vick, 1990).

4.2.3 Grout curtains

Grouting is a process in which fluids (grouts) are injected into the soil in order to reduce seepage and compressibility of soil, and increase the shear strength (Craig, 2004). The suspension type grouts consist of soil, cement, lime, asphalt emulsion etc while the solution type grouts include a wide variety of chemicals (Murthy, 2003). Grout curtains have been used to reduce foundation permeability for water retention dams and can be installed to a depth of 30 m or more. This method is costly; therefore, it is not widely used in tailings impoundment for seepage control (Vick, 1990).

4.2.4 Liners

The whole floor of the impoundment can be covered with low permeability tailings. This cover of tailings is termed as liner as shown in Figure 13. Liners can be constructed on any dry surface, without care for the nature of subsurface soil, rock, or groundwater conditions. The main types of liners include tailings slimes, clay liners, and synthetic liners (Vick, 1990).

Slimes liners are economical in seepage control of tailings, with effectiveness comparable to clay or synthetic liners. The portion of slimes must be more than 40 % passing through 0.075 mm sieve. The slimes must have consolidated permeability of approximately 10^{-6} cm/sec. Slimes liners can resist major foundation settlement and seismic liquefaction (Vick, 1990).

Clay liners have been used to reduce seepage from water storage reservoirs and toxic waste impoundments. Clay liners also consist of compacted soils that incorporate additives such as commercial bentonite. Clays with high plasticity and high placement moisture content generally show flexibility and lower permeability, and high shrinkage and cracking on drying (Vick, 1990).

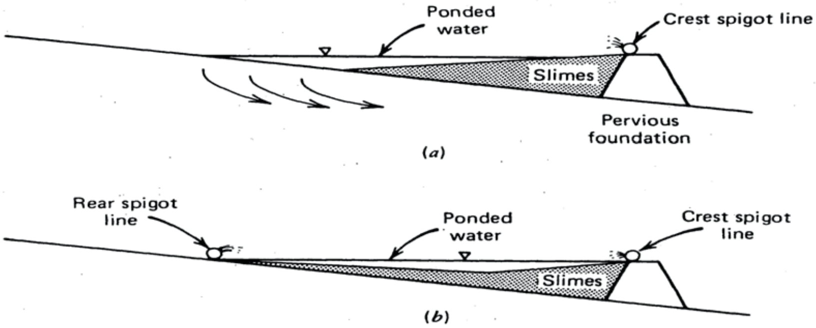

Figure 13. Control of seepage by slimes spigotting procedures. (a) Major seepage at water foundation contact, (b) Foundation sealing by rear spigotting of slimes (Vick, 1990).

5. STABILITY ANALYSIS OF TAILINGS EMBANKMENTS

The stability of a tailings embankment reduces during the construction period. In order to improve the stability of an embankment, the tailings dams are constructed in stages. Numerical analysis can be performed to check the stability of tailings embankments. The pore water pressures that develop during the construction of a tailings embankment and the conditions for stability analysis are discussed below.

5.1 Pore pressures in tailings embankments

The pore pressures (initial static pore pressures, initial excess pore pressures, and pore pressures due to shearing) that develop during construction stage of a tailings embankment are shown in Figure 14. The initial static pore pressures u_s occur due to steady state seepage flow without any external loading on the embankment. In stability analysis, the reasonable assumption is that the pore pressure at a particular point is related to its depth D below the phreatic surface (Figure 14a).

The initial excess pore pressures u_e may develop in an upstream embankment due to quick rate of raising, which does not allow dissipation of pore pressures (Figure 14b). Similarly, in case of soft clay foundation, the excess pore pressures can occur in the foundation material. For very coarse and permeable soils, the pore pressure due to shearing u_f may dissipate quickly (Figure 14c). For dense compacted soils, negative pore pressures occur due to dilatancy during shear. The negative pore pressures are neglected in stability analysis. For loose fine–grained soils, large pore pressures develop due to rapid changes in shear stress. The changes in shear stress are dependent not only on applied loading but on unloading also. For example, unloading due to removal of material at the toe, can cause changes in shear stress, hence, the pore pressure may increase (Vick, 1990). The combined effect of the three types of pore pressures is shown in Figure 14d. The additional parameters used in Figure 14 are defined as: γ_w is the unit weight of water, γ_t is the total unit weight, and H is the depth of soil layer.

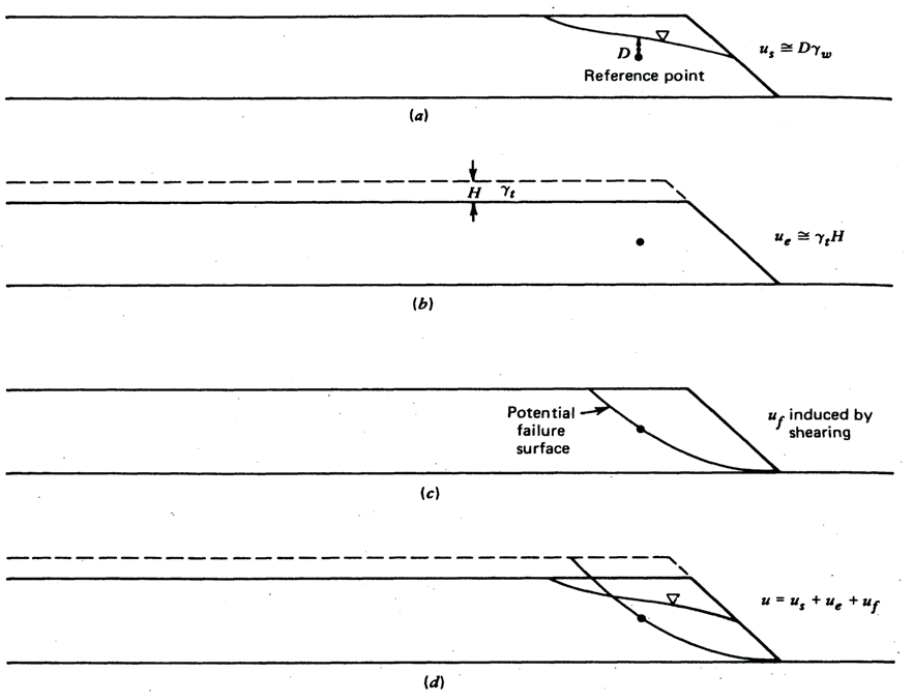

Figure 14. Pore pressures in stability analysis. (a) Initial static pore pressure due to seepage, (b) Initial excess pore pressure due to uniform rapid loading, (c) Pore pressure due to shear, (d) Combined pore pressure conditions (Vick, 1990).

5.2 Conditions of analysis for tailings embankments

For conventional water dams, the following critical loading conditions occur during the life of the dam; (i) end of construction, (ii) staged construction, (iii) long term steady seepage and (iv) rapid drawdown. The relevance of these conditions with respect to tailings dams is discussed below.

5.2.1 End of construction

For conventional water dams, the loads due to successive raising of the dam cause compression of the fill and increase of pore pressures. Normally the pore pressures become high when the dam reaches full height, however, the pore pressures may become critical at any intermediate stage. This condition can be dangerous for either the upstream or the downstream slopes (Singh and Varshney, 1995).

The factors affecting construction pore pressure are compaction moisture content, soil type, and rate of construction etc. An embankment compacted wet of optimum can sustain larger differential settlements without cracking; while an embankment compacted dry of optimum will be more brittle and liable to cracking. However, the construction pore pressures in a fill compacted dry of optimum are much less than those in a fill compacted wet of optimum (Singh and Varshney, 1995). The construction pore pressures increase with compressibility of the soil. The high pore pressures can develop in clayey soils due to their compressibility. The low pore pressures can develop in silts and silty sands of low plasticity due to their low compressibility (Singh and Varshney, 1995).

In case of tailings dams, when starter dikes are constructed on soft silts or clays, significant dissipation of load-induced pore pressure may not occur during construction, and if failure occurs, the full pore pressure due to shearing is experienced by the foundation material (Vick, 1990). This type of loading is usually analysed using the undrained shear strength S_u and $\phi = 0$ approach as shown in Figure 15(a).

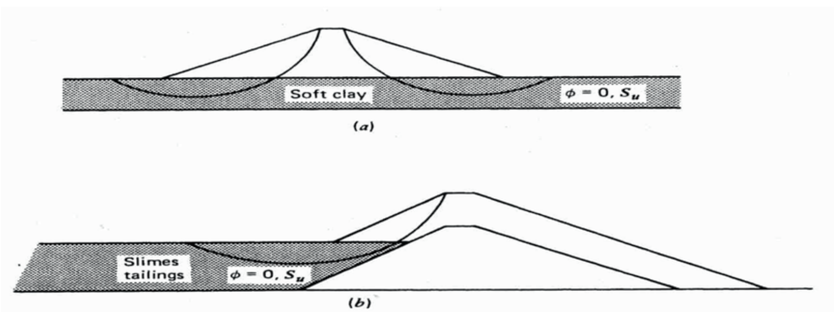

Figure 15. End of construction analysis for tailings embankments. (a) Starter dike constructed rapidly on soft clay foundation, (b) Centreline raise constructed on soft slimes (Vick, 1990).

For soft, normally consolidated clays, S_u usually increases with depth. The increase in S_u with depth can be taken into consideration by dividing the foundation material into various horizontal layers. Figure 15(b) shows centreline embankment raises. When the raises are high and are constructed quickly, the stability of the upstream fill placed over the slimes is determined by undrained analysis.

5.2.2 Staged construction

The staged construction analysis may be applicable to downstream, centreline and upstream embankments constructed on soft foundations. However, this analysis is commonly used for upstream embankments that are constructed rapidly. During staged construction, the load-induced pore pressures dissipate significantly due to slow loading. However, the increase in initial pore pressures cannot be neglected due to increased rate of embankment height. For upstream embankments, raised at a rate less than 4.5-9 m/year, the excess pore pressures are assumed to dissipate sufficiently and staged construction analysis is not applied. The staged construction analysis (Vick, 1990) is shown in Figure 16.

At time t_1, when a new raise is added, it can generate excess pore pressures in the first raise along with initial pore pressures due to seepage. Before the addition of a second raise, some dissipation of excess pore pressures of the first raise will occur. However, the pore pressures will not dissipate completely; there will remain some residual pore pressures. When a second raise is added at time t_2, there will be residual pore pressures from the previous step plus excess pore pressures due to second raise. Similarly, this procedure is repeated for the subsequent raises, where excess pore water pressures can dissipate and develop simultaneously. The pore pressure predictions for staged construction analyses should be verified by field measurements (Vick, 1990).

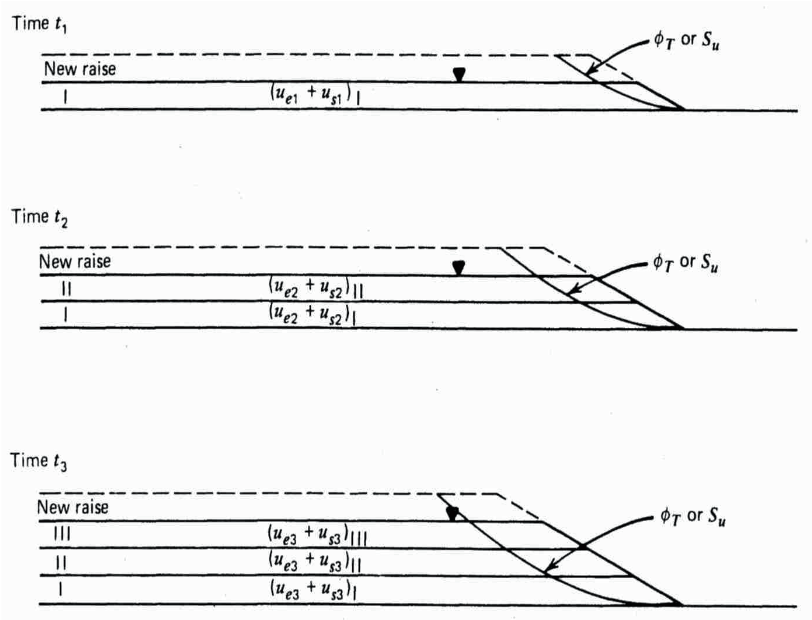

Figure 16. Staged construction analysis for rapid raising of upstream embankment (Vick, 1990).

Since tailings dams are constructed in stages in order to allow time for consolidation. The drainage due to consolidation improves the stability of a tailings embankment and the foundation. During construction of a tailings embankment, positive excess pore water pressures can develop in foundation soil or in slimes. The construction period of a tailings dam is considered critical from stability point of view. Hence, the staged construction condition is applicable for either continuous controlled rate of construction or construction of embankments in several stages. The stability of upstream tailings dams during construction can be strengthened by the application of vertical drains and by berms along the downstream side (Ladd, 1991).

In conventional effective stress analysis (ESA), the staged construction is considered as the consolidated drained case because of the assumption that potential failure can occur gradually and shear induced pore pressures dissipate completely. The factor of safety computed with ESA is higher and unrealistic because the most failures during staged construction occur in undrained conditions (Ladd, 1991). On the other hand, the staged construction is assumed as consolidated undrained case in undrained strength analysis (USA). In this case, the failure occurs very quickly without dissipation of shear induced pore pressures. The factor of safety determined from undrained strength analysis can be reliable because the undrained shear strength C_u of normally consolidated soils is less than the drained strength (Ladd, 1991).

5.2.3 Long-term

For conventional water dams, long-term stability analysis is applicable when internal stresses and pore pressures are in equilibrium and steady state seepage conditions occur under full reservoir level and as a result, the whole soil mass below the phreatic surface develops positive pore pressures. The seepage forces act towards the downstream slope. Hence, a steady state seepage condition is dangerous for downstream slope (Singh and Varshney, 1995). Long-term analyses for tailings embankments are applicable under conditions similar to those defined for conventional water dams, but with some further assumptions. The condition for long term is that there will be no rapid change in external loading. Long-term analyses are performed when the raised embankments attain maximum height. For slowly raised embankments, it is assumed that the pore pressures and internal stresses due to previous raises will be in equilibrium. The further assumption is that the steady seepage condition can occur when the embankment reaches maximum height. These assumptions make lowest estimate of the long-term pore pressures (Vick, 1990).

There are two different opinions of the researchers whether or not the pore pressures induced by shearing at failure should be included in long-term analysis. Johnson (1975) suggests that neglecting the shear induced pore pressures may cause high shear strength. However, the effective–stress parameters (without taking into consideration the pore pressures induced by shear at failure) can be used in long-term analysis (Kealy and Soderberg, 1969; Wahler, 1974) as shown in Figure 17.

The properties of very loose tailings deposits may be similar to that of natural deposits of sensitive clay. For sensitive clay, even a small initial slip in a slope can cause a rapid change in the loading conditions at the toe of slope and can produce a series of slides resulting in failure of the slope (Bishop and Bjerrum, 1960). This situation may also occur in tailings embankments constructed of very loose material (Bishop, 1973). Figure 18 illustrates the long-term analysis of tailings embankments (Vick, 1990).

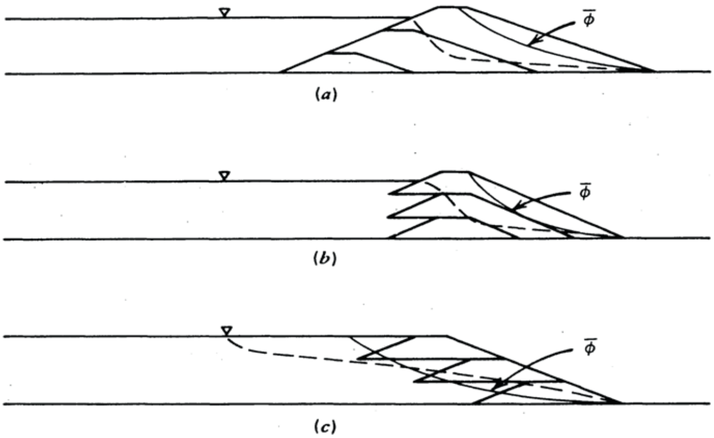

Figure 17. Long-term analysis of various types of tailings embankments. (a) Downstream, (b) Centreline, (c) Upstream (Vick, 1990).

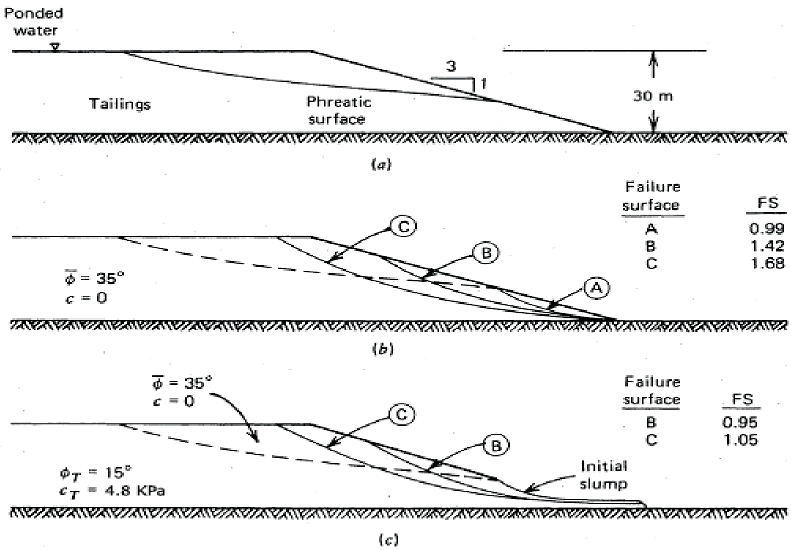

Figure 18. Progressive failure under drained and undrained loading conditions. (a) Geometry, material and phreatic conditions, (b) Effective-stress analysis, long-term condition (c) Total-stress analysis, after change in loading produced by initial slump (Vick, 1990).

Figure 18(b) shows the effective stress analysis for an upstream embankment for long-term condition. Three failure surfaces A, B and C are shown for different factors of safety (FS). Failure surface A (FS = 0.99) indicates that a sloughing-type slide can occur in saturated material near the toe. Generally, this small sloughing-type slide is considered dangerous for overall stability of the embankment (Vick, 1990). If such sloughing occurs quickly, it will violate the nonfailure assumptions of long-term analysis. Changes in stress resulting from sloughing can increase pore pressures in remaining part of the embankment. Undrained analysis using total stress parameters can be used to model these new conditions occurring due to sloughing (Vick, 1990). Figure 18(c) shows the total stress analysis (the pore pressures induced by changes in shear stress are considered). In this case, failure may occur along surface B (FS = 0.95) and the failure surface C (FS = 1.05) has marginal stability (Vick, 1990).

5.2.4 Rapid drawdown

For conventional water dams, rapid drawdown occurs when the reservoir is lowered quickly. The soil inside the embankment remains saturated. Seepage can occur from the saturated embankment towards both upstream and downstream slopes. The drawdown condition is dangerous for the upstream slope because the upstream water pressure does not counterbalance seepage force (Singh and Varshney, 1995). In case of tailings embankments, the breach of the embankment can create this condition. Therefore, the rapid drawdown condition is not directly applicable to stability analysis of tailings embankments (Vick, 1990).

6. RECLAMATION OF TAILINGS IMPOUNDMENTS

When the mining operation ceases, the deposition of the tailings into the impoundment ends. If looked from the broad perspective, the deposition of tailings stops but not the disposal. Hence, tailings management must be continuous until the permanent physical stability and environmental safety of the tailings dams and impoundments are assured. The fundamental objectives of reclamation are: long term structural stability of the tailings dams and impoundments, erosion stability, prevention of environmental contamination, and return of the disturbed area to the productive use (Vick, 1990). These objectives are discussed below.

6.1 Long time stability of the impoundment

The phreatic surface can be lower, when the discharge of tailings stops due to closure of mining operation. The stability of embankment slopes can be higher at closure than during the mining operation period (Vick, 1990). Hence, it is usually assumed that any slope that was stable during operation will also be stable after abandonment; if there will be no accumulation of water in the impoundment. It is also assumed that measures will be taken during reclamation to stop entry of water in the impoundment (Vick, 1990).

There is the risk of liquefaction of loose-deposited tailings during mining operation in high seismic areas. When the mining operation ends, the loose tailings get dry, consolidate with time, and hence, the risk for liquefaction may be reduced after abandonment (Vick, 1990).

Hydrologically induced failures are the major cause of mass instability of abandoned tailings deposits. The accumulation of run off water in the impoundment may cause slope failure or seismic instability, overtopping and erosion (Vick, 1990). Because of the possibility of accumulation of runoff water, hydrological stability is a major concern during operation, and reclamation stage. The construction of diversion ditches, spillways or culverts to divert long time runoff is not suitable due to high cost and maintenance in future. The accumulation of water can be prevented by capping the impoundment with mine waste material with nominal slope of 0.5-1% peaked at impoundment centre and sloped towards its perimeter (Vick, 1990). An additional material will also be needed to prevent water ponding at depressions that occur due to settlement of slimes under the weight of capping material. Commonly, an additional 3 m or more of capping material is needed to reduce the settlement of the slimes zone (Vick, 1990).

6.2 Long term erosion stability

Wind erosion is a problem on flat surfaces, while water erosion is a problem on embankment slopes. Tailings embankment slopes flatter than 3:1 (H:V) are considered erosion resistant and conducive to vegetation growth. Slopes flatter than 5:1 are more stable (Vick, 1990).

6.3 Environmental contamination

The leaching of the contaminants from tailings into the ground water is harmful to the environment. The drains in the tailings dams can be plugged due to deposition of salts, e.g. gypsum and ferrous salts. The long-term degradation of protective layers is possible due to chemical weathering of cover materials, liners and ripraps (Robertson and Skermer, 1988).

Acid Mine Drainage (AMD) or Acid Rock Drainage (ARD) is the major environmental problems faced by the mining industry. The AMD phenomenon occurs in base metal (iron, nickel, lead, zinc and copper), gold, uranium, coal and lignite mining industry. AMD is produced by the oxidation of sulphide minerals, mainly pyrite and pyrrhotite, in the presence of air, water and bacteria, resulting in the formation of acidic solutions with increased concentrations of sulphate anions and dissolved metals (Mylona *et al*., 2004).

Improper deposition and rehabilitation of tailings can produce acid drainage that may occur for hundreds of years or more after mining closure. AMD produces sulphuric acid and toxic metals, which contaminate soil and ground water. The acids generated can kill living organisms in water systems for years causing problems for land use. The leaching of the contaminants produced due to oxidation of pyrite (if present), can be prevented by providing a clay cap over the impoundment during abandonment and reclamation. The water covers prevent the entry of oxygen and hence, can stop the AMD generation. The AMD is a very complex problem and needs careful measures to control chemical reaction and prevent drainage in the ground water (Mylona *et al*., 2004).

6.4 Return of land to productive use

During mining operation, the natural flora and fauna of the land is disturbed. The purpose of reclamation process is to make the land usable to some acceptable level with vegetation, forestry plantations etc. Furthermore, the development of the basic infrastructure is intended for commercial development of the area affected by the mining operation.

6.5 Stablization methods

The aim of stabilization of tailings dams and impoundments is to control the erosion and release of contaminants to the ground water. The tailings dams and impoundments can be stabilized with the help of ripraps, vegetation and different covers (Vick, 1990) as mentioned below.

6.5.1 Ripraps

The purpose of ripraps (small pieces of rock, gravel and mine waste) is to resist the impact of falling raindrops. Hence, a thin layer of riprap can serve this purpose very well. However, the ripraps are generally not conducive for vegetation growth and even provision of this thin layer for the whole impoundment will be costly (Vick, 1990).

6.5.2 Chemical stabilization

Chemical stabilizing agents used for temporary control of erosion, include electrometric polymers, calcium lignosulfate (a paper mill waste), asphalt emulsions, sodium silicates, and resinous adhesives. Generally, the reapplication of chemical agents is required every year. Hence, the use of chemical agents will be much costly and therefore, the chemical stablization is not suitable as permanent reclamation measure (Vick, 1990).

6.5.3 Vegetative stabilization

Vegetation is commonly used for stablization of tailings impoundments. A vegetative cover can minimize wind and water erosion. Re-vegetation can be established by some simple efforts in the presence of favourable climate and tailings with favourable chemical composition. However, the achievement of re-vegetation becomes difficult and costly in dry climates or for tailings having low PH, or high concentrations of heavy metals or salts (Vick, 1990). Many types of tailings provide a poor growth medium on the basis of texture, fertility, toxicity, or all the three. It is obvious that considerable effort may be required to modify the tailings to provide conditions conducive to re-vegetation. The alternative is to cover the entire impoundment with topsoil. Topsoil is commonly applied to the impoundment surface in depths ranging from 15 cm to 1 m (Vick, 1990).

6.5.4 Water covers

In water cover system, free water is used as an oxygen diffusion barrier. The oxygen diffusion coefficient is 10^4 times less in water than in air. Hence, the use of water cover can eliminate the sulphide oxidation.

Water covers have been implemented in tailings impoundments at Stekenjokk and Kristineberg, Sweden. The water cover can reduce the sulphide oxidation rate of the deposited tailings. However, in the water cover system, the pore pressures may cause slope failures (Bjelkevik, 2005).

6.5.5 Dry covers

The dry cover systems of tailings impoundments can be composed of multiple layers as shown in Table 9 (Rumer and Mitchell, 1996). The selection of the cover system is based on site-specific factors such as climate, environmental risk of disposal area, availability of borrow material, cost etc. Although both natural and synthetic covers may be cost-effective when applied in relatively small disposal areas, they may not be feasible for large tailings disposal facilities.

Table 9. Layers of the final cover at waste disposal sites (Rumer and Mitchell, 1996).

	Layer	Primary functions	Potential materials	Factors affecting performance
1	Surface layer	• Separation of underlying layers from the ground surface • Resistance to wind and water erosion • Protection of underlying layers from temperature and moisture extremes	• Topsoil vegetated • Geosynthetic layer over topsoil • Cobbles • Paving material	Erosion, evapotranspiration, vegetation
2	Protection layer	• Storage of infiltrated water until its removal by evapotranspiration • Separation of waste from humans, burrowing animals and plant roots • Protection of underlying layers from wet-dry and freeze-thaw cycles, which may cause cracking	• Soil • Cobbles • Recycled or reused Waste (e.g., fly ash, bottom ash and paper mill sludge)	Erosion, slope failure due to pore pressure build up, animal burrows
3	Drainage layer	• Reduction of water head on the barrier layer • Reduction of pore pressures in the overlying layers, thus increasing slope stability • Reduction of the time during which the overlying layers are saturated following rainfall events, thereby decreasing erosion	• Sand or gravel • Geonet or geocomposite • Recycled or reused waste	Clogging, insufficient capacity and drainage outlets
4	Hydraulic and/or oxygen barrier layer	• Prevention of water percolation • Prevent oxygen diffusion	• Compacted clay • Geomembrane • Geosynthetic clay liner • Recycled waste • Asphalt	Cracking due to desiccation, deformation from settlement or seismic action, root penetration
5	Foundation layer	• Foundation for the cover	• Sand or gravel • Soil • Waste	Adequate strength

The dry cover has been successfully applied for the remediation of Uranium tailings in the Ranstad tailings facility in Sweden (Sundblad, 2003). This cover consists of the different layers placed on tailings such as moraine (0-0.3m), clay-moraine (0.2 m), limestone (0.2 m), moraine (1.2 m), and topsoil (0.2 m) from bottom to top respectively.

7. ANISOTROPY

Anisotropy is the change in soil behaviour with direction of loading. Anisotropy occurs due to different factors such as deposition, stress strain history of soil, and changes in loading conditions (Seah, 1990). Anisotropy in soils is measured with: conventional axisymmetric triaxial cell, true triaxial apparatus, plane strain device, direct simple shear device, torsional shear hollow cylinder, and directional shear cell. The torsional shear hollow cylinder and directional shear cell give realistic predictions of anisotropy (Seah, 1990). There are two essential causes of anisotropy in soils (Budhu, 2007):

(a) Structural anisotropy: occurs due to formation of soil fabric during deposition. The symmetries occur due to depositional history of soils.

(b) Stress-induced anisotropy: happens due to difference in stresses in different directions.

Transverse anisotropy also called cross anisotropy (horizontal plane is isotropic) is the most common type of anisotropy in soils. Generally, stress-strain characteristics and strength of a soil in vertical (z direction) is different from horizontal (x and y) directions. For transverse anisotropy, the elastic parameters are the same in the lateral directions but are different in the vertical direction. For full description of anisotropic soil behaviour, 21 elastic constants are needed (Love, 1927). For transverse anisotropy, only five elastic constants (E_h, E_v, v_{hh}, v_{vh}, G_{vh}) are needed.

The incremental stress-strain relation to represent cross anisotropy (Wood, 1990) is:

$$\begin{bmatrix} \delta\varepsilon_{xx} \\ \delta\varepsilon_{yy} \\ \delta\varepsilon_{zz} \\ \delta\gamma_{yz} \\ \delta\gamma_{zx} \\ \delta\gamma_{xy} \end{bmatrix} = \begin{bmatrix} 1/E_h & -v_{hh}/E_h & -v_{vh}/E_v & 0 & 0 & 0 \\ -v_{hh}/E_h & 1/E_h & -v_{vh}/E_v & 0 & 0 & 0 \\ -v_{vh}/E_v & -v_{vh}/E_v & 1/E_v & 0 & 0 & 0 \\ 0 & 0 & 0 & 1/2G_{vh} & 0 & 0 \\ 0 & 0 & 0 & 0 & 1/2G_{vh} & 0 \\ 0 & 0 & 0 & 0 & 0 & 2(1+v_{hh})/E_h \end{bmatrix} \begin{bmatrix} \delta\sigma'_{xx} \\ \delta\sigma'_{yy} \\ \delta\sigma'_{zz} \\ \delta\tau_{yz} \\ \delta\tau_{zx} \\ \delta\tau_{xy} \end{bmatrix} \tag{6}$$

Where $\delta\sigma'_{xx}$, $\delta\sigma'_{yy}$, $\delta\sigma'_{zz}$ are the effective normal stress increments in x, y, and z axes respectively; $\delta\tau_{yz}$, $\delta\tau_{zx}$, $\delta\tau_{xy}$ denote the shear stress increments; $\delta\varepsilon_{xx}$, $\delta\varepsilon_{yy}$, $\delta\varepsilon_{zz}$ represent the normal strain increments; $\delta\gamma_{yz}$, $\delta\gamma_{zx}$, $\delta\gamma_{xy}$ are the shear strain increments; E_h, E_v are the Young's moduli in horizontal and vertical directions respectively; ν_{vh} is the Poisson's ratio when the load is applied in the vertical direction; ν_{hh} is the Poisson's ratio when the load acts on horizontal direction, and G_{vh} is the shear modulus in horizontal direction when the load is applied in vertical direction.

Graham and Houlsby (1983) are of the view that from conventional triaxial compression tests of soil; more than 3 elastic constants can not be taken. Out of these three elastic constants, two constants (E and ν) describe isotropic elastic response, and the third constant α describes some anisotropy.

The incremental stress strain relation for this case (Graham and Houlsby, 1983) is expressed as:

$$\begin{bmatrix} \delta\varepsilon_{xx} \\ \delta\varepsilon_{yy} \\ \delta\varepsilon_{zz} \\ \delta\gamma_{yz} \\ \delta\gamma_{zx} \\ \delta\gamma_{xy} \end{bmatrix} = \frac{1}{E*} \begin{bmatrix} 1/\alpha^2 & -\nu^*/\alpha^2 & -\nu^*/\alpha & 0 & 0 & 0 \\ -\nu^*/\alpha^2 & 1/\alpha^2 & -\nu^*/\alpha & 0 & 0 & 0 \\ -\nu^*/\alpha & -\nu^*/\alpha & 1 & 0 & 0 & 0 \\ 0 & 0 & 0 & 2(1+\nu*)/\alpha & 0 & 0 \\ 0 & 0 & 0 & 0 & 2(1+\nu*)/\alpha & 0 \\ 0 & 0 & 0 & 0 & 0 & 2(1+\nu*)/\alpha^2 \end{bmatrix} \begin{bmatrix} \delta\sigma'_{xx} \\ \delta\sigma'_{yy} \\ \delta\sigma'_{zz} \\ \delta\tau_{yz} \\ \delta\tau_{zx} \\ \delta\tau_{xy} \end{bmatrix} \quad (7)$$

where, E^* and ν^* are the modified values of Young's modulus and Poisson's ratio for the soil respectively, and α is an anisotropy parameter.

For normally consolidated or lightly overconsolidated soft clays, yielding can occur at small increase of stresses and hence, plastic deformations will be more important than elastic deformations. Therefore, for simplicity, the elastic behaviour is assumed to be isotropic (Wheeler *et al.*, 2003).

The direction of load can vary the unconsolidated undrained shear strength of saturated clays. Anisotropy phenomenon is shown in Figure 19 (Das, 1997). The direction H and V are parallel and perpendicular to the bedding plane respectively. The undrained shear strength $S_{u(i)}$ of a soil sample with its axis inclined at an angle i with the horizontal direction (Das, 1997) is given by:

$$S_{u(i)} = \frac{\sigma_1 - \sigma_3}{2} \quad (8)$$

The soil becomes isotropic when the undrained strength is the same ($S_{u(i)} = S_{u(H)} = S_{u(V)}$) in any direction. Casagrande and Carrillo (1944) suggested the following equation for undrained shear strength of soil when the load acts at an angle *i* with the horizontal direction:

$$S_{u(i)} = S_{u(H)} + \left[S_{u(V)} - S_{u(H)}\right]\sin^2 i \tag{9}$$

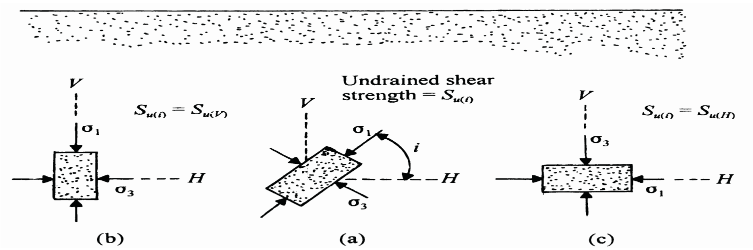

Figure 19. Strength anisotropy in clay (Das, 1997).

The ratio of undrained shear strength in vertical direction to undrained shear strength in horizontal direction is called coefficient of anisotropy (Das, 1997) and is described as:

$$K = \frac{S_{u(V)}}{S_{u(H)}} \tag{10}$$

For natural soils, the value of *K* ranges from 0.75 to 2.0. For overconsolidated clays, the value of *K* is less than 1 (Das, 1997).

Seah (1990) performed series of undrained shear strength tests of Boston Blue clay with directional shear cell. The shearing was done with different orientations of the major principal stress to the direction α of deposition. The undrained shear strength *Su* (normalized by vertical consolidation stress σ'_p) reduces up to 50% as α increases (Figure 20).

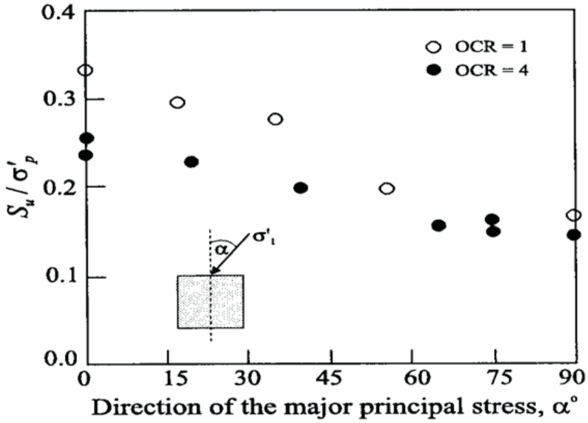

Figure 20. Undrained strength anisotropy of Boston Blue clay (Seah, 1990).

Hight (1998) conducted series of hollow cylinder tests on K_0 normally consolidated Ham river sand (Figure 21). It is observed that the drained friction angle ϕ' decreases with α .

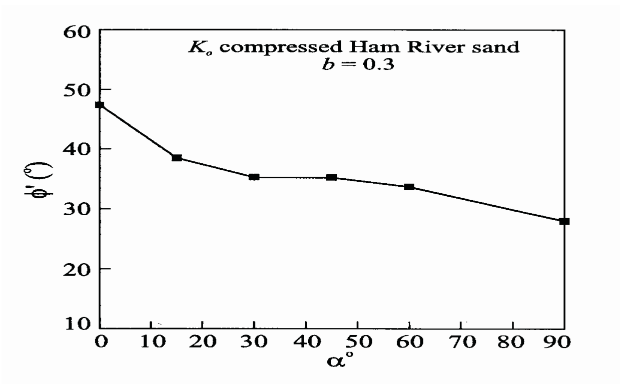

Figure 21. Effect of orientation of major principal stress on drained friction angle of sand (Hight, 1998).

8. CYCLIC LOADING

The loose saturated sand under undrained conditions tends to contract due to seismic action, the pore water pressure resists this contraction and results in increase in pore water pressure and decrease in effective stress. The pore water pressure increases with repeated cycles of loading.

Because of high degree of saturation and loose densities, the tailings are sensitive to liquefaction. Liquefaction of tailings can lead to instability and failure of tailings impoundments. Loose uncompacted saturated sands at relative densities of 30-50% are vulnerable to liquefaction (Vick, 1990). For tailings samples, when pore pressure equals confining pressure, the initial liquefaction can start. Generally, the initial liquefaction can initiate at 10% of cyclic strain. Liquefaction due to earthquake loading is a concern in upstream tailings dams (Vick, 1990). Seismic action on tailings dams may cause settlement, horizontal movement, cracking, pore pressure increase, slope slumping, slope failure, liquefaction, internal erosion, seepage increase and impoundment breaching (Engels *et al.*, 2004). Seed (1979) remarks that tailings, due to their loose deposition and normal consolidation are more susceptible to liquefaction than natural soil deposits.

During undrained cyclic loading of tailings, the pore pressures can build up and cause large shear deformations and low strength (Wijewickreme *et al.*, 2005) as shown in Figure 22.

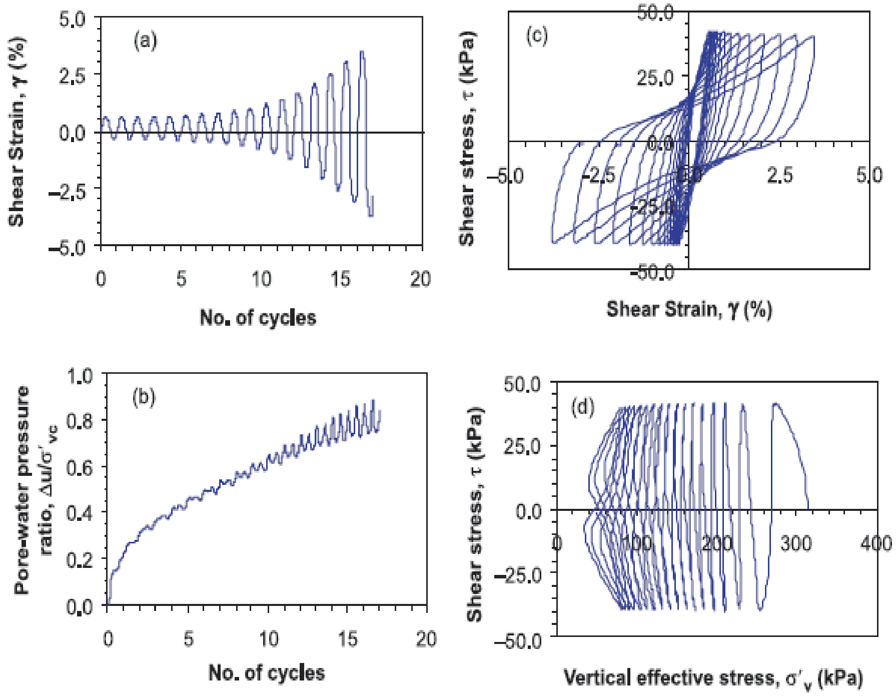

Figure 22. Typical response of copper–gold–zinc tailings in constant-volume cyclic Direct simple Shear (DSS) loading (Initial effective confining stress σ'_{vc} = 314 kPa). (a) Shear strain versus number of cycles, (b) Equivalent excess pore-water pressure ratio versus number of cycles, (c) stress– strain response, (d) stress path response (Wijewickreme *et al.*, 2005).

Ishihara *et al*. (1980) conducted cyclic triaxial tests on tailings material (Figures 23 to 25). These figures show that cyclic strength of tailings (sands, low/high plasticity slimes) decreases with increase in the void ratio. However, the cyclic strength of slimes is found to be lower than that of the sands at the same void ratio. At a very large void ratio, the cyclic strength of sands and slimes becomes almost similar. The fine-grained tailings with plasticity index of 15 to 20 showed higher cyclic strength as compared to the nonplastic tailings (Ishihara *et al.*, 1980).

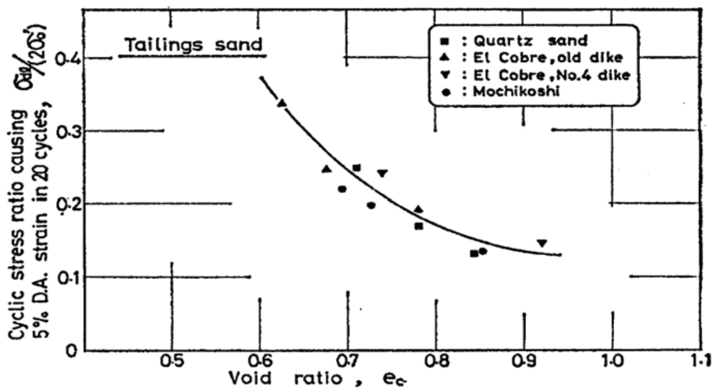

Figure 23. Cyclic strength vs. void ratio relationship of tailings sands (Ishihara *et al.*, 1980).

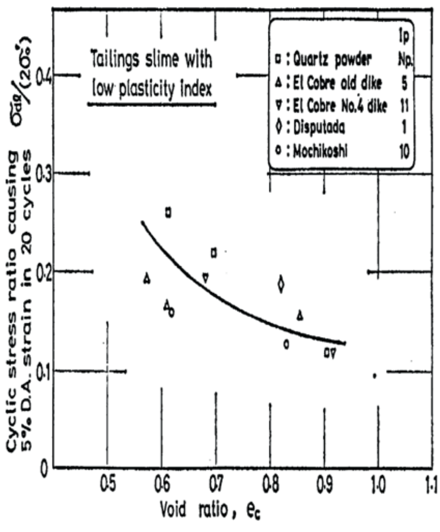

Figure 24. Cyclic strength vs. void ratio of low plasticity tailings slimes (Ishihara *et al.*, 1980).

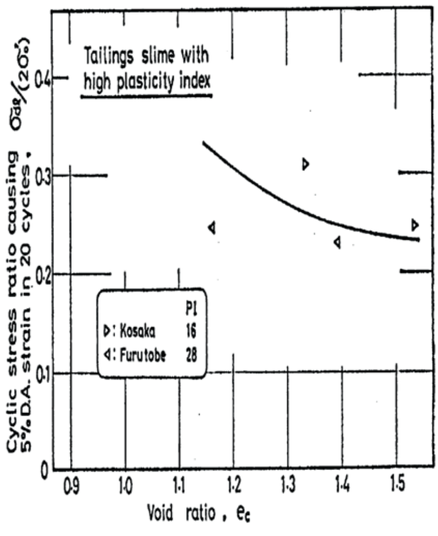

Figure 25. Cyclic strength vs. void ratio of high plasticity slimes (Ishihara *et al.*, 1980).

However, Vick (1990) describes that slimes tailings show higher cyclic strength than the sand tailings (Figure 26).

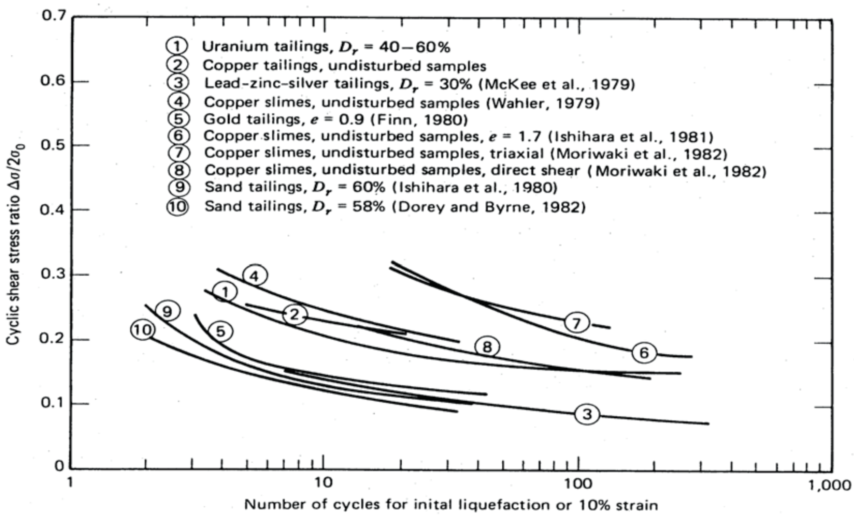

Figure 26. Cyclic shear strength of tailings (Vick, 1990).

9. TIME-DEPENDENT BEHAVIOUR OF SOILS

The consolidation settlement consists of two parts, i.e., primary consolidation and secondary compression or creep. The primary consolidation occurs when the excess pore water pressure diminishes and the load is transferred to the soil particles. A constant vertical effective stress can cause changes in soil fabric (internal structure) with respect to time. The deformation produced due to a constant vertical effective stress is called secondary compression or creep. The physical reasons for creep in soils may be expulsion of water from micro pores or viscous deformation of the soil structure (Budhu, 2007). The primary consolidation and secondary compression may occur simultaneously from the start of loading (Craig, 2004). However, for simplification, it is assumed that secondary compression occurs after the primary consolidation completes (Budhu, 2007).

The rate of secondary compression in the Oedometer test can be defined by the slope C_α of the final part of the compression-log time curve as shown in Figure 27. The slope C_α is also called the secondary compression index and is expressed (Budhu, 2007) as:

$$C_\alpha = \frac{(e_t - e_p)}{log(t/t_p)}; \qquad t > t_p \tag{11}$$

where (t_p, e_p) is the coordinate at the intersection of tangents to the primary consolidation and secondary compression parts of the void ratio versus logarithm of time curve and (t, e_t) is the coordinate of any point on the secondary compression curve as shown in Figure 27. The secondary consolidation settlement ρ_{sc} can be expressed (Budhu, 2007) as:

$$\rho_{sc} = \frac{H_0}{(1+e_p)} C_\alpha \log\left(\frac{t}{t_p}\right) \tag{12}$$

where H_0 is the initial height of the soil sample.

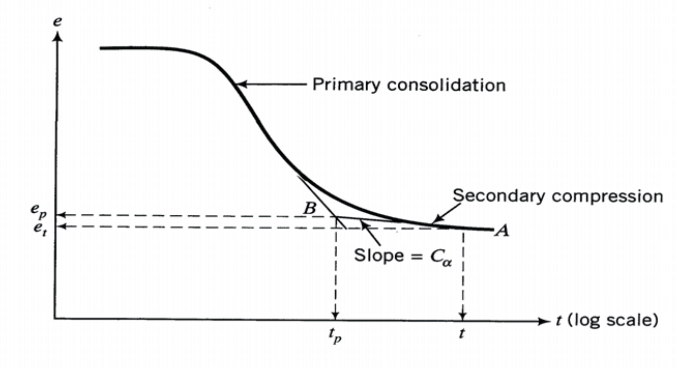

Figure 27. Primary consolidation and secondary compression (Budhu, 2007).

Based on the coefficient of secondary consolidation Mesri (1973), classified the secondary compressibility as shown in Table 10.

Table 10. Classification of secondary compressibility (Mesri, 1973).

C_α	Secondary compressibility
<0.002	very low
0.002-0.004	low
0.004-0.008	medium
0.008-0.016	high
0.016-0.032	very high

Creep can be divided into volumetric creep and deviatoric creep. In volumetric creep, the void ratio decreases with time at constant effective stress. In deviatoric creep, the shear strain increases with time at constant shear or deviatoric stress.

The time-dependent deformations in soils occur due to various factors such as soil structure interaction, stress history, drainage conditions, and changes in temperature, pressure, and biochemical environment with time (Mitchell and Soga, 2005).

9.1 General characteristics of creep in soils

The general characteristics of creep behaviour of some soils are described below.

- An increase in deviatoric stress level shows increased creep rate (Figure 28).

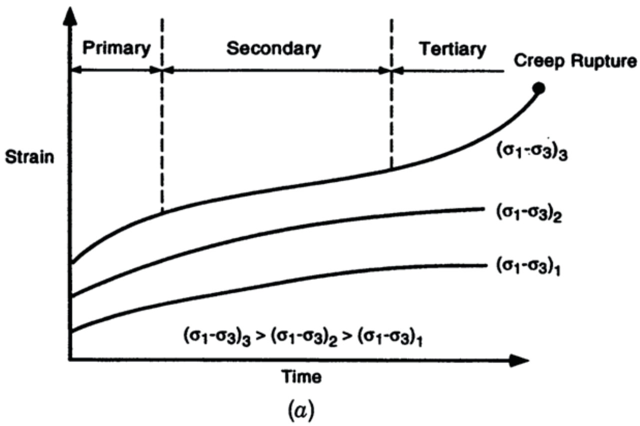

Figure 28. Creep under constant stress rate with deviator stress for undrained compression (Mitchell and Soga, 2005).

- Figure 29 shows drained triaxial compression creep of London clay (Bishop, 1966), and Figure 30 demonstrates undrained triaxial compression creep of soft Osaka clay (Murayama and Shibata, 1958). Both the Figures 29 and 30 display that the logarithm of strain rate decreases linearly with increase in the logarithm of time.

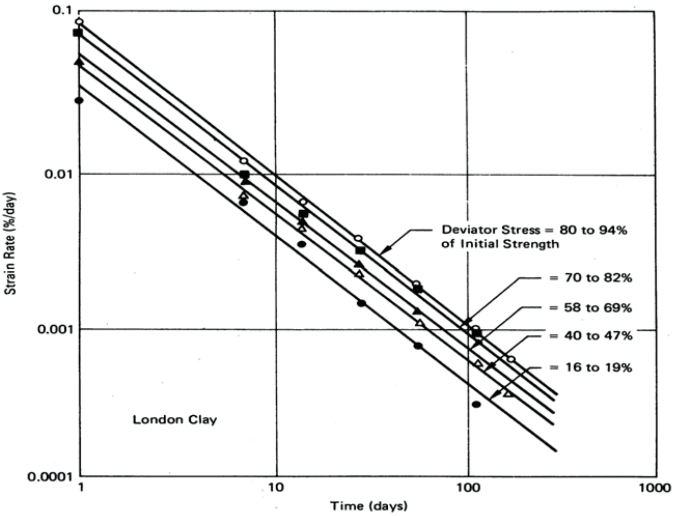

Figure 29. Strain rate vs. time relationships during drained creep of London clay (Bishop, 1966).

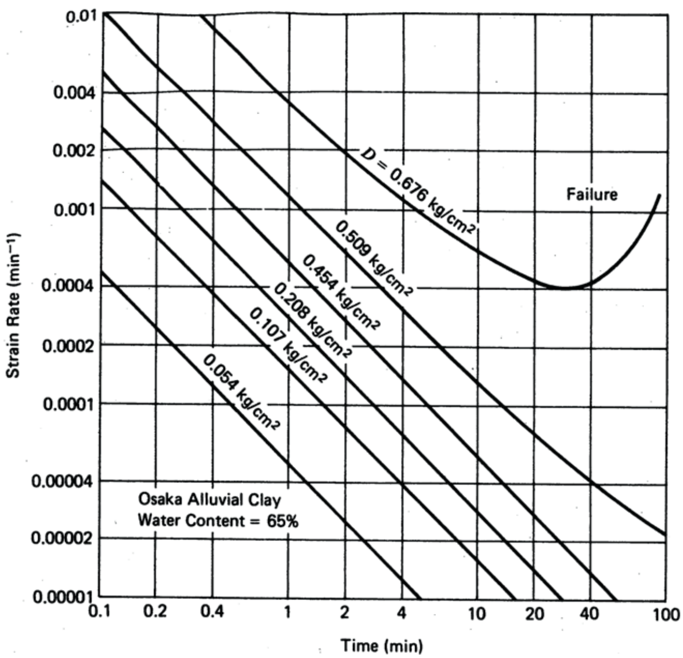

Figure 30. Strain rate vs. time relationship during undrained creep of Alluvial clay (Murayama and Shibata, 1958).

- The undrained strength of saturated clay increases with increase in rate of strain (Figure 31 and 32).

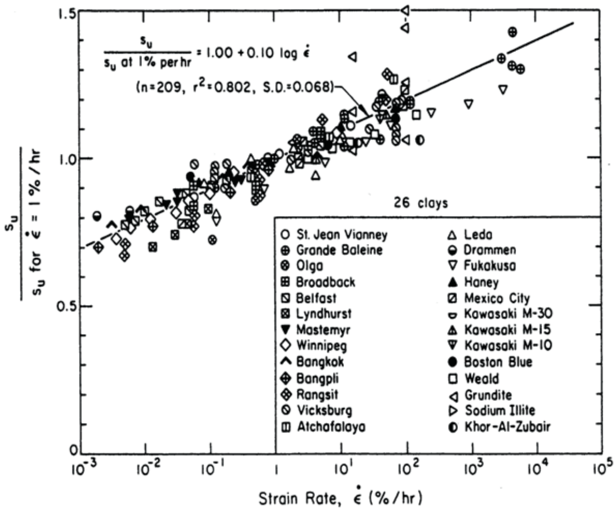

Figure 31. Effect of strain rate on undrained strength (Kulhawy and Mayne, 1990).

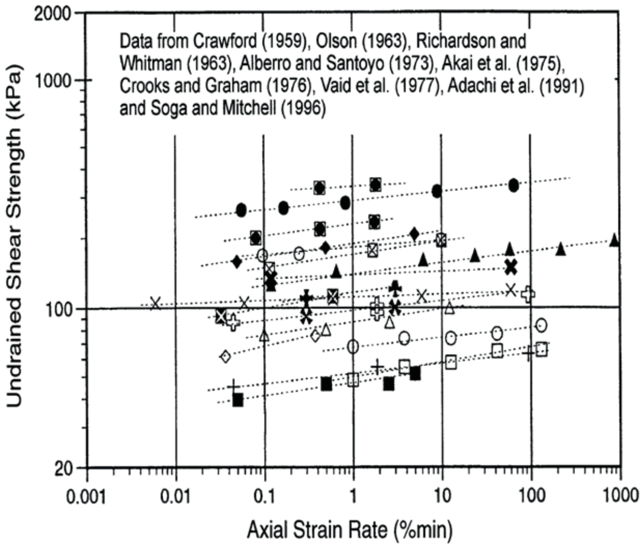

Figure 32. Strain rate dependence on undrained shear strength determined using constant strain rate CU tests (Soga and Mitchell, 1996).

- Organic matter in soil may cause high plasticity, high shrinkage, high compressibility, low hydraulic conductivity, and low strength. In general, the creep rate increases with organic content, clay content, and plasticity index as illustrated in Figures 33 and 34 (Mitchell and Soga, 2005).

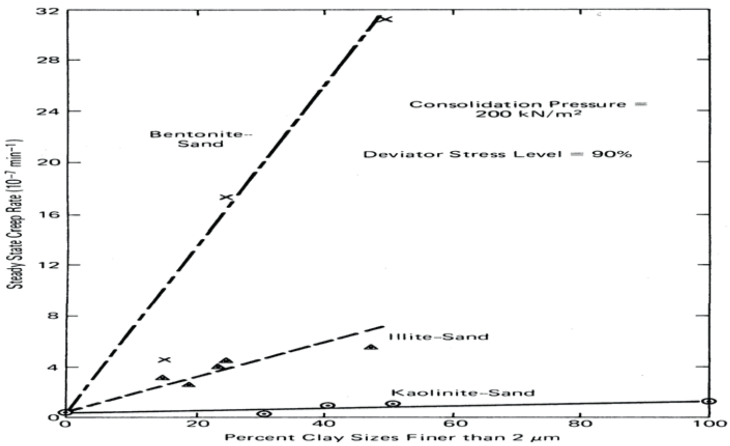

Figure 33. Effect of amount and type of clay on steady state creep rate (Mitchell and Soga, 2005).

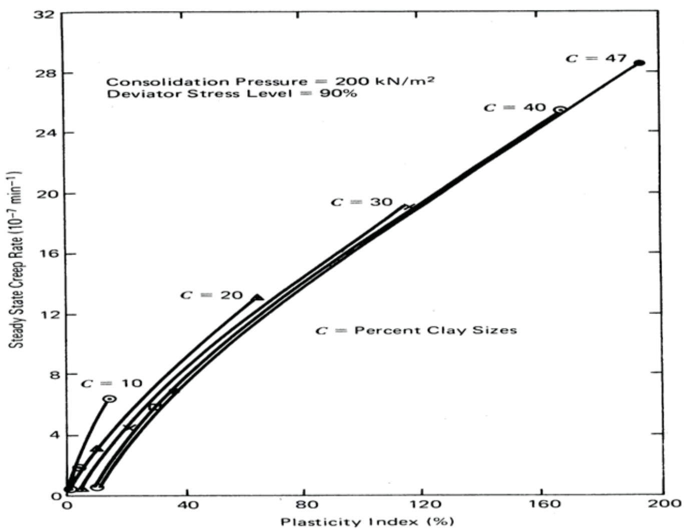

Figure 34. Relationship between clay content, plasticity index, and creep rate (Mitchell and Soga, 2005).

- With increase in temperature, the pore pressure of soil increases and the strength reduces. Hence, creep rate increases with higher temperatures (Figure 35).

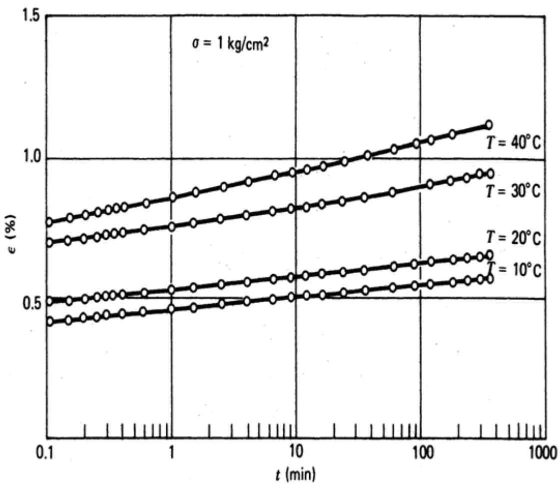

Figure 35. Creep curves for Osaka clay tested at different temperatures- undrained triaxial compression (Murayama, 1969).

- Undrained stress-strain-pore pressure response of normally consolidated natural Olga clay (Lefebvre and LeBouef, 1987) is shown in Figure 36. It describes that the deviator stress increases with increase in strain rate. The pore pressure was higher at slower strain rates because more creep can occur at slow loading.

- The most active clays usually show the greatest time-dependent response (smectite > illite > kaolinite). This is because the smaller the particle size, the greater is the specific surface, and the greater is the water adsorption (Mitchell and Soga, 2005).

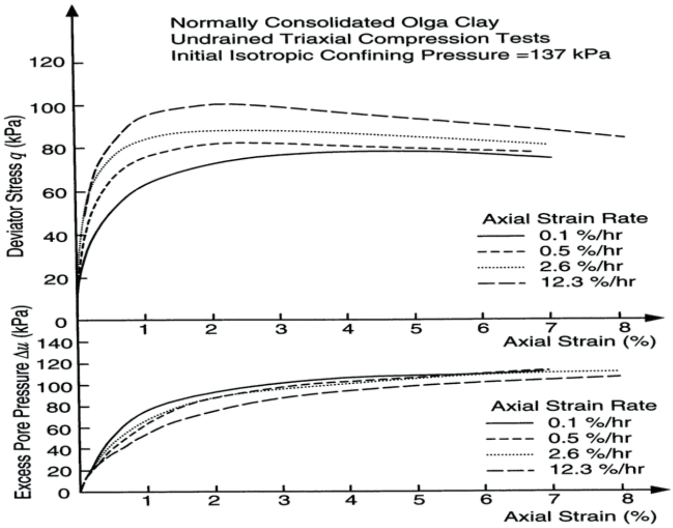

Figure 36. Stress-strain and pore pressure-strain curves for normally consolidated Olga clay (Lefebvre and LeBouef, 1987).

9.2 Tests for time-dependent response of a material

The time-dependent response of a material can be measured with the three standard tests i.e. the creep test, the relaxation test, and the constant strain rate test (Ottosen and Ristinmaa, 2005).

In the creep test, the stress σ_0 is applied immediately and then kept constant (Figure 37a) and as a result the strain may vary from immediate strain ε_0 to creep strain ε^{cr} (Figure 37b). In the relaxation test, the strain ε_0 is applied immediately and then kept constant (Figure 38a) and as a result the stress decreases slowly with time (Figure 38b).

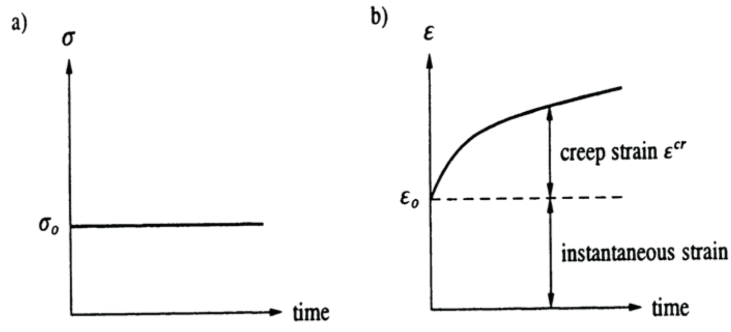

Figure 37. Creep test. (a) Stress history, (b) Strain history (Ottosen and Ristinmaa, 2005).

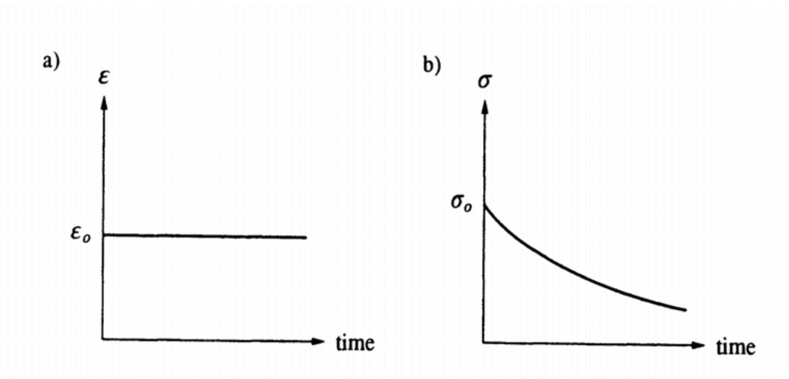

Figure 38. Relaxation tests. (a) Strain history, (b) Stress history (Ottosen and Ristinmaa, 2005).

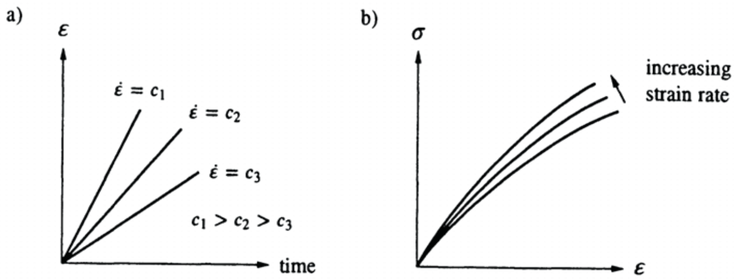

Figure 39. Constant strain-rate test. (a) Strain history for three tests, (b) Corresponding stress-strain responses (Ottosen and Ristinmaa, 2005).

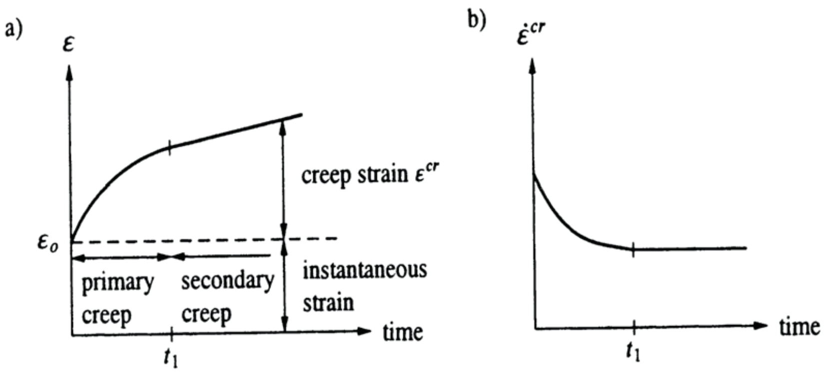

Figure 40. Creep test for a small stress. (a) Strain history, (b) Creep strain rate $\dot{\varepsilon}^{cr}$ (Ottosen and Ristinmaa, 2005).

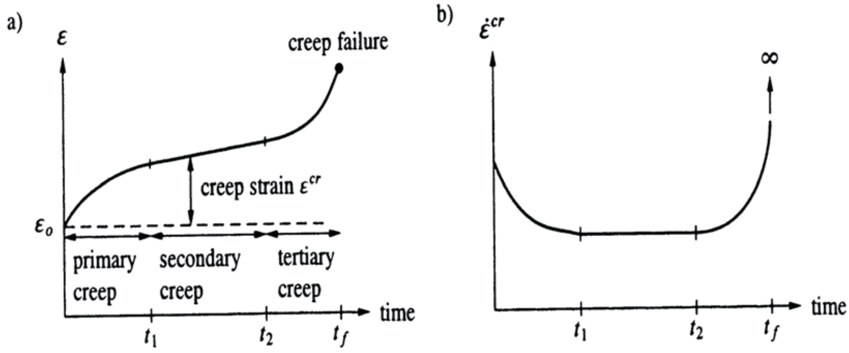

Figure 41. Creep test for a large stress. (a) Strain history, (b) Creep strain rate $\dot{\varepsilon}^{cr}$ (Ottosen and Ristinmaa, 2005).

In the constant strain-rate test, the total strain rate $\dot{\varepsilon} = d\varepsilon/dt =$ constant is applied to the material and the stress response is measured. Figure 39 depicts that material becomes stiffer with increase in strain rate.

The creep test for small-applied stress is shown in Figure 40. The primary creep (transient creep) occurs up to time t_1, and the secondary creep (stationary creep) occurs after time t_1. Figure 40(b) shows that creep strain rate $\dot{\varepsilon}^{cr} = d\varepsilon^{cr}/dt$ decreases during primary creep and is constant during secondary creep. Figure 41 demonstrates the creep response of a material when the applied stress is large. The tertiary creep occurs after time t_2, in this portion the creep strain rate $\dot{\varepsilon}^{cr}$ increases and creep failure occurs at time t_f (Figure 41b).

9.3 Creep in Sands

Creep occurs in all soils, but the rate of creep depends on the soil type (Lade and Liu, 1998). At the same stress state, creep in sands is less than in clays (Murayama *et al.*, 1984; Lade *et al.*, 1997). At high stresses, the particles of sand can crush and increase the amount of creep (Yamamuro and Lade 1996). Loose sands and sands consisting of weak particles generally show more creep than dense sands or sands with strong particles. Creep in sands occurs due to slippage and fracture of particles (Lade and Liu, 1998). Loose sands with weak grains show more slippage and crushing of particles (Bjerrum, 1973; Bopp and Lade, 1997).

The properties of granular materials such as stress-strain, compressibility, permeability, and pore pressures depend on the integrity of the particles (Lade and Yamamuro, 1996). The crushing of the particles may cause changes in the above-mentioned properties.

In high earth dams, the loads due to the embankments can break the particles of the underlying soils. Hence, the larger particles break into smaller particles. The increase of fine particles can cause low permeability, more compressibility, and increase in pore water pressure.

More crushing of the particles can occur at high stresses and strains. The particle breakage is a function of time and can occur at constant stress (Lade and Yamamuro, 1996). Generally, large and angular particles can crush more easily. More particle crushing occurs in triaxial tests than in one-dimensional compression tests at the same mean stress (Daoudadji and Hicher, 2009).

The large primary settlements of dams and embankments are usually followed by significant creep settlements in later years. In natural slopes, slides may occur due to continuous displacement and strength reduction caused by creep (Vermeer and Neher, 1999).

Very little data about creep behaviour of tailings is found in the literature. The coefficient of secondary compression of tailings C_α and its classification by Mesri (1973) is presented in Table 11.

Table 11. Coefficient of secondary compression of tailings.

Coefficient of secondary compression C_α	Location	Classification of secondary compressibility (Mesri, 1973)	Source
0.005	Gold tailings South Africa	medium	Chang, 2009
0.0205	Blue lagoon or Slimes pond (Bulgaria)	very high	Germanov, 2003
0.0128	Oxidative Pond (Bulgaria)	high	Germanov, 2003
0.0016	Tailings dam (Bulgaria)	low	Germanov, 2003

As far as long time stability of tailings dams is concerned, there are fair chances of crushing of tailings (angular particles). This crushing of angular particles may result in fine particles and the presence of fine particles may enhance the creep rate.

9.4 Creep in Clays

Following four case studies have been selected regarding the creep behaviour of clay. The case studies are presented below.

9.4.1 Bratteröd test site

Claesson (2003), observed settlements from five test sites in Sweden (Änggården, Bratteröd, Hanhals, Lundby Strand and Lilla Mellösa). The one-dimensional consolidation model presented by Alen (1998) was used for numerical analysis. This model takes into consideration the creep effects.

At Bratteröd test site, the deposit of natural clay is about 35 m deep with thin layers of sandy silt and/or shell deposits. The ground water level was about 1.0 m below the ground surface. The settlement vs. time response of the test site is shown in Figure 42.

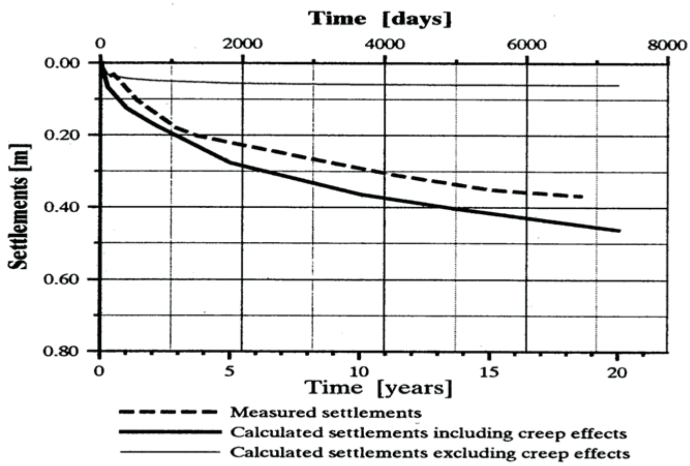

Figure 42. Calculated and measured settlements for section 0/920 at the Bratteröd (Claesson, 2003).

The calculated settlement (excluding creep effects) was 0.06 m. The calculated settlement of 0.06 m makes only 15% of the measured settlement after 18 years. The Alen model overestimated the predicted settlement (0.45 m) as compared with the measured settlement of 0.38 m (Claesson, 2003).

9.4.2 Skå Edeby test embankment

Skå Edeby site is located at 25 km west of Stockholm and was built in 1961. The embankment has a height of 1.5 m, crest width 4 m, and side slopes of 1:1.5. The soil under the embankment consists of soft clay with a thickness of 15 m on top of till or rock. The numerical analysis of this site was performed using both the soft soil model and the soft soil creep model (Neher *et al.*, 2001).

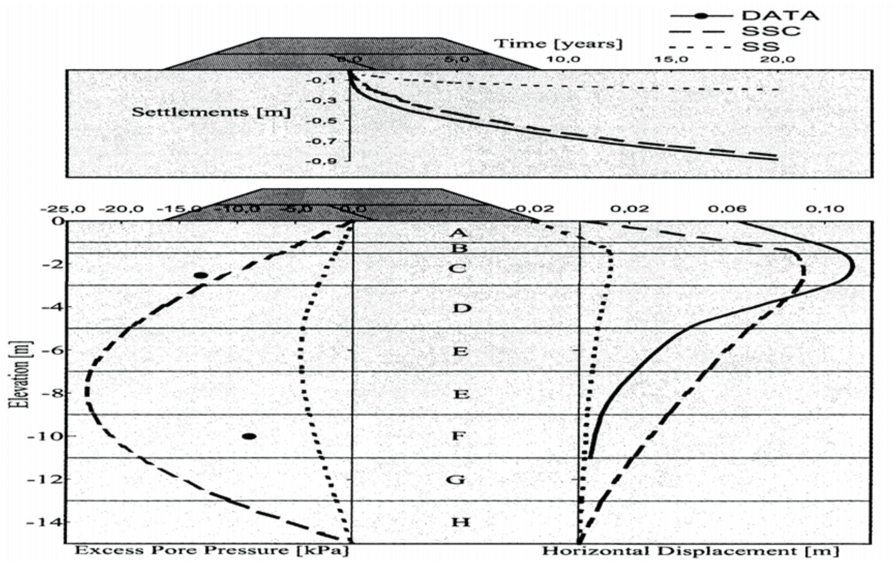

Figure 43. Time- Settlement-Curve; Pore-pressure distribution after 10 years and horizontal displacements after 10 years (Neher *et al.*, 2001).

The soft soil clay layer was divided into 9 sub-layers with different compressibility parameters and overconsolidation ratios (OCR). The soft clay was almost normally consolidated (OCR≈1) except the upper 2 m clay layer that had a high OCR value. The results show that the settlements, pore pressures, and horizontal displacements are highly underestimated by the Soft Soil (SS) model, whereas the results of the Soft Soil Creep (SSC) model are in agreement with field measurements (Figure 43).

9.4.3 Leaning tower of Pisa

The leaning tower of Pisa is a classic example of differential settlement. The tower is 58.4 m high with a foundation diameter of 19.6 m. The construction of the tower started in 1173 and by the end of 1178 when two-thirds of the tower was completed, it tilted. Over the past 800 years, the south side has tilted more than the north side, giving about a 2 m differential settlement and a 5.5^0 inclination. The cross-section and foundation profile are shown in Figures 44 and 45 respectively.

Mitchell and Soga (1995) conducted triaxial creep tests on the Pisa clay. The samples were taken from four different depths of 6 m, 10 m, 14 m and 19 m corresponding to layers A_1, B_1, B_2, and B_3 respectively as shown in Figure 46. The specimens were 3.4 cm in diameter and 8.9 cm in height. For each step of the test, a constant load was applied instantly and then was allowed to last for 7 days. Drainage was allowed at the top and bottom of the specimen. A backpressure of 98 kpa was applied to maintain saturation. The axial strain vs. time response is shown in Figure 47.

The results indicate that the sample taken from 10 m depth showed very large axial strain (up to 16%) due to its highly plastic nature and relatively large tower loads. The sample taken at 6 m depth also showed large deformations (up to 9%) due to very large tower load increments. The tests show that creep occurs in the clayey silt layer A_1' and the highly plastic clay layer B_1 (Figure 46).

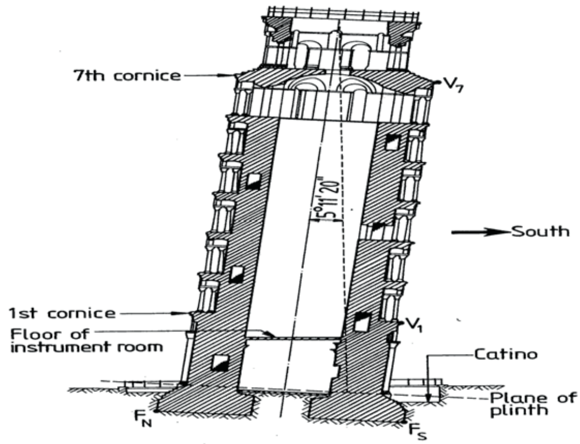

Figure 44. Cross-section through tower (Bai, 1998).

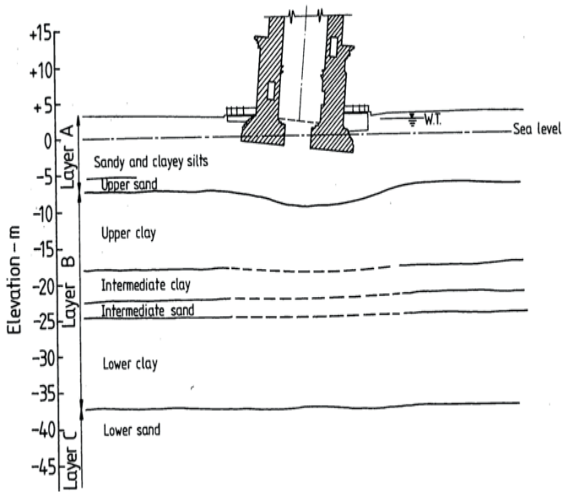

Figure 45. Foundation soil profile of tower (Bai, 1998).

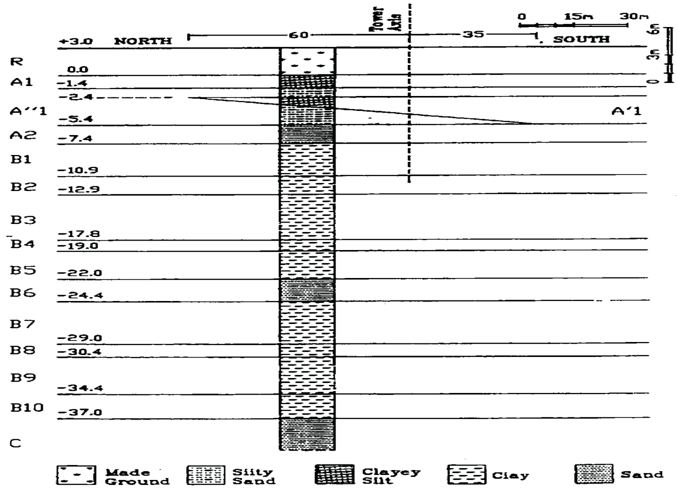

Figure 46. The assumed initial soil profile at Pisa tower (Calabresi *et al*., 1992).

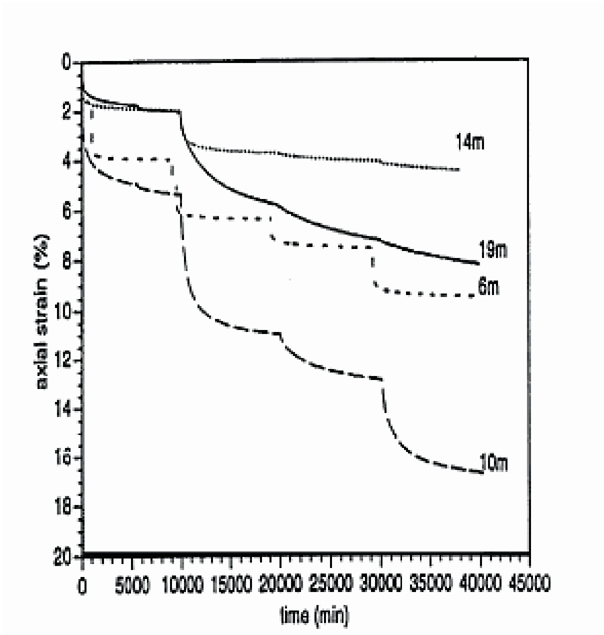

Figure 47. Axial strain vs. time relationship (Mitchell and Soga, 1995).

Mitchell and Soga (1995) performed 3-dimensional and plane strain finite element analyses using elastic and elasto-plastic models. The predicted final rotation in year 1990 was 3.5 degrees and the observed one was 5.5 degrees. The final maximum settlement in 1990 was 1.6 m that can be compared to a measured settlement of 2.8 m. It was concluded that the difference in calculated and observed values was due to the time independent behaviour of the Cam Clay model used (no consideration for creep) and the small strain formulation in finite element software utilized.

Bai (1998) performed plane strain visco-plastic analysis of foundation of Pisa tower using a double yield surface constitutive model for the stress-strain-time behaviour of cohesive soils (Borja *et al.*, 1990). It was concluded (Bai, 1998) that:

- A total settlement of 3.3 m and a tilting angle of 3.4 degrees were obtained.
- The total vertical displacements of the footing under both non-creep and creep cases were compared as shown in Figure 48. An additional settlement of 1 m and a tilting of 1.7 degrees were obtained in the computation when creep was taken into consideration.

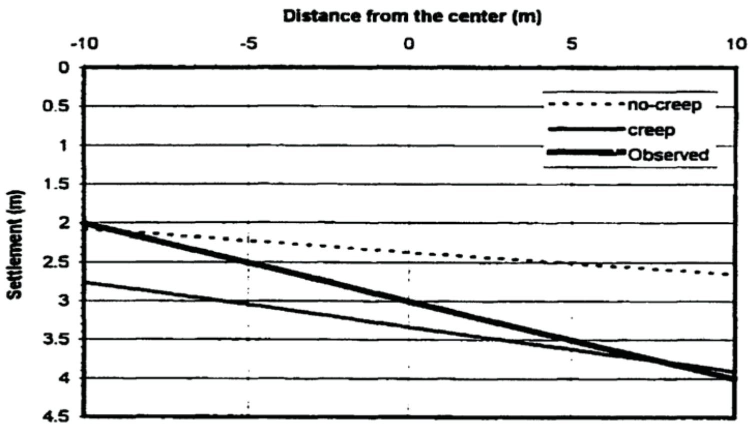

Figure 48. Comparison of the final settlement of the footing (Bai, 1998).

9.4.4 Road embankment construction with the Soft Soil Creep model

This is a solved example taken from the PLAXIS manual (Brinkgreve *et al.*, 2008). Figure 49 shows the cross section of the road embankment. In the example, the clay layer is modelled with the Soft Soil Creep model (SSC), while peat and sand layers are modelled with the Mohr-Coulomb (MC) model. When using the SSC model for clay layer instead of the MC model, the safety factor becomes lower during construction of the embankment. Figure 50 shows the results of the safety factor analysis after the construction of the first layer of the embankment (after 5 days) with both MC model (safety factor = 1.11) and SSC model (safety factor = 1.01). The SSC model shows lower factor of safety due to the irreversible volumetric creep. At this low safety factor, the soil has reached its failure state and the calculation of other phases is not possible.

Figure 51 shows a comparison of the vertical displacements at point *A* computed with both the SSC model and the MC model. The horizontal displacements at point *B* predicted by the SSC model and the MC model are shown in Figure 52. As compared to the MC model, the SSC model shows little difference in the vertical displacements, but much larger differences in the horizontal displacements (because the material is close to failure due to creep effect).

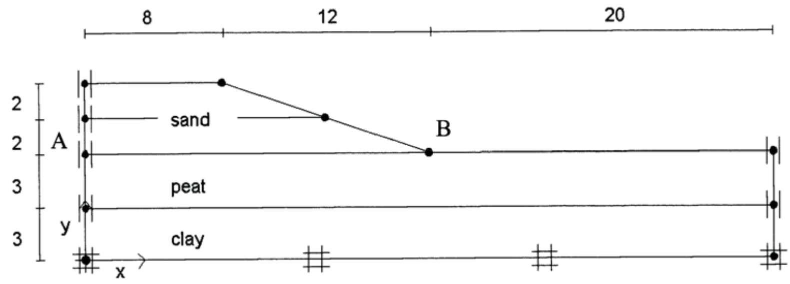

Figure 49. Geometry model of road embankment project (Brinkgreve *et al.*, 2008).

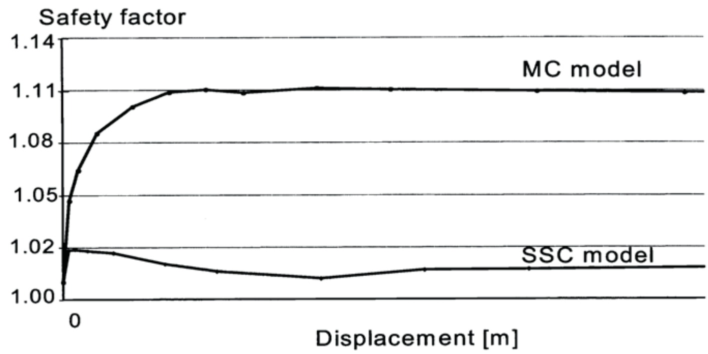

Figure 50. Safety factor analysis using MC model and SSC model (Brinkgreve *et al.*, 2008).

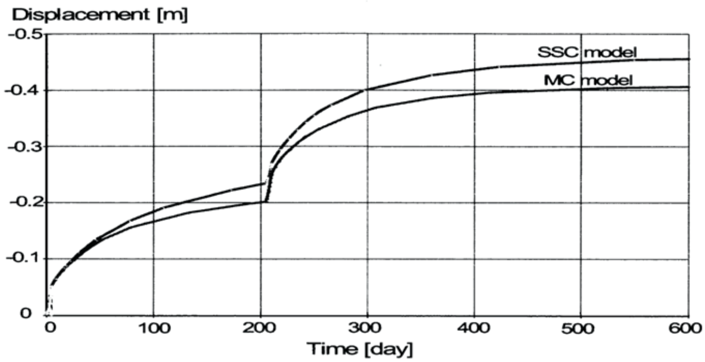

Figure 51. SSC model vs. MC model-vertical displacements at point *A* (Brinkgreve *et al.*, 2008).

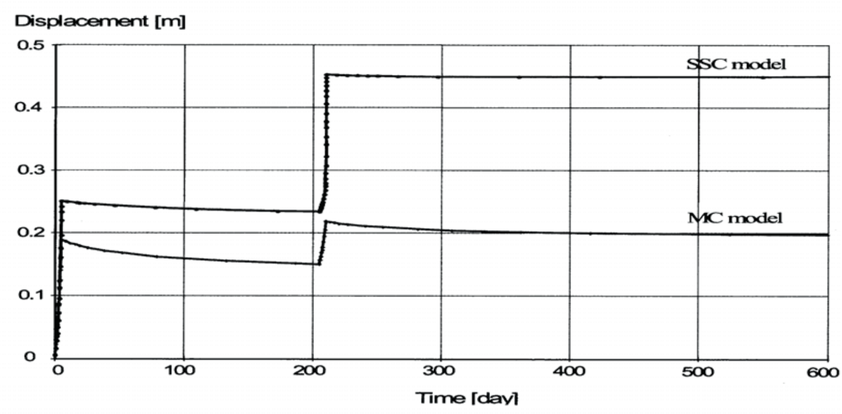

Figure 52. SSC model vs. MC model-horizontal displacements at point *B* (Brinkgreve *et al.*, 2008).

The MC model does not show reduction of mean effective stress during undrained loading and leads to over prediction of the stability when using effective strength parameters. However, the SSC model considers the effect of reduced mean effective stress during undrained loading. The SSC model gives more realistic prediction of time-dependent behaviour of soft-soil (Brinkgreve *et al.*, 2008).

10. CONSTITUTIVE SOIL MODELS

Soils are not linearly elastic and perfectly plastic for the entire range of loading, rather soils are complex materials showing non-linear, anisotropic and time-dependent behaviour when subjected to stresses. Brinkgreve (2005) describes the following features of soil behaviour:

(a) The dissipation of excess pore water pressure due to consolidation causes change in effective stress and deformation.
(b) Soil stiffness is not constant, but it depends on various factors (such as stress level, stress path, strain level, time, density, permeability, over-consolidation, anisotropy etc).
(c) Most soils have very small elastic region and show irreversible deformation from start of loading.
(d) Shear strength of the soil depends upon confining effective stress level, loading speed, time, density, over-consolidation, anisotropy etc.
(e) In soft soils, when excess pore water pressure dissipates, the settlement may continue with time due to creep.

Presently a large number of constitutive models capturing different aspects of soil behaviour are available in the literature. Only a few constitutive models are implemented in commonly used commercial software such as PLAXIS, Geostudio etc. Hence, the geotechnical professionals are aware of only those constitutive models that are implemented in such commercial programs. Therefore, the constitutive soil models implemented in the finite element code PLAXIS 2D are discussed here.

10.1 Mohr-Coulomb model

The Mohr-Coulomb (MC) model is an elastic-perfectly plastic model, containing five model parameters, i.e. Young's modulus *E and* Poisson's ratio v for soil elasticity; friction angle ϕ and cohesion c for soil plasticity and the dilatancy angle ψ. Although the increase of stiffness with depth can be taken into account, this model does not include stress-dependency, stress-path dependency or anisotropic stiffness. As far as its strength behaviour is concerned, this model is suitable to analyse the stability of dams, slopes, and embankments. However, the model does not show softening behaviour after peak strength. The soft soils, like normally consolidated clays, generally show a decreasing mean effective stress during shearing, whereas the Mohr-Coulomb model gives a constant mean effective stress. Hence, the MC model over predicts shear strength (Brinkgreve, 2005).

10.2 Modified Cam Clay model

The Modified Cam Clay (MCC) Model uses a logarithmic relationship between the mean effective stress p' and the void ratio *e*. Hence, the model involves a linear stress-dependency of the stiffness, which is more realistic for normally consolidated clays. For highly overconsolidated soils, the MCC model predicts an unrealistic elastic range which leads to an unrealistic high peak strength, followed by softening behaviour until the critical state is reached. Hence, the MCC model is not suitable for highly over-consolidated soils. The MCC model is suitable for soft soils such as normally consolidated clays (Brinkgreve, 2005).

Further shortcomings of the MCC model (Hau, 2003) are:

- It assumes the soil isotropic, whereas natural soils are anisotropic due to the mode of deposition.
- It overestimates the failure stresses on the dry side (i.e. states to the left of the critical state line). It predicts peak strength in undrained heavily overconsolidated clay, which is not usually observed in experiments.
- It cannot successfully predict the behaviour of sand, because the sand does not closely follow the associated flow rule.
- The MCC model, on primary loading produces large plastic strains, but on subsequent unloading-reloading cycles within the yield surface, only produces purely elastic strains.

10.3 Hardening Soil model

The hardening soil model (Schanz *et al.*, 1998) is a true second order model for soils in general (soft as well as hard soils), for most types of applications. The model, in an undrained loading shows a reduction in mean effective stress for soft soils and increase in mean effective stress for hard soils respectively. This model can accurately predict displacement and failure for general type of soils in various geotechnical applications. The model does not include anisotropy and time dependent behaviour (Brinkgreve, 2005).

10.4 Hardening Soil model with small strain stiffness

The Hardening Soil model with small strain stiffness (HSsmall) is a modification of the Hardening Soil model. At low strain levels, most soils show a higher stiffness than at engineering strain levels. The stiffness varies non-linearly with strain. This behaviour is captured by HSsmall model (Brinkgreve *et al.*, 2008).

11.5 Soft Soil model

The Soft Soil (SS) model is a Cam-Clay type of model for predicting the behaviour of normally consolidated soils (clays, clayey silts and peat). The hardening soil model supersedes the SS model. The SS model does not over predict the shear strength for overconsolidated states of stress. The SS model works well in primary loading conditions, such as embankment or foundation construction. The model has no advantages over the Mohr-Coulomb model in unloading situations, such as excavations or tunnel construction (Brinkgreve, 2005).

10.6 Soft Soil Creep model

The Soft Soil Creep (SSC) model is suitable for prediction of creep related settlement of embankments and foundations in soft soils (normally consolidated clays, silts and peat). The SSC model over predicts the range of elastic behaviour in unloading situations such as excavations and tunnel construction. In these situations, the SSC model hardly supersedes the Mohr-Coulomb model (Brinkgreve *et al.*, 2008).

11. CONCLUSIONS

Tailings show complex material behaviour with respect to high compressibility, structural heterogeneity, anisotropy, permeability, consolidation and void ratio. The factors such as internal and external erosion, seepage, and natural events (rainfalls, floods, and earthquakes) have strong influence on stability of tailings dams and impoundments. For long time stability (more than 1000 years) of tailings dams and impoundments, the convenient assumption is that the phreatic surface control measures (cores, drains, and filters) and seepage control measures (cut-off trenches, slurry walls, and grout curtains) will not function properly. Hence, excessive pore water pressures will build up in the dam body. Moreover, it is assumed that in the long time, heavy rainfalls, floods, and severe earthquakes may occur. All these conditions necessitate for comprehensive understanding of the mechanical behaviour of tailings. Reliable predictions about long time stability of tailings dams and impoundments can be made with proper understanding of tailings material behaviour with regard to anisotropy, cyclic loading, particle crushing, and creep effects.

The constitutive model plays a key role in finite element analyses. The selection of a constitutive model for the numerical analyses of tailings dams and impoundments requires an in-depth understanding of the features of tailings material (anisotropy, cyclic loading, particle crushing and creep) and understanding of the assumptions and limitations made in the constitutive model. Hence, the validity of a constitutive model for tailings material should be confirmed by comparing the model predictions with laboratory tests and field measurements. Reliable numerical modelling of tailings dams and impoundments will also help in formulating the criteria for assessment of the long time stability of the tailings dams.

REFERENCES

Alen, C. (1998). *On probability in geotechnics. Volume, 1, 2. PhD Thesis.* Department of Geotechnical Engineering, Chalmers University of Technology, Göteborg, Sweden.

Barnekow, U., Haase, M., and Wels, C. (1999). Geomechanical fine tailings characterization and 1-D consolidation modelling of slimes zones at WISMUT tailings impoundments. *Soft tailings stablization workshop; part-II: Practice and experiences*; Chemnitz, Germany; June 23-25, 1999.

Bai, J. (1998). *Creep analysis of the leaning tower of Pisa. Doctoral Thesis*. Department of Civil and Environmental Engineering, University of Alberta, Canada.

Bishop, A., and Bjerrum, L. (1960). The relevance of the triaxial test to the solution of stability problems. *Research conference on shear strength of cohesive soils,* ASCE, University of Colorado, 437-501.

Bishop, A.W. (1966). The strength of soils and engineering materials. *Géotechnique,* **16**(2), 89-130.

Bishop, A. (1973). The stability of tips and spoil heaps. *Quart. J. of Eng. Geology,* Vol.6, 335-376.

Blight, G., and Steffen, D. (1979). Geotechnics of gold mine waste disposal. *Current geotechnical practice in mine waste disposal.* ASCE, 1-52.

Bjelkevik, A. (2005). *Water cover closure design for tailings dams*. *State of the art report.* Department of Civil and Environmental Engineering, Luleå University of Technology, Luleå, Sweden.

Bjelkevik, A., and Knutsson, S. (2005). Swedish Tailings–Comparison of Mechanical properties between Tailings and natural Geological Materials. *In proceedings of Securing the Future, International Conference on Mining and the environment, metals and energy recovery.* Skellefteå, Sweden. June 27-July 1, 2005.

Bjerrum, L. (1973). Problems of soil mechanics and construction on soft clays and structurally unstable soils. *In proceedings of the 8th International Conference of Soil Mechanics and Foundation Engineering.,* **3**, 111-159.

Bopp, P.A., and Lade, P.V. (1997). Effects of initial density on soil instability at high pressures. *J. Geotech. and Geoenviron. Engrg.*, **123**(7), 671-677

Borja, R.I., Hsieh, H.S., and Kavazanjian, E.J. (1990). Double-yield-surface model-II: Implementation and verification. *Journal of Geotechnical Engineering Division.* **116** (GT9), 1402-1421.

Brinkgreve, R.B.J., Broere, W., and Waterman, D. (2008). PLAXIS 2D - version 9.0 ISBN 978-90-76016-06-1.

Brinkgreve, R.B.J. (2005). Selection of soil models and parameters for geotechnical engineering application. *In proceedings of Geo-Frontiers Conference*, ASCE, Austin, TX, January 24-26, 2005.

Budhu, M. (2007). *Soil Mechanics and Foundations.* 2nd edition. John Wiley and Sons, Inc. ISBN 0-471-43117-6.

Calabresi, G., Rampello, S., and Callisto. L. (1992). Geotechnical characterization of the tower's subsoil within the framework of the critical state theory. Universita di Roma, Dipartimento di Ingegneria struttural.

Casagrande, A., and Carrillo, N. (1944). Shear failure of anisotropic materials, in contribution to Soil Mechanics 1941-1953, Boston society of civil engineers, Boston, Mass.

Chang, H.N. 2009). *The effect of fabric on the behaviour of gold tailings. Doctoral Thesis.* Department of Civil Engineering, Built Environment and Information Technology, University of Pretoria.

Chapuis, R.P. (2004). Predicting the saturated hydraulic conductivity of sand and gravel using effective diameter and void ratio. *Can. Geotech. J.*, *41* (5), 787-795.

Claesson, P. (2003). *Long-term settlements in soft clays. Doctoral Thesis.* Department of Geotechnical Enginerring, Chalmers University of Technology, Göteborg, Sweden.

Craig, R.F. (2004). *Craig's Soil Mechanics.* 7th edition. Spon Press, Taylor and Francis Group, London and New York. ISBN 0-415-32702-4.

Daouadji, A., and Hicher, P.Y. (2009). An enhanced constitutive model for crushable granular materials. *Int. J. Numer. Anal. Meth. Geomech.*, **34**(6), 555–580.

Das, B.M. (1998). *Principles of Geotechnical Engineering.* 4th edition. PWS publishing company, 20 Park Plaza, Boston. ISBN 0-534-95179-1.

Das, B.M. (1997). *Advanced Soil Mechanics.* 2nd edition. Taylor and Francis Publishers. ISBN 1-56032-561-5.

Engels, J., Schönhardt, M., Witt, K.J., Benkovics, I., Berta, Z., Csövári, M., Georgescu, D.P., Radulescu, C.A., Zlagnean, M., Bőhm, J., Debreczeni, Á., Gombkötő, I., Koffa, E., Mylona, E., Paspaliaris, I., and Xenidis, A. (2004). Tailings management facilities - Intervention actions for risk reduction. A European research and technological development project. http://www.tailsafe.bam.de/pdf-documents/TAILSAFE_Intervention_Actions.pdf (Dec. 12, 2009).

Fell, R., MacGregor, P., Stapledon, D., and Bell, G. (2005). *Geotechnical Engineering of Dams.* Balkema, Leiden, ISBN 041536440x.

Gens, A., and Alonso, E.E. (2006). Aznalcóllar dam failure. Part 2: Stability conditions and failure mechanism. *Géotechnique*, **56**(3), 185-201.

Germanov, T. (2003). Geotechnical properties of industrial waste deposits in Bulgaria. *In proceedings of 13th International conference on Soil Mechanics and Geotechnical Engineeering ECSMGE, Prague*, ISBN 80-86769-00-3 (Vol. 1). http://www.uacg.bg/UACEG_site/acadstaff/userfiles/publ_bg_312_germanov_13ECSMGE-2003.pdf (Dec. 22, 2009).

Gibsson, R.E., England, G.L., and Hussey, M.J.L. (1967). The theory of one-dimensional consolidation of saturated clays-I. Finite non-linear consolidation of thin homogenous layers. *Géotechnique*, **17**(2), 261-273.

Gibsson, R.E., Schiffman, RL., and Cargill, K.W. (1981). The theory of one-dimensional consolidation of saturated clays. II. Finite non-linear consolidation of thick homogenous layers. *Can. Geoteh. J.,* **18**(2), 280-293.

Graham, J., and Houlsby, G.T. (1983). Anisotropic elasticity of natural clay. *Géotechnique,* **33**(2), 165-180.

Hau, K.W. (2003). *Application of a three-surface kinematic hardening model to the repeated loading of thinly surfaced pavements. PhD Thesis.* Department of Civil Engineering, University of Nottingham, UK.

Hight, D. W. (1998). Soil characterization: The importance of structure and anisotropy. *38th Rankine Lecture*, British Geotechnical Society, London.

ICOLD. (1996). A guide to tailings dams and impoundments-design, construction, use and rehabilitation. *Bulletin no*. 106.

Ishihara, K., Troncoso J., Kawase Y., and Takahashi, Y. (1980). Cyclic Strength Characteristics of Tailings Materials. *Soils and Foundations*, *Japanese Society of Soil Mechanics and Foundation Engineering*, **20** (4), 127-142.

Jewell, J. R. (1998). An Introduction to Tailings. *Case Studies on Tailings Management.* United Nations publications. ISBN 1-895720-29-x.

Johnson, S. (1975). Analysis and design relating to embankments. Analysis and design in geotechnical engineering, ASCE, **2** , 1-48.

Kealy, C., and Soderberg, R. (1969). Design of dams for mill tailings. *U.S Bureau of mines,* IC 8410.

Kulhawy, F.H., and Mayne, P.W. (1990). *Manual on Estimating Soil Properties for Foundation Design.* Final Report, Project 1493-6, EL-6800, Electric Power Research Institute, Palo Alto, CA.

Ladd, C.C. (1991). Stability evaluation during staged construction. *Journal of geotechnical engineering,* **117**(4), 540-615.

Lade, P.V., Yamamuro, J.A., and Bopp, P.A. (1997). Influence of time effects on instability of granular materials, *Computers and Geotechnics,* **20**(3/ 4), 179–193.

Lade, P.V., and Liu, C.T. (1998). Experimental study of drained creep behaviour of sand. *Journal of Engineering Mechanics.,* **124**(8), 912-920.

Lade P.V., and Yamamuro, J.A. (1996). Significance of particle crushing in granualr materials. *Journal of geotechnical engineering,* **122** (4), 309-316.

Lefebvre, G., and LeBouef, D. (1987). Rate effects and cyclic loading of sensitive clays. *Journal of Geotechnical Engineering*, ASCE, **113**(5), 467–489.

Love, A.E.H. (1927). *The Mathematical Theory of Elasticity.* Cambridge University Press, Cambridge.

Mesri, G. (1973). Coefficient of secondary compression. *J. Soil Mech. Found. Div.*, ASCE, Vol. 99, No. SM1, 123-137.

Mitchell, J.K., and Soga, K. (2005). *Fundamentals of Soil Behavior.* 3rd edition. John wiley and sons, inc. ISBN 0471463027.

Mitchell, J.K., and Soga, K. (1995). Numerical and experimental studies related to the performance and stablization of the tower of Pisa. *Report to the Consorzio Progetto Torre di Pisa.*

Mittal, H., and Morgenstern, N. (1975). Parameters for the design of tailings dams. *Can. Geotech. J.,* **13**, 277-293.

Mittal, H., and Morgenstern, N. (1976). Seepage control in tailings dams. *Can. Geotech. J.*, **12**, 235-261.

Murthy, V.N.S. (2003). *Geotechnical Engineering: Principles and Practices of Soil Mechanics and Foundation Engineering.* Marcle Dekker, inc. ISBN 0-8247-0873-3.

Murayama, S., and Shibata, T. (1958). On the rheological characteristics of clays, Part I, *Bulletin No. 26,* Disaster Prevention Research Institute, Kyoto, Japan.

Murayama, S. (1969). Effect of temperature on elasticity of clays, *Highway Research Board Special Report* 103, 194–202.

Murayama, S., Michihiro, K., and Sakagami, T. (1984). Creep characteristics of sands. *Soils and Foundations,* **24**(2), 1–15.

Mylona, E., Xenidis, A., and Paspaliarris, I. (2004). Implementation and improvement of closure and restoration plans for disused tailings facilities. A European research and technological development project. (http://www.tailsafe.bam.de/pdf-documents/TAILSAFE_Closure_and_Remediation.pdf) (Dec. 10, 2009).

Neher, H.P., Wehnert, M., and Bonnier, P.G. (2001). An evaluation of soft soil models based on trial embankments. *In Proceedings of the 10th International Conference on Computer Methods and Advances in Geomechanics (IACMAG), Tuscon*: 373-378. Rotterdam, A.A. Balkema.

Olalla, C., and Cuellar, V. (2001). Failure mechanism of the Aznalcóllar dam, Sevile, Spain. *Géotechnique,* **51**(5), 399-406.

Ottosen, N., and Ristinmaa., M. (2005). *The Mechanics of Constitutive Modeling*. 1st edition. Elsevier Ltd. ISBN 0-008-044606-X.

Pousette, K. (2007). Laboratorieförsök på anrikningssand från Aitik. Ödometerförsök, skjuvförsök, triaxialförsök. Internal working document, Luleå University of Technology, Luleå, Sweden.

Priscu, C. (1999). *Behaviour of mine tailings dams under high tailings deposition rates. Doctoral Thesis*. Department of Mining and Metallurgical Engineering, McGill University, Montreal, Canada.

Psarropoulos, P.N., and Tsompanakis, Y. (2008). Stability of tailings dams under static and seismic loading. *Can. Geotech. J.,* **45** (5), 663-675.

Rico, M., Benito, G., Salgueiro, A.R., Herrero, A.D., and Pereira, H.G. (2008). Reported tailings dam failures. A review of the European incidents in the worldwide context. *Journal of hazardous materials.* **152**(2), 846-852.

Robertson, A.M., and Skermer, N.A. (1988). Design considerations for the long-term stability of mine wastes. http://www.robertsongeoconsultants.com/publications/long_term.pdf (Dec. 20, 2009).

Rumer, R.R., and Mitchell, J.K. (1996). Assessment of barrier containment technologies. *Product of the international containment technology workshop*, Baltimore, Maryland, August 29-31.

Seah, T.H. (1990). *Ansitropy of resedimented Boston Blue Clay. Doctor of Science Thesis*. Department of Civil Engineering, Massachusetts Institute of Technology (MIT), USA.

Seed, H. (1979). Soil liquefaction and cyclic mobility evaluation for level ground during earthquakes. *Journ. Geotech. Eng. Div.,* **105** (GT2), 201-255.

Seneviratne, N.H., Fahey, M., Newson, T.A., and Fujiyasu, Y. (1996). Numerical modelling of consolidation and evaporation of slurried mine tailings. *International journal for numerical and analytical methods in geomechanics.*, **20**(9), 647-671.

Shanz, T., Vermeer, P.A., and Bonnier, P.G. (1998). The hardening soil model: formulation and verification. *In proceedings of the International symposium Beyond 2000 in computational Geotechnics -10 years of PLAXIS International.* Balkema, Amsterdam, ISBN 905809040x.

Singh, B., and Varshney, R.S. (1995). *Engineering for Embankment Dams.* A.A. Balkema/Rotterdam. ISBN 905410 2799.

Soga, K., and Mitchell, J. K. (1996). Rate-dependent deformation of structured natural clays. In: T.G. Sheahan and V. N. Kaliakin (Eds.), *Measuring and Modeling Time Dependent Soil Behavior,* Geotechnical Special Publication No. 61, ASCE, New York, 243–257.

Sundblad, B. (2003). Ten years experience of a multi-layer cover for Uranium mill tailings in Ranstad Sweden. *In proceedings of Mining and the Environment III*, Sudbury, Ontario, Canada, 25-28 May 2003.

Terzaghi, K. (1925). *Erdbaumechanik auf Bodenphysikalischer Grundlage,* Deuticke, Vienna.

Vermeer, P.A., and Neher, H.P. (1999). A soft soil model that accounts for creep. *In proceedings of the International symposium Beyond 2000 in computational Geotechnics-10 years of PLAXIS International.* Balkema, Amsterdam, ISBN 905809040x.

Vick, S.G. (1990). *Planning, design, and analysis of tailings dams*. 2nd edition. BiTech Publishers Ltd, Canada. ISBN 0-921095-12-0.

Volpe, R. (1979). Physical and engineering properties of copper tailings. *Current Geotechnical practice in mine waste disposal.* ASCE, 242-260.

Wahler, W.A. (1974). Evaluation of mill tailings disposal practices and potential dam stability problems in Southwestern United States. *U.S. Bureau of mines ,* OFR50(1)-75-OFR50(5)-75.

Wheeler, S.J., Näätänen, A., Karstunen, M., and Lojander, M. (2003). An anisotropic elastoplastic model for soft clays. *Can. Geotech. J.,* **40**(2), 403-418.

Wijewickreme, D., Sanin, M.V., and Greenaway, G.R. (2005). Cyclic shear response of fine-grained mine tailings. *Can. Geotech .J.*, **42**(5), 1408-1421.

Witt, K.J., Schönhardt, M., Saarela, J., Frilander, R., Csicsak, J., Csővari, M., Várhegyi, A., Georgescu, D. P., Radulescu, C.A., Zlagnean, M., Bõhm, J., Debreczeni, A., Gombkötõ, I., Xenidis, A., Koffa, E., Kourtis, A., and Engels, J. (2004). Tailings management facilities-risks and reliability. A European research and technological development project. http://www.tailsafe.bam.de/pdf-documents/TAILSAFE_Risk_and_Reliability.pdf (Dec. 15, 2009).

Witt, K.J., Wudtke, R.B., and Engles, J. (2005). Implementation and improvement of design and authorization procedures for proposed tailings facilities. A European research and technological development project. http://www.tailsafe.bam.de/pdf-documents/TAILSAFE_Design_and_Authorisation.pdf (Dec. 20, 2009).

Wood, D.M. (1990). *Soil behaviour and critical state soil mechanics.* Cambridge University Press. ISBN 0-521-3249-4.

Yamamuro, J.A., and Lade, P.V. (1996). Drained sand behavior in axisymmetric tests at high pressures. *Journal of Geotechnical Engineering,* **122**(2), 109–119.

Paper I

NUMERICAL ANALYSIS OF STRENGTHENING BY ROCKFILL EMBANKMENTS ON AN UPSTREAM TAILINGS DAM

L. Ormann, M.A. Zardari, H. Mattsson, A. Bjelkevik, and S. Knutsson

To be submitted to Canadian Geotechnical Journal

Numerical analysis of strengthening by rockfill embankments on an upstream tailings dam

Linda Ormann, Muhammad Auchar Zardari, Hans Mattsson, Annika Bjelkevik, and Sven Knutsson

L. Ormann, and A. Bjelkevik

SWECO Infrastructure AB, Gjörwellsgatan 22, P.O. Box 34044, SE-100 26 Stockholm, Sweden

M. A. Zardari, H. Mattsson, [1] **and S. Knutsson**

Department of Civil, Environmental and Natural Resources Engineering, Luleå University of Technology, SE-971 87 Luleå, Sweden

[1]Corresponding author

e-mail: hans.mattsson@ltu.se, Tel.: +46-920-492147, Fax: +46-920-492075

Abstract

The consolidation process might be slow in an upstream tailings dam; therefore, the stability can reduce due to increase in excess pore pressures when the dam is raised. The safety of the dam can be enhanced by constructing rockfill banks on the downstream side. This paper presents a case study for strengthening of an upstream tailings dam with rockfill banks. The finite element analyses were performed for modelling the staged construction of the dam and for optimizing the volume of the rockfill banks. The dam has been raised in eleven stages; each stage consists of a raising phase and a consolidation phase. The study shows that the slope stability of the dam reduced due to increase of excess pore pressures during the raising phase. The stability of the dam was successfully improved by utilizing rockfill banks as supports on the downstream side. A technique has been presented to minimize the volume of the rockfill banks so that required stability can be accomplished at minimum cost. This paper shows that the finite element method can be a useful tool for modelling the consolidation behaviour of an upstream tailings dam and minimizing the volume of the rockfill banks that may be needed to maintain the stability of the dam during staged construction.

Key words: consolidation, optimization, rockfill banks, slope stability, staged construction, tailings dams.

Introduction

This paper presents a case study of a finite element analysis on a tailings dam. The overall objective is that the description will serve as an example of how advanced numerical software can be utilized for examining the slope stability of dams.

The tailings dam in Aitik in north of Sweden is the subject of the study. The design method for the dam is mainly upstream construction; see e.g., Vick (1990). Compared to e.g., the downstream construction method and the centreline construction method, the upstream construction method has the disadvantage that stability problems might occur if the dam is raised too fast.

As the Aitik tailings dam is raised primarily with the upstream construction method, new dikes are step by step constructed mainly on the tailings beach. A rapid rate of raise results in excess pore pressures within the tailings. These excess pore pressures will gradually dissipate during the consolidation process and effective stresses and shear strengths will increase. This implies that the stability of the tailings dam is expected to be most critical just after a new dike is constructed. The time for consolidation depends mainly on the permeability of the soils in the structure and the drainage conditions in the surroundings. If the consolidation process is not completed when a new dike is built, excess pore pressures will remain in the structure and they might successively increase for each new raising of the dam and cause a potential dangerous stability situation. However, to increase the safety of the dam, rockfill banks can be gradually constructed as support fillings at the downstream toe.

It is seen that the slope stability of this type of tailings dam is closely related to the consolidation process. The consolidation process for a tailings dam is complex and as a consequence of this it is appropriate to model the stability with advanced numerical software, based on e.g., the finite element method.

In this case study, the commercial finite element software PLAXIS (Brinkgreve et al. 2008) has been used for analyzing the stability of the Aitik dam. For eleven subsequent yearly raises in a section of the tailings dam, the consolidation process and the associated stability have been modelled with the software. It was concluded that rockfill banks were required at the downstream toe in order to obtain safety factors that were high enough for the slopes to be sufficiently stable. Thus, an optimization analysis was performed to examine when the rockfill banks were needed and where to place those to minimize the volume of rockfill required for support. The results of this study have been previously published in a report (Ormann 2008).

To the authors´ knowledge, just a few case studies of tailings dams analysed with the finite element method have been presented in the literature; e.g., Saad and Mitri (2010); Zandarín et al. (2009); Psarropoulos and Tsompanakis (2008); Gens and Alonso (2006); Priscu (1999); Priscu et al. (1999); and Desai et al. (1998). However, no optimization analysis to minimize the amount of rockfill discussed in this study, were mentioned in those references. Engineers who carry out numerical analyses need specialist knowledge in a wide range of technical subjects. Commercial software is often user friendly that makes it easy to produce results, even wrong ones. Therefore, it seems important that more case studies of this type are published to share with others the experiences from simulations as well as potential restrictions and pitfalls involved. It will probably facilitate for someone else to repeat and maybe improve the same kind of numerical analyses.

The Aitik tailings dam

Aitik is an open pit copper mine located close to Gällivare in the north of Sweden. Boliden Mineral AB is the mining company managing Aitik. The mining activities started in 1968. Today the production level is about 18 million tonnes of ore yearly, but the annual production level is planned to be doubled in the future.

Tailings are the waste products obtained during extraction of minerals from the ore. The particle size of tailings varies from medium sand to clay sized particles. In Aitik the tailings are pumped to the tailings disposal area and discharged by spigotting from the dam embankments. The tailings impoundment, shown in Fig. 1, is spread over a 13 square kilometre area and is limited by the topography and four dams A-B, C-D, E-F (including E-F2 extension), and G-H. The clarification pond is situated downstream of dam E-F.

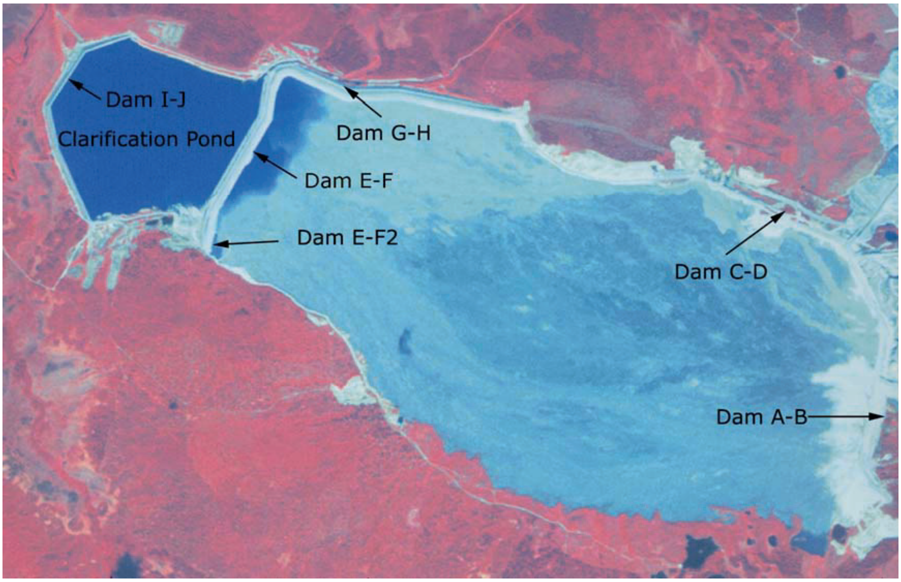

Fig. 1. Aerial view of Aitik tailings dam and impoundment (Photo courtesy of Boliden Mineral AB).

It is interesting to notice that a large failure occurred in the Aitik tailings dam in the year 2000. Dam E-F2 failed over a length of 120 meters. As a result, 2.5 million cubic meters of water was discharged into the clarification pond. When the water level in the clarification pond reached the maximum level permitted, clarified water was further discharged from the clarification pond into rivers outside Aitik. No definite conclusion what caused the failure was reached (Göransson et al. 2001).

The finite element analysis in this case study has been performed on a section of dam E-F, see Fig. 2. Dam E-F is considered as the most important dam to study since the consequences of a failure there are regarded to be more serious for humans and the surrounding environment than failures in other dams in the tailings pond. The dam E-F has been constructed by the upstream method. The different material zones are presented in Fig. 2.

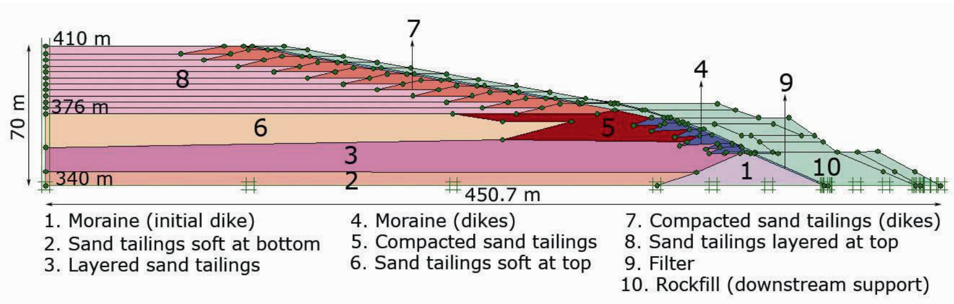

Fig. 2. Cross section of dam E-F.

The finite element model

It has been assumed that the stored tailings and the dam are raised 3 meter per year starting from the level 376 m above mean sea level. The present level of the dam in year 2010 is 385 m. The slope inclination of the dam E-F from level 376 m to 410 m is 1:6 (vertical to horizontal). Figure 2 shows the expected appearance of dam section E-F in year 2018.

The stability of the dam E-F was analysed with PLAXIS 2D, which is a finite element program for numerical analysis of geotechnical structures. As the dam is a long straight section, plane strain condition was adopted in the numerical analysis. It has been assumed that the raising of the dam (from level 376 m to 410 m) consists of eleven stages. Each stage comprises a raising phase of 10 days and a consolidation phase of 355 days. The consolidation analyses were performed for staged construction to determine strength gain due to dissipation of excess pore pressures. The stability of the dam for each raising was evaluated with factors of safety. If the safety factor was less than 1.5 during a raise (GruvRIDAS 2007), a rockfill bank was added on the downstream side to increase slope stability. Therefore, an optimization analysis was also performed to minimize the volume of rockfill banks required for slope stability during staged construction.

The finite element model of the dam including future raises (up to level 410 m) is shown in Fig. 3. The finite element mesh in each cluster is composed of 15 node triangular elements. The computations were initially performed with different levels of coarseness of the mesh (fine, and very fine). There was only a slight difference in the computed results from analyses with fine and very fine mesh. Therefore, the fine mesh was utilized in the analysis to save computational time. The horizontal displacements are assumed to be zero along the left vertical boundary. A fixed base was adopted since the bottom of the dam lies on a dense and impervious moraine deposit. Flow of water can occur through all boundaries in the finite element model of the dam except at the left vertical boundary and the base.

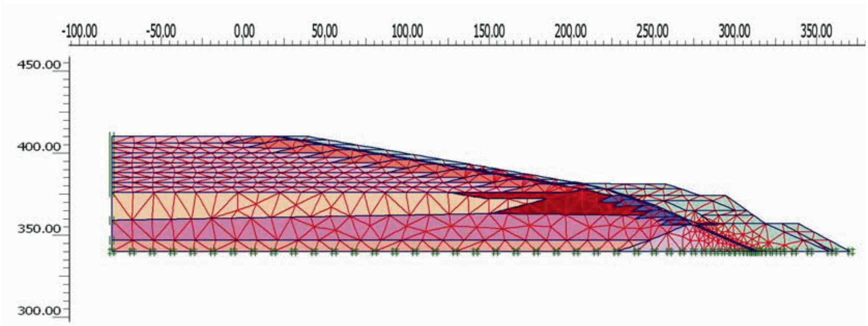

Fig. 3. Finite element model of dam E-F.

The Mohr-Coulomb (MC) model was chosen for all the materials (tailings, rockfill and filter) in the dam. The MC model is a simple elastic – plastic model, which contains five model parameters that can be easily determined from laboratory tests. The parameters of the MC model (except Poisson's ratio and angle of dilatancy), were evaluated from field and laboratory tests, and are presented in Table 1 (Jonasson 2007; Pousette 2007; Jonasson 2008). The Poisson's ratio is assumed to be 0.33 for all the materials, which is a suitable value for this type of analysis (Brinkgreve et al. 2008). The angle of dilatancy is assumed to be zero everywhere; a convenient assumption for loose and contractant soil which the major portion of the dam consists of.

Table 1. Parameters of the Mohr-Coulomb model (Jonasson 2007; Pousette 2007; Jonasson 2008).

Material type	γ_{unsat} (kN/m^3)	γ_{sat} (kN/m^3)	k_x (m/s)	k_y (m/s)	E (kN/m^2)	c' (kN/m^2)	φ' (º)
Moraine (initial dike)	20	22	9.95×10^{-8}	4.98×10^{-8}	20000	1	35
Sand tailings soft at bottom	18	18	9.95×10^{-8}	1×10^{-8}	9800	6	18
Layered sand tailings	17	18.5	5.5×10^{-7}	5.56×10^{-8}	9312	9.5	22
Moraine (dikes)	20	22	4.98×10^{-8}	1×10^{-8}	20000	1	37
Compacted sand tailings	16	19	1×10^{-6}	9.95×10^{-8}	8790	13	26
Sand tailings soft at top	18	18	9.95×10^{-8}	1×10^{-8}	3048	6	18
Compacted sand tailings (dikes)	16	19	1×10^{-6}	9.95×10^{-8}	7200	13	26
Sand tailings layered at top	17	18.5	5.5×10^{-7}	5.56×10^{-8}	3895	9.5	22
Filter	18	20	1×10^{-3}	1×10^{-3}	20000	1	32
Rockfill (downstream support)	18	20	1×10^{-1}	1×10^{-1}	40000	1	42

Note: γ_{unsat} is the unit weight above phreatic level, γ_{sat} is the unit weight below phreatic level, k_x is the hydraulic conductivity in horizontal direction, k_y is the hydraulic conductivity in vertical direction, E is the Young's modulus, c' is the effective cohesion and φ' is the effective friction angle.

The phreatic level of the dam was determined with Piezometers. The phreatic level increases from the downstream to the upstream side and finally coincides with the surface level. This trend for the phreatic level was assumed for all raises of the dam (Fig. 4 and 5).

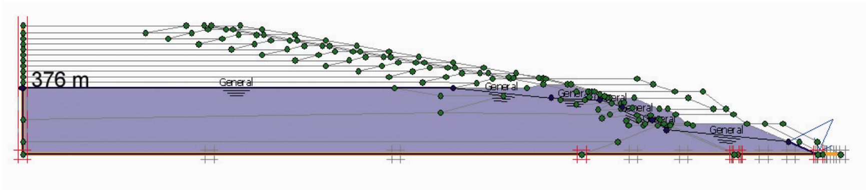

Fig. 4. Phreatic level of the dam E-F for the first raising (elevation 376 m).

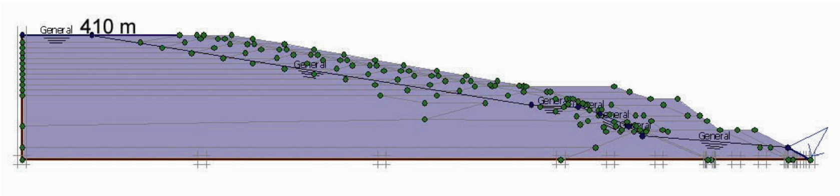

Fig. 5. Phreatic level of the dam E-F for the last raising (elevation 410 m).

The undrained shear strength of the loose tailings was determined from direct shear tests. The failure was evaluated at 0.15 % of shear strain (SGF 2004). The undrained shear strength results were in agreement with the MC model predictions. Therefore, in this case it can be interpreted that the undrained shear strength of the loose tailings is not over predicted with the MC model, which generally over estimates the undrained shear strength of normally consolidated clays (Brinkgreve 2005). Moreover, the results from the finite element analyses have been validated with hand calculations.

The finite element analyses

Stability analyses

Slope stability is determined with a factor of safety. The safety factor is defined as the available shear strength of the soil divided by the shear stress required for equilibrium along the failure surface. In the finite element program PLAXIS, the safety factors are computed with a phi-c reduction technique. In this technique, the strength parameters, i.e., the friction angle φ and the cohesion c of the soil are lowered gradually in the same proportion until a failure of the structure occurs (Brinkgreve et al. 2008). The Swedish safety guidelines document GruvRIDAS (2007) recommends a minimum safety factor of 1.5 for slope stability at the end of construction and during normal operation conditions for tailings dams.

The consolidation and safety analyses were initially performed on the dam section E-F with the previously existing rockfill banks on the downstream side (Fig. 6). It is noted that Fig. 6 and Fig. 2 are exactly the same in all aspects (dimensions and material zones) except the number of rockfill banks on the downstream side. Factors of safety were computed for all the eleven raisings from level 376 m to 410 m. In this case, the factors of safety directly after the raising phase were 1.47, 1.48, 1.43 and 1.37 after first, second, third and fourth raisings respectively. The gradual decrease of the value of the safety factor (from second to eleventh raising) indicates that the safety is not enough that might imply potential instability problems for the dam.

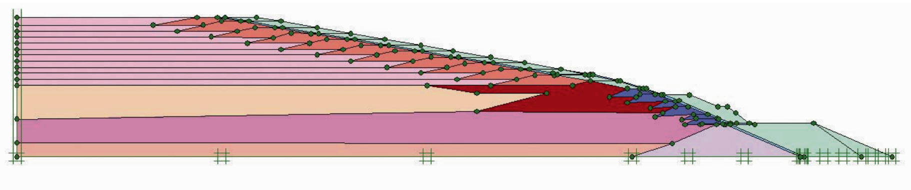

Fig. 6. Cross section of dam E-F with only previously existing rockfill banks on the downstream side.

To increase the stability of the dam during raising, one of the possible solutions is to provide rockfill banks on the downstream side. An optimal technique for gradual strengthening of the dam with rockfill banks (during staged construction) was obtained from the finite element analyses. To improve the slope stability during second rasing, a rockfill bank P (Fig. 7) was placed on the downstream side at the start. The volume of the rockfill bank P was minimized by changing the width and height of the bank until a safety factor of approximately 1.5 was achieved. After adding the rockfill bank P in the beginning of the second raising, the safety factors were computed again for third to eleventh raisings. It was observed that during third raising the slope was stable enough, so there was no need for a rockfill bank at this stage. However, the safety factors were still not adequate to ensure enough slope stability for fourth to eleventh raisings. Therefore, following the similar procedure as described for increasing the slope stability during the second raising, the rockfill banks Q, R, S, T, U, V and W were proposed for fourth to tenth raisings respectively (Fig. 7). The slope stability was sufficient during eleventh raising; so, no rockfill bank was added then.

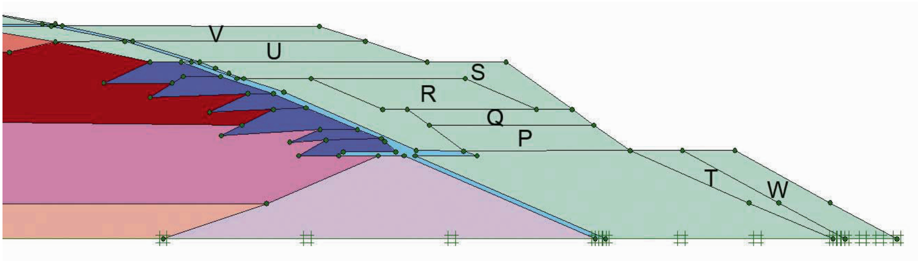

Fig. 7. Placement of the rockfill banks on the downstream side to increase slope stability during construction (optimal case No. IX).

Table 2 summarizes the discussed scheme to enhance the stability of the dam with rockfill banks on the downstream side. Table 2 shows that no rockfill banks were provided for case No. I, whereas the other cases (II to IX) contained an increasing number of rockfill banks. Case No. IX (Fig. 7) turned out to be the optimal case.

Table 2. Rockfill banks proposed for each raising in various computation cases.

Case No.	Raising 1	Raising 2	Raising 3	Raising 4	Raising 5	Raising 6	Raising 7	Raising 8	Raising 9	Raising 10	Raising 11
I	-	-	-	-	-	-	-	-	-	-	-
II	-	P	-	-	-	-	-	-	-	-	-
III	-	P	-	Q	-	-	-	-	-	-	-
IV	-	P	-	Q	R	-	-	-	-	-	-
V	-	P	-	Q	R	S	-	-	-	-	-
VI	-	P	-	Q	R	S	T	-	-	-	-
VII	-	P	-	Q	R	S	T	U	-	-	-
VIII	-	P	-	Q	R	S	T	U	V	-	-
IX	-	P	-	Q	R	S	T	U	V	W	-

The factors of safety with respect to time in years, for all the cases, are presented in Fig. 8. For each case, the factors of safety reduced after every raising and increased due to the following consolidation. The reason is that the effective stresses increase at the same rate as the excess pore pressures dissipate and consequently, the shear strength increases gradually during consolidation. This means that the lowest stability of the dam is always found directly after a raising phase. For cases II to IX, the safety factors increased progressively with addition of rockfill banks on the downstream side as compared to case No. I (Fig. 8). The weight of the rockfill banks on the downstream toe increased the resistance against sliding, which in turn increased the slope stability.

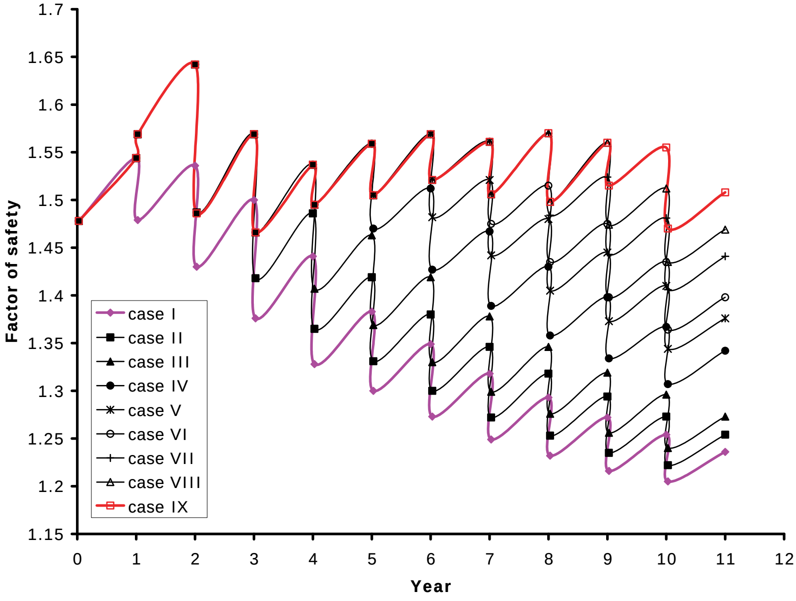

Fig. 8. Factor of safety vs. time in year.

As mentioned earlier, the volume of the rockfill banks was minimized with optimization technique by gradually increasing the width and height of a bank until a safety factor of 1.5 was obtained. This optimization served two purposes i.e. (*i*) to minimize the weight of a rockfill that is necessary to increase the resisting force along the failure surface in order to avoid the condition in which the over weight of the rockfill bank may increase the sliding force and reduce the stability, and (*ii*) to reduce the construction cost by utilizing the minimum volume of a rockfill bank without compromise on slope stability. The case No. IX was considered to be the optimum case, because the safety factors of approximately 1.5 were attained for all the eleven raises. The safety analyses showed that the dam is stable up to eleventh raising (level 410 m), if the rockfill banks are constructed in accordance with case No. IX.

Excess pore pressures

If there is not enough time for the excess pore pressures to dissipate after each new raising of the dam they might successively increase and venture the stability. Therefore, it is interesting to look a little bit closer on the magnitudes of the excess pore pressures that developed in this analysis. Excess pore pressures after the second and eleventh raising phase and their associated subsequent consolidation phase, respectively, are presented for case No. IX in Fig. 9-12.

It is seen in Fig. 9 and 10 that after each raising, relatively high excess pore pressures were observed in the material zones 2, 3, and 6 (cf. Fig. 2), particularly the maximum excess pore pressures occurred in these zones directly below the corresponding embankment. The occurrence of high excess pore pressures in the lower part of the dam is due to the presence of an impermeable base, and the low permeability of the materials in the zones 2 and 6. The excess pore pressures increased after each raising (Fig. 9 and 10) and decreased during the consolidation (Fig. 11 and 12). The excess pore pressures also increased cumulatively with the increase in dam height, and the centre of highest excess pore pressures moved gradually inwards the dam body as the dam height was increased (Fig. 9 and 10).

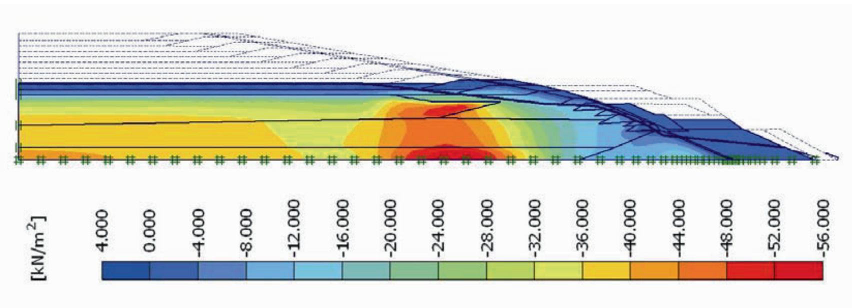

Fig. 9. Excess pore pressures after second raising.

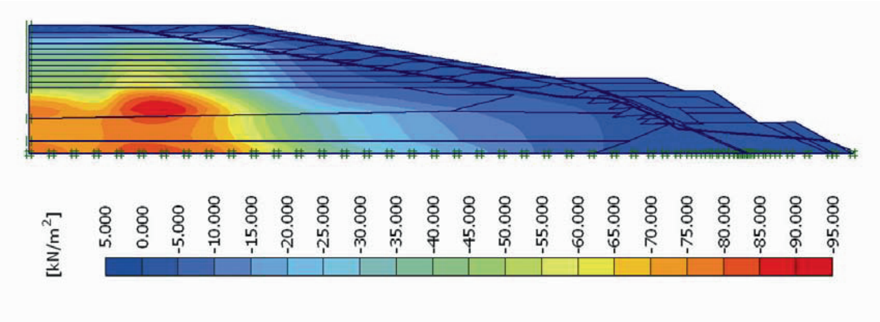

Fig. 10. Excess pore pressures after eleventh raising.

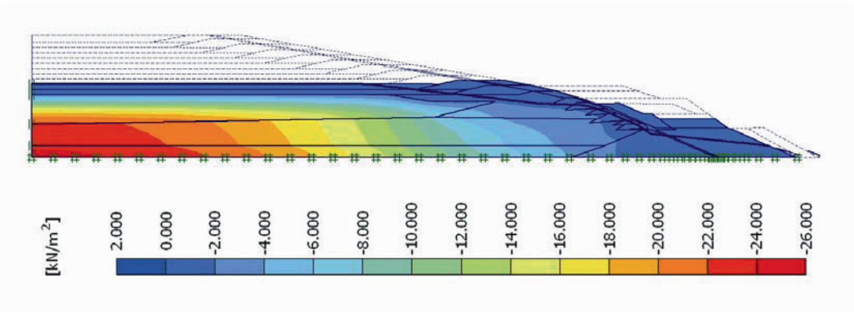

Fig. 11. Excess pore pressures after consolidation of second raising.

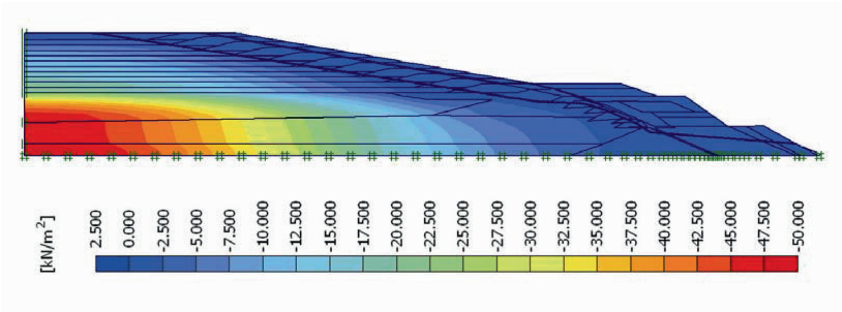

Fig. 12. Excess pore pressures after consolidation of eleventh raising.

Concluding remarks

This study points out that it might take a long time for the excess pore pressures to dissipate during consolidation when an upstream tailings dam is sequentially raised. If excess pore pressures are gradually built up, it might lead to a critical stability situation.

By using the finite element method, an optimization technique has been presented to minimize the volume of the rockfill banks. In this technique, both consolidation and safety analyses are carried out and safety factors are computed for each raising. If the safety factor is less than 1.5, a rockfill bank is placed on the downstream side to improve the stability. The volume of a rockfill bank is minimized by gradually increasing the width and height of the bank until the desired slope stability is achieved.

It is believed that with this finite element method based optimization technique, the desired slope stability of an upstream tailings dam can be accomplished by utilizing minimum volume of rockfill banks, which can result in significant construction cost savings.

Acknowledgements

The authors would like to thank Ms. Kerstin Pousette at Luleå University of Technology, Sweden, and Mr. Fredrik Jonasson at SWECO VBB Luleå, Sweden, for performing laboratory and field tests and for evaluation of material parameters.

The “IRIS” project within the EU Fp7 framework together with Luleå University of Technology and "Swedish Hydropower Centre - SVC" are acknowledged for financial support, which made the work possible. SVC has been established by the Swedish Energy Agency, Elforsk and Svenska Kraftnät together with Luleå University of Technology, The Royal Institute of Technology, Chalmers University of Technology and Uppsala University. Participating hydro power companies are: Andritz Hydro Inepar Sweden, Andritz Waplans, E.ON Vattenkraft Sverige, Fortum Generation, Holmen Energi, Jämtkraft, Karlstads Energi, Linde Energi, Mälarenergi, Skellefteå Kraft, Sollefteåforsens, Statkraft Sverige, Statoil Lubricants, Sweco Infrastructure, Sweco Energuide, SveMin, Umeå Energi, Vattenfall Research and Development, Vattenfall Vattenkraft, VG Power and WSP. Boliden Mining is to be acknowledged for giving access to site information.

References

Brinkgreve, R.B.J., Broere, W., and Waterman, D. 2008. PLAXIS user's manual – version 9. PLAXIS bv, the Netherlands.

Brinkgreve, R.B.J. 2005. Selection of soil models and parameters for geotechnical engineering application. *In* Proceedings of Geo-Frontiers Conference, ASCE, Austin, TX, January 24-26, 2005. American Society of Civil Engineers, USA, pp. 69-98.

Desai, C.S., Shao, C., White, D., and Davis, S. 1998. Stability analysis for consolidation and dynamic response of mine tailing dam. *In* Proceedings of the Fifth International Conference on Tailings and Mine Waste '98, Fort Collins, Colorado, 26-28 January 1998. A.A Balkema Publishers, Rotterdam, the Netherlands, pp. 193-200.

Gens, A., and Alonso, E.E. 2006. Aznalcóllar dam failure. Part 2: Stability conditions and failure mechanism. Géotechnique, **56** (3): 185-201.

Göransson, T., Benckert, A., Lindvall, M., and Ritzén, R. 2001. Dam failure at the Aitik mine: Investigations, conclusions and measures taken. *In* Proceedings of Securing the future – International Conference on Mining and the Environment, Skellefteå, Sweden, 25 June-1July 2001. The Swedish Mining Association, Skellefteå, pp. 1-13.

GruvRIDAS. 2007. Gruvindustrins riktlinjer för dammsäkerhet. Svensk Energi AB/ SveMin, Stockholm (in Swedish).

Jonasson, F. 2007. Geoteknisk provtagning av anrikningssand damm E-F och G-H Aitik. PM Geoteknik Uppdragsnummer 2473649, SWECO VBB, Luleå, Sweden (in Swedish).

Jonasson, F. 2008. PM Förslag på materialparametrar för "Övriga Material" vid beräkning i Plaxis. Uppdragsnummer 2166133310, SWECO VBB, Luleå, Sweden (in Swedish).

Ormann, L. 2008. Stabilitet damm EF Aitik. Uppdragsnummer 2166133, SWECO Infrastructure AB, Stockholm, Sweden (in Swedish).

Pousette, K. 2007. Laboratorieförsök på anrikningssand från Aitik. Internal working document, Luleå University of Technology, Luleå, Sweden (in Swedish).

Priscu, C. 1999. Behavior of mine tailings dams under high tailings deposition rates. Ph.D thesis, Department of Mining and Metallurgical Engineering, McGill University, Montreal, Canada.

Priscu, C., Mitri, H.S., Keira, H., and Jacobsz, S.W. 1999. Evaluation of mine tailings dams behaviour - A case study. *In* Proceedings of the Sixth International Conference on Tailings and Mine Waste '99, Fort Collins, Colorado, 24-27 January 1999. A.A Balkema Publishers, Rotterdam, the Netherlands, pp. 325- 334.

Psarropoulos, P.N., and Tsompanakis, Y. 2008. Stability of tailings dams under static and seismic loading. Canadian Geotechnical Journal, **45**(5): 663-675. doi: 10.1139/T08-014.

Saad, B., and Mitri, H. 2010. Staged construction analysis of surface tailings disposal facilities. International Journal of Mining, Reclamation and Environment, **24**(1): 44-63. doi:10.1080/17480930902951293.

SGF. 2004. Direkta skjuvförsök – en vägledning. Swedish Geotechnical Society, Linköping, Sweden (in Swedish).

Vick, S.G. 1990. Planning, design and analysis of tailings dams. BiTech Publishers Ltd. Richmond, B.C.

Zandarín, M.T., Oldecop, L.A., Rodríguez, R., and Zabala, F. 2009. The role of capillary water in the stability of tailing dams. Engineering Geology, **105**(1-2): 108–118. doi:10.1016/j.enggeo.2008.12.003.

Paper II

NUMERICAL ANALYSIS OF CURVED EMBANKMENT OF AN UPSTREAM TAILINGS DAM

L. Ormann, M.A. Zardari, H. Mattsson, A. Bjelkevik, and S. Knutsson

To be submitted to Electronic Journal of Geotechnical Engineering

Numerical Analysis of Curved Embankment of an Upstream Tailings Dam

Linda Ormann
Geotechnical Engineer, SWECO Infrastructure AB, Gjörwellsgatan 22, Stockholm, Sweden
Email: linda.ormann@sweco.se

Muhammad Auchar Zardari
Ph.D student, Department of Civil, Environmental and Natural Resources Engineering, Luleå University of Technology, Luleå, Sweden
Email: muhammad.zardari@ltu.se

Hans Mattsson
Assistant Professor, Department of Civil, Environmental and Natural Resources Engineering, Luleå University of Technology, Luleå, Sweden
Email: hans.mattsson@ltu.se

Annika Bjelkevik
Geotechnical Engineer, SWECO Infrastructure AB, Gjörwellsgatan 22, Stockholm, Sweden
Email: annika.bjelkevik@sweco.se

Sven Knutsson
Professor, Department of Civil, Environmental and Natural Resources Engineering, Luleå University of Technology, Luleå, Sweden
Email: sven.knutsson@ltu.se

ABSTRACT

A curved embankment (corner) of an upstream tailings dam was analyzed with the finite element method to identify possible zones of low compressive stresses susceptible to hydraulic fracturing that might initiate internal erosion. The embankment was also analyzed as a straight section, with the same cross section as in the corner, in order to compare compressive stresses in the corner and the straight section. The analysis showed that in comparison to the straight section of the dam, the compressive stresses in the corner were (*i*) much lower above the phreatic level, in the rockfill banks and the filter zones, and (*ii*) fairly lower below the phreatic level. The rockfill and the filter contain coarse materials, which are not sensitive to hydraulic fracturing and internal erosion. An increase in radius of the corner is proposed to avoid too low compressive stresses that may develop due to future raisings. The slope stability analysis showed that the corner is currently stable, but an additional rock fill bank on the downstream toe is required for future raisings.

KEYWORDS: tailings dams, curved embankments, cracks, internal erosion, hydraulic fracturing, slope stability.

INTRODUCTION

A case study of a finite element analysis of an upstream tailings dam named Aitik, located in the north of Sweden, is presented. This study investigates the potential risk of hydraulic fracturing followed by internal erosion in the corner between the dam sections E-F and G-H (Figure 1). The corner E-F/G-H can be considered as a curved embankment in which retained tailings exert lateral earth pressure on the inner side of the embankment. Consequently, low compressive stresses (and even tensile stresses) may develop near the surface along the outer side of the embankment. Thus, the zones of low compressive stresses in the corner may be sensitive to hydraulic fracturing and internal erosion.

In embankments, cracks or weak zones can appear even at very small tensile stresses. If no cracks develop immediately due to small deformations, cracking may occur later by hydraulic fracturing (Sherard, 1986; Kjaernsli *et al*., 1992). Internal erosion can then initiate through these cracks. Hydraulic fracturing in an embankment dam may occur through the zones of low compressive stresses, i.e. along the plane of minor effective principal stress (Kjaernsli *et al*., 1992). Hydraulic fracturing due to high water pressures might have caused leakage or failure of many embankment dams (Sherard, 1986; Singh and Varshney, 1995).

Recently in Hungary, on October 4, 2010, Ajka tailings pond failed at a corner section. In this incident, 0.6 million cubic meters of sludge was released, which killed ten and injured 120 people (WISE, 2010). The possible causes of the failure of Ajka tailings pond were (*i*) generation of excess tensile stresses in the corner, and (*ii*) differences in cross sections of the two dikes that formed the corner (Zanbak, 2010).

In a report (SWECO, 2005), it has been mentioned that low compressive stresses (and tensile stresses) might arise at the corner E-F/G-H. Since then, the dam has been raised, and the corner has become sharper.

In this paper, the corner E-F/G-H was analyzed with the finite element program PLAXIS 2D (Brinkgreve, 2002) in order to locate the zones of low compressive stresses that may be susceptible to hydraulic fracturing and internal erosion. The results of this study have been previously published in a report (Ormann and Bjelkevik, 2009).

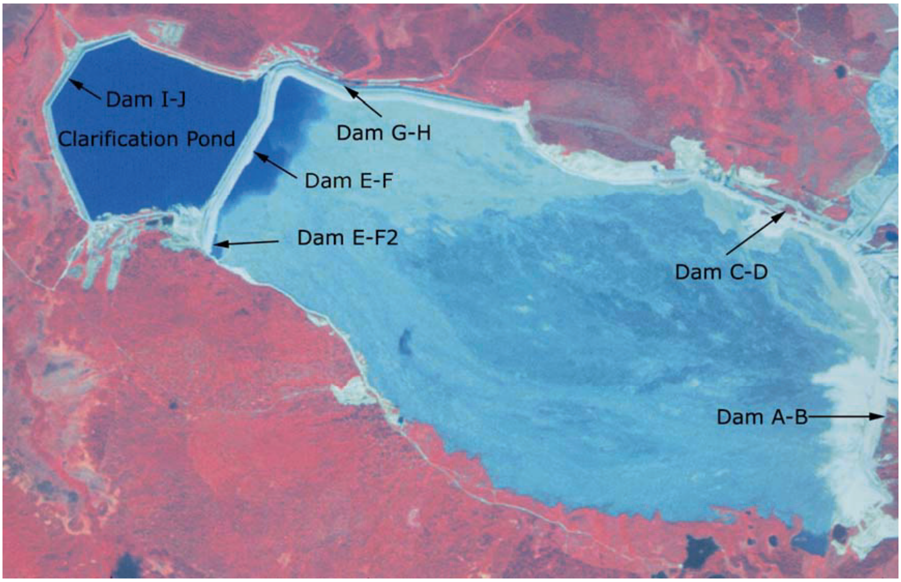

Figure 1: Aerial view of Aitik tailings dam and impoundment (Photo courtesy of Boliden Mineral AB).

FINITE ELEMENT MODEL

The stability of the corner E-F/G-H was analysed with PLAXIS 2D, which is a finite element program for numerical analysis of geotechnical structures. The corner represents a complex three-dimensional geometry. An axisymmetric condition was assumed to model this geometry in two-dimensional space. This condition can be used for circular structures with an almost uniform cross section with load distribution around the central axis. In an axisymmetric condition, the *x*-coordinate represents the radius, and the *y*-coordinate denotes the axial line of symmetry.

It is previously mentioned that due to horizontal pressure of retained tailings at the inner side of the corner, too low compressive stresses may occur near the surface along the outer side of the corner. It is assumed that if the corner is straightened, then the compressive stresses may be sufficiently high to resist hydraulic fracturing and internal erosion. Therefore, it is important to compare the compressive stresses in the corner with the straight section of the dam. Hence, the corner was also modelled with a plane strain condition, which is appropriate for any geotechnical structure - whose length is large compared with its cross section. Figure 2 illustrates the difference between a plane strain and an axisymmetric condition (Brinkgreve, 2002). In this paper, the compressive stresses are taken as positive and the tensile stresses as negative.

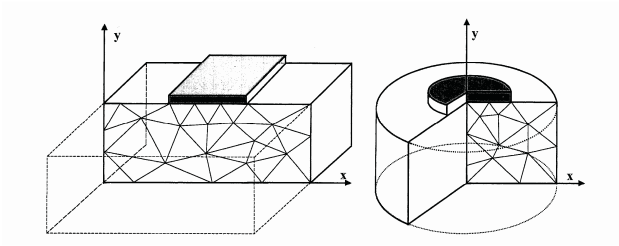

Figure 2: (*a*) Plane strain condition, and (*b*) Axisymmetric condition (Brinkgreve, 2002).

It has been assumed that the stored tailings and the dam are raised 3 meter per year starting from the level 376 m above mean sea level. The crest level of the dam is 2 m above the level of the stored tailings. The present crest level of the dam in year 2010 is 387 m. The cross section of the corner is shown in figure 3. The estimated radius is 195 m (Figure 4). It is supposed that the dam is to be raised in stages with the upstream construction method with side slope of 1:6 (vertical to horizontal). Each stage comprises a raising phase of 10 days and a consolidation phase of 355 days.

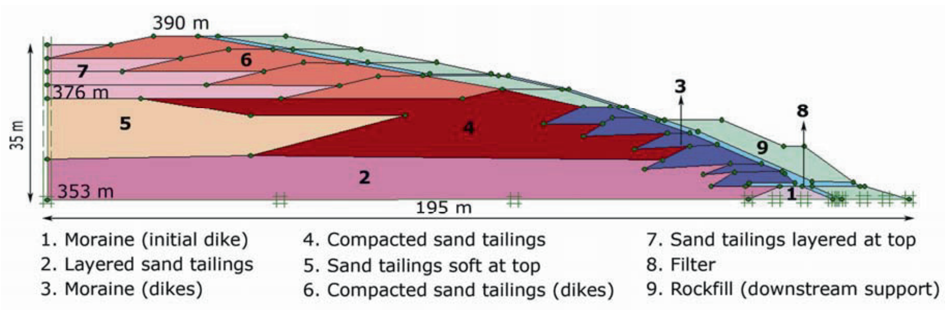

Figure 3: Cross section of corner E-F/G-H.

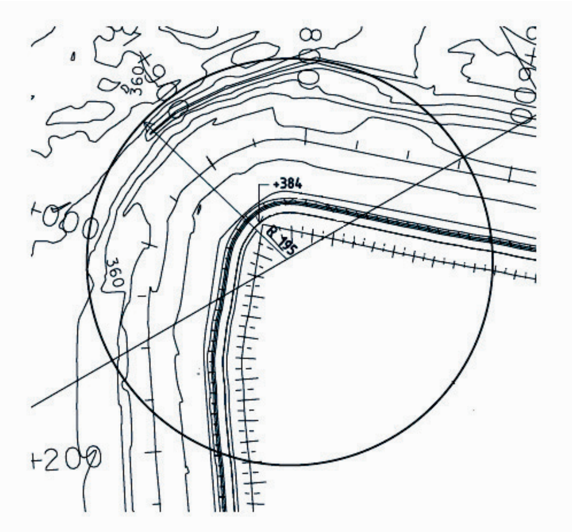

Figure 4: Plan of existing corner between the dam sections E-F and G-H.
The radius is 195 m.

The finite element model of the corner is presented in figure 5. The finite element mesh in each cluster is composed of 15 node triangular elements. The computations were initially performed with different levels of coarseness of the mesh (fine, and very fine). There was a small difference in the results from the computations done with the fine and the very fine mesh. Therefore, the fine mesh was used in the analysis to save computational time. The horizontal displacements are assumed to be zero along the left vertical boundary. A fixed base was used assuming that the bottom of the dam lies on a dense and impervious moraine deposit. Water flow can occur through all boundaries in the geometry, except at the left vertical boundary and the base.

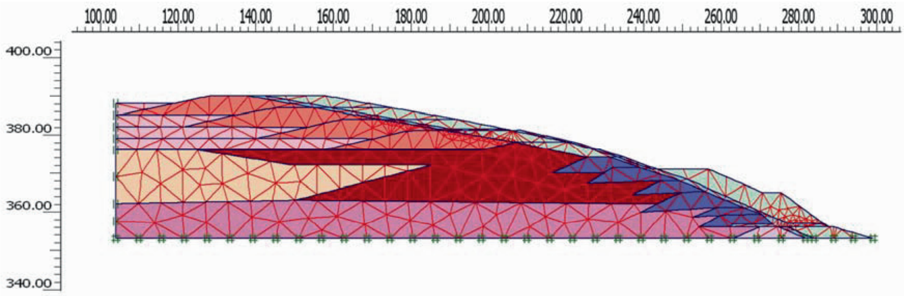

Figure 5: Finite element mesh of corner E-F/G-H.

The Mohr-Coulomb (MC) model was applied to all the materials (tailings, rockfill, and filter) in the dam. The MC model is a simple elastic - plastic model, which contains five model parameters that can be easily determined from laboratory tests. The parameters of the MC model (except Poisson's ratio and angle of dilatancy), were evaluated from field and laboratory tests, and are presented in Table 1 (Jonasson, 2007; Pousette, 2007; Jonasson, 2008). The Poisson's ratio is assumed to be 0.33 for all the materials, which is a representative value for this type of analysis (Brinkgreve, 2002). The angle of dilatancy of each material is assumed to be zero, which is a convenient assumption for loose and contractant soil e.g. tailings that occupy the major portion of the dam.

The undrained shear strength of loose tailings was determined from direct shear tests. The failure was evaluated at 0.15 % of shear strain (SGF, 2004). The undrained shear strength results were in agreement with the MC model predictions. Therefore, in this case it can be interpreted that the undrained shear strength of loose tailings is not over predicted with the MC model, which generally over estimates the undrained shear strength of normally consolidated clays (Brinkgreve, 2005).

As mentioned earlier, the possible risks of hydraulic fracturing followed by internal erosion in the corner have been investigated in this study. The hydraulic fracturing can occur along the plane of the minor effective principal stress. Therefore, it is important to locate the position of the minor effective principal stress in the corner. In this connection, consolidation analysis was performed for staged construction of the dam. The minor effective principal stress was calculated from the results of the consolidation analysis. In addition to this, safety analysis was also carried out to determine the slope stability of the dam.

Table 1. Parameters of the Mohr-Coulomb model (Jonasson, 2007; Pousette, 2007; Jonasson, 2008).

Material type	γ_{unsat} (kN/m^3)	γ_{sat} (kN/m^3)	k_x (m/s)	k_y (m/s)	E (kN/m^2)	c' (kN/m^2)	φ' (º)
Moraine (initial dike)	20	22	9.95×10^{-8}	4.98×10^{-8}	20000	1	35
Layered sand tailings	17	18.5	5.5×10^{-7}	5.56×10^{-8}	9312	9.5	22
Moraine (dikes)	20	22	4.98×10^{-8}	1×10^{-8}	20000	1	37
Compacted sand tailings	16	19	1×10^{-6}	9.95×10^{-8}	8790	13	26
Sand tailings soft at top	18	18	9.95×10^{-8}	1×10^{-8}	3048	6	18
Compacted sand tailings (dikes)	16	19	1×10^{-6}	9.95×10^{-8}	7200	13	26
Sand tailings layered at top	17	18.5	5.5×10^{-7}	5.56×10^{-8}	3895	9.5	22
Filter	18	20	1×10^{-3}	1×10^{-3}	20000	1	32
Rockfill (downstream support)	18	20	1×10^{-1}	1×10^{-1}	40000	1	42

Note: γ_{unsat} is the unit weight above phreatic level, γ_{sat} is the unit weight below phreatic level, k_x is the hydraulic conductivity in horizontal direction, k_y is the hydraulic conductivity in vertical direction, E is the Young's modulus, c' is the effective cohesion and φ' is the effective friction angle.

FINITE ELEMENT ANALYSIS

Evaluation of minor effective principal stress

An element of a soil under an embankment can be subjected to three principal stresses acting on three mutually perpendicular planes. For the geometry of the corner E-F/G-H, two of the principal stresses act in the *x-y* plane, and the third principal stress occurs in the *z* direction along the length of the dam. Hence, the normal effective stress σ'_{zz} in the *z* direction is also a principal stress. The major effective principal stress σ'_1 and the minor effective principal stress σ'_2 in the *x-y* plane can be calculated according to Das (1997):

$$\sigma'_{1,2} = \frac{1}{2}\left(\sigma'_x + \sigma'_y\right) \pm \sqrt{\left(\frac{\sigma'_x + \sigma'_y}{2}\right)^2 + \tau_{xy}^2} \qquad (1)$$

where σ'_x and σ'_y are the effective normal stress components in the *x* and *y* directions respectively, and τ_{xy} is the shear stress component in the *x-y* plane. The values of these stress components were directly obtained from the results of the finite element analysis of the corner.

The major effective principal stress occurred in the *x-y* plane. As stated earlier, for this analysis, it is essential to locate the minor effective principal stress in the three dimensional space. Therefore, the minor effective principal stress σ'_2 in the *x-y* plane was compared to the effective normal stress σ'_{zz} in the *z* direction. Figure 6 illustrates the ratio σ'_{zz} / σ'_2 of the effective normal stress in the *z* direction and the minor effective principal stress in the *x-y* plane. If the ratio is less than one, the effective normal stress in the *z* direction is the minor effective principal stress in the three dimensional space. In the upper parts of the geometry, the effective normal stress in the z direction, dominates as the minor effective principal stress in the three dimensional space. When the ratio is equal to one, the minor effective principal stress in the x-y plane and the effective normal stress in the z direction are equal. If the ratio is greater than one, the minor effective principal stress in the x-y plane acts as the minor effective principal stress in the three dimensional space. The ratio of 1 to 1.2 indicates that the effective normal stress in the z direction is approximately of the same magnitude as the minor effective principal stress in the x-y plane. It is obvious that the minor effective principal stress in the three dimensional space is located either in the x-y plane or in the z direction.

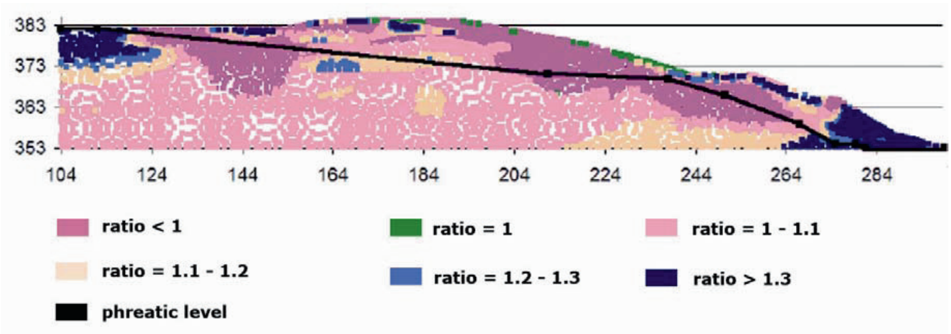

Figure 6: The ratio of the effective normal stress in the z direction and the minor effective principal stress in the x-y plane for the axisymmetric condition (crest level +384 m).

The numerical analysis was carried out with both axisymmetric and plane strain conditions. This was done in order to compare the principal stresses σ'_2 and σ'_{zz} in the axisymmetric and the plane strain cases. For this purpose, an absolute norm N_{abs} was computed for σ'_2 and σ'_{zz} (equations 2 and 3).

$$N_{abs} = \sigma_2'^{\,axs} - \sigma_2'^{\,pls} \tag{2}$$

$$N_{abs} = \sigma_{zz}'^{\,axs} - \sigma_{zz}'^{\,pls} \tag{3}$$

where the superscripts "*axs*" and "*pls*" represent the axisymmetric and the plane strain conditions respectively. The absolute norm shows that there was (*i*) small difference in magnitude of the minor effective principal stress σ'_2 in the *x-y* plane for the plane strain and the axisymmetric cases (Figure 7), and (*ii*) large reduction of the effective normal stress σ'_{zz} in the *z* direction in the axisymmetric condition compared to the plane strain condition (see e.g. Figure 8b). Therefore, the effective normal stress σ'_{zz} in the *z* direction is examined in more detail in the next section.

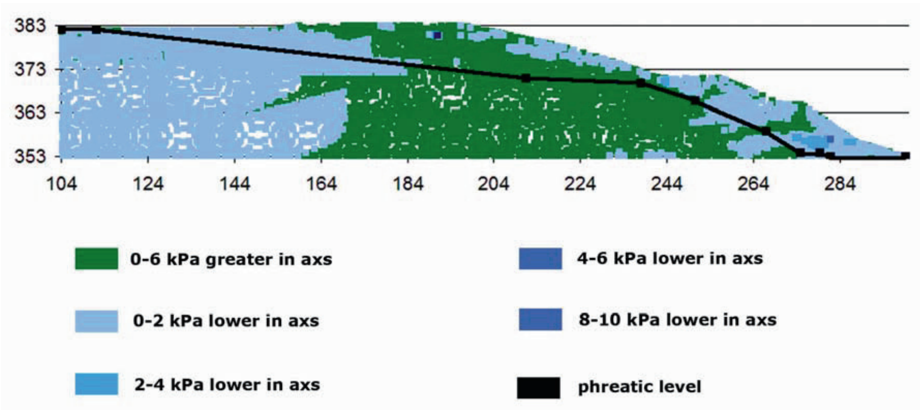

Figure 7: Absolute norm (difference) of the minor effective principal stress in the *x-y* plane for the axisymmetric and the plane strain conditions (crest level +384 m).

Effective normal stress in the *z* direction

It was concluded in the previous section that the effective normal stress in the longitudinal *z* direction in the corner need to be further studied to assess the zones of low compressive stresses that might be sensitive to hydraulic fracturing and internal erosion.

In addition to examining the magnitude of the effective normal stress in the *z* direction in the corner, it is important to find out how much the effective normal stress in the *z* direction in the corner is reduced compared to the straight section. This was done by calculating (*i*) the absolute norm N_{abs} (equation 3), and (*ii*) the relative norm N_{rel} (equation 4).

$$N_{rel} = 100 \times \left(\sigma'^{\,axs}_{zz} - \sigma'^{\,pls}_{zz} \right) / \sigma'^{\,pls}_{zz} \tag{4}$$

An absolute norm here shows the difference in magnitude of the effective normal stress in the *z* direction in the corner and the straight section. For small values of the absolute norm, it may be interpreted that the difference of the effective normal stress in the *z* direction between the corner and the straight section is negligible. In fact, that difference might be considerable, if it is evaluated in percentage. Therefore, the relative norm is useful for this purpose. The relative norm indicates reduction in percentage of the effective normal stress in the *z* direction in the corner compared to the straight section. A disadvantage with the relative norm is that extremely large norm values can be obtained even for small absolute deviations, if the value of the effective normal stress $\sigma'^{\,pls}_{zz}$ approaches zero. However, in this type of analysis both the absolute norm and the relative norm are of significance, and are therefore, studied together.

Figures 8a-9a show the magnitude of the effective normal stress σ'_{zz} in the z direction for the axisymmetric condition. The figures indicate that the effective normal stress in the z direction increases with depth of the embankment, and low compressive stresses (and tensile stresses) occur only on the vicinity of the embankment surface. This is consistent with the findings of Sherard (1986) that the internal compressive stresses in an embankment increase with depth.

The absolute and relative norms (Figures 8b-9b and 8c-9c) illustrate that the effective normal stress in the z direction in major portion of the cross section was lower in the axisymmetric case compared to the plane strain case. The largest difference of the effective normal stress in the z direction (between the axisymmetric and plane strain conditions) occurred above the phreatic level, in rockfill banks and the filter zones. This area is not susceptible to hydraulic fracturing (and consequently to internal erosion), because the material is mainly coarse grained and no water flow occurs above the phreatic level. Hydraulic fracturing takes place only in materials with low permeability such as dense cores of clay or moraine and not in the coarse-grained permeable material such as gravel and stones (Kjaernsli *et al.*, 1992).

Figures 8b-9b and 8c-9c depict that the effective normal stress in the z direction also reduced moderately below the phreatic level in axisymmetric condition compared to the plane strain condition. A comparison of figures 8b-9b and 8c-9c indicates that the absolute and relative norm values were gradually increased with successive raisings of the dam. This implies that with every new raise, the effective normal stress in the z direction in the corner was reduced compared to the straight section. Therefore, it is interpreted that when the dam will be raised higher, the effective normal stress in the z direction in axisymmetric case can reduce significantly even under the phreatic level.

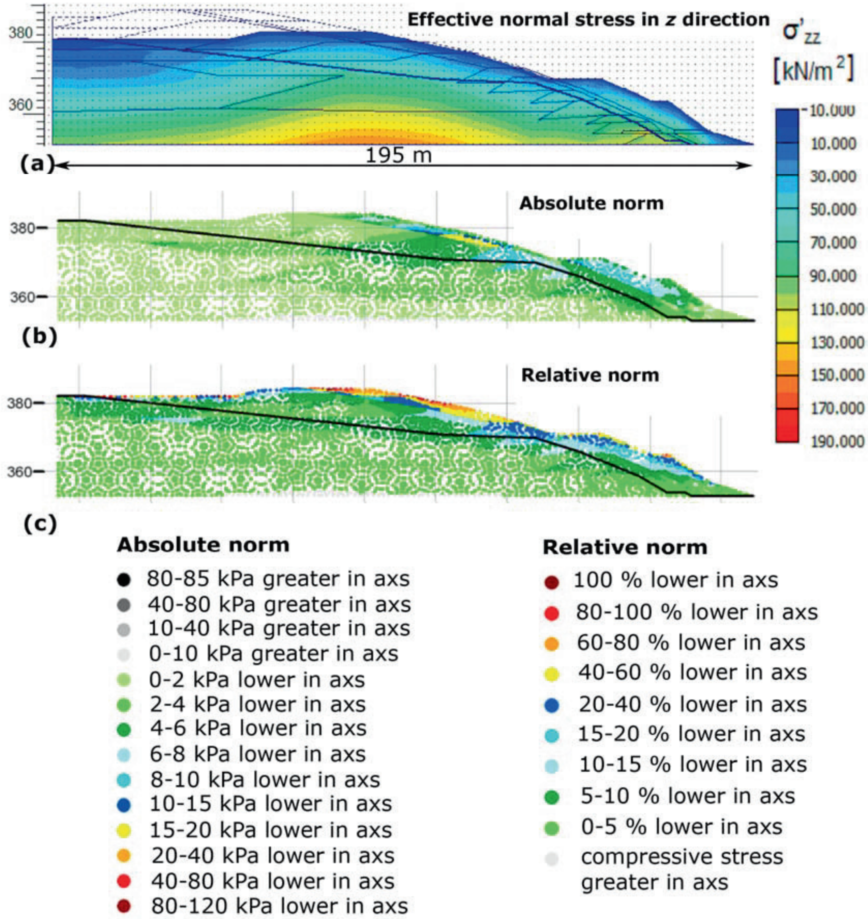

Figure 8: (*a*) Effective normal stress σ'_{zz} in the z direction in the axisymmetric condition (crest level +384 m). The correlation of σ'_{zz} for the axisymmetric and the plane strain conditions, (*b*) absolute norm, and (*c*) relative norm.

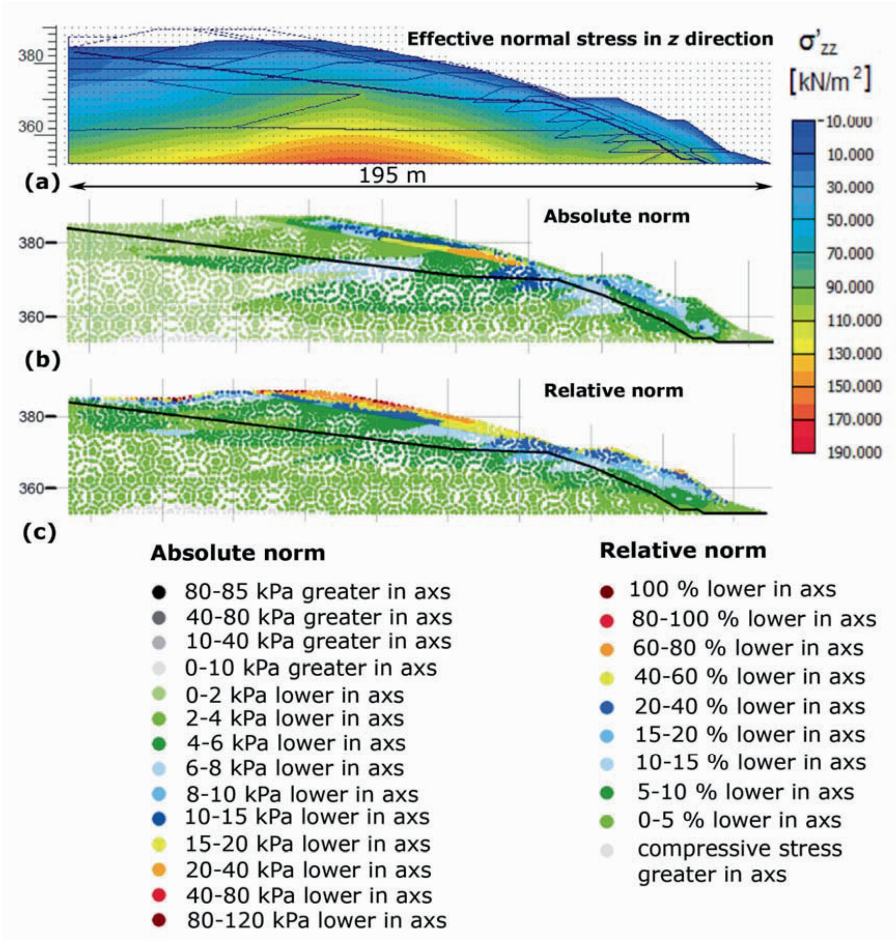

Figure 9: (*a*) Effective normal stress σ'_{zz} in the *z* direction in the axisymmetric condition (crest level +387 m). The correlation of σ'_{zz} for the axisymmetric and the plane strain conditions, (*b*) absolute norm, and (*c*) relative norm.

The corner will be narrower, if raised continuously with side slope of 1:6, and within a few years, the crest of the dam will be so sharp that the dam sections E-F and G-H might meet and collapse. Presently the corner is stable. However, it might be unstable after future raisings. It is recommended to increase the radius of the corner. This can be done by increasing the side slope of the corner from 1:6 to 1:12. With a larger radius, a wider beach can be maintained which will help to reduce the height of the phreatic level in the embankment (Vick, 1990). This implies that a small portion of the embankment may be saturated, which can result in low pore pressures and increased strength. As the corner widens, the stress situation resemble more of the plane strain condition, with increasing compressive stresses in the dam longitudinally.

Slope stability Analysis

The slope stability of a dam can be evaluated with the factors of safety. In the safety guidelines document for Swedish tailings dams GruvRIDAS (2007), a safety factor of 1.5 is recommended for slope stability at the end of construction and during normal operation conditions, and 1.3 for extreme conditions. Table 2 shows the safety factors obtained from the safety analysis of the corner.

Table 2: Safety factors for the corner E-F/G-H.

Crest level	Factor of safety
Level +384 m before consolidation	1.43
Level +384 m after yearly consolidation	1.47
Level +387 m before consolidation	1.44
Level +387 m after yearly consolidation	1.47
Level +390 m before consolidation	1.43
Level +390 m after yearly consolidation	1.47

The safety factors are approximately 1.5; therefore, the slope stability of the corner is considered satisfactory for present raising level. The safety factors may reduce during future raisings of the dam. In order to maintain desired slope stability of the dam (i.e. safety factor of 1.5) for next raisings, it is recommended to provide an additional rockfill bank on the downstream side.

CONCLUSIONS

The results of the finite element analysis have shown that the effective normal stress in the longitudinal *z* direction acts as the minor effective principal stress in the upper part of the corner. In comparison to the straight section of the dam, the effective normal stress in the *z* direction in the corner was (*i*) much lower above the phreatic level, in the rockfill banks and the filter zones, and (*ii*) moderately lower below the phreatic level. The rockfill and the filter contain coarse materials, which are not influenced by hydraulic fracturing and internal erosion. Larger reductions of the effective normal stresses in the *z* direction are expected, even below the phreatic level, as the dam height is gradually increased. For future raisings, it has been proposed to increase the radius of the corner by increasing the slope inclination of the corner section from 1:6 to 1:12. Currently the dam section in the corner has adequate slope stability, but for future raisings, an additional rockfill bank on the downstream side will be needed.

Admittedly, the corner is not circular, but due to its uniform cross section, an axisymmetric condition was applied. Hence, the obtained results might differ slightly from reality; in this regard, three dimensional finite element analyses can give further insight into the problem.

This paper shows that the finite element method can be a good tool to investigate the risks of hydraulic fracturing followed by internal erosion in the zones of low compressive stresses in a curved embankment of a tailings dam.

ACKNOWLEDGEMENTS

The authors would like to thank Ms. Kerstin Pousette at Luleå University of Technology, Sweden, and Mr. Fredrik Jonasson at SWECO VBB Luleå, Sweden, for performing laboratory and field tests and for evaluation of material parameters.

The “IRIS” project within the EU Fp7 framework together with Luleå University of Technology and "Swedish Hydropower Centre - SVC" are acknowledged for financial support, which made the work possible. SVC has been established by the Swedish Energy Agency, Elforsk and Svenska Kraftnät together with Luleå University of Technology, The Royal Institute of Technology, Chalmers University of Technology and Uppsala University. Participating hydro power companies are: Andritz Hydro Inepar Sweden, Andritz Waplans, E.ON Vattenkraft Sverige, Fortum Generation, Holmen Energi, Jämtkraft, Karlstads Energi, Linde Energi, Mälarenergi, Skellefteå Kraft, Sollefteåforsens, Statkraft Sverige, Statoil Lubricants, Sweco Infrastructure, Sweco Energuide, SveMin, Umeå Energi, Vattenfall Research and Development, Vattenfall Vattenkraft, VG Power and WSP. Boliden Mining is to be acknowledged for giving access to site information.

REFERENCES

1. Brinkgreve, R.B.J (2002) “PLAXIS user’s manual- version 8.2,” Delft University of Technology and PLAXIS b.v., The Netherlands. ISBN 9058095088.
2. Brinkgreve, R.B.J (2005) “Selection of soil models and parameters for geotechnical engineering application,” *In* proceedings of Geo-Frontiers Conference, ASCE, Austin, TX, January 24-26, 2005.
3. Das, B.M (1997) “Advanced Soil Mechanics,” 2nd edition, Taylor and Francis. ISBN 1-56032-561-5.

4. GruvRIDAS (2007) "Gruvindustrins riktlinjer för dammsäkerhet," Svensk Energi AB/ SveMin, Stockholm (in Swedish).

5. Jonasson, F (2007) "Geoteknisk provtagning av anrikningssand dam EF och GH Aitik," SWECO VBB, Luleå, Sweden (in Swedish).

6. Jonasson, F (2008) "PM Förslag på materialparametrar för Övriga Material vid beräkning i Plaxis," Uppdragsnummer 2166133310, SWECO VBB, Luleå, Sweden (in Swedish).

7. Kjærnsli, B., Valstad, T., and Höeg, K (1992) "Rockfill Dams," In the series Hydropower Development, Vol. 10, Norwegian Institute of Technology, Trondheim, ISBN 82-7598-014-3.

8. Ormann, L., and Bjelkevik, A (2009) "Hållfasthetsanalys av hörnet GH/EF i Aitikdammen," Uppdragsnummer 2168007350, SWECO Infrastructure AB, Stockholm, Sweden (in Swedish).

9. Pousette, K (2007) "Laboratorieförsök på anrikningssand från Aitik. Internal working document, Luleå University of Technology, Luleå, Sweden (in Swedish).

10. Sherard, J.L (1986) "Hydraulic fracturing in embankment dams," *Journal of Geotechnical Engineering*, Vol. 112, No. 10, pp 905-927.

11. SGF (2004) "Direkta skjuvförsök – en vägledning," Swedish Geotechnical Society, Linköping, Sweden (in Swedish).

12. Singh, B., and Varshney, R.S (1995) "Engineering for Embankment Dams," A.A. Balkema/Rotterdam. ISBN 905410 2799.

13. SWECO, VBB (2005) "Aitik dammar 2005," SWECO Infrastructure AB, Stockholm, Sweden (in Swedish).

14. Vick, S.G (1990) "Planning, design, and analysis of tailings dams," 2nd edition, BiTech Publishers Ltd, Canada. ISBN 0-921095-12-0.

15. WISE (2010) “The Kolontár red mud dam failure,” Available from web http://wise-uranium.org/mdafko.html#CAUSES [cited 29 November 2010].

16. Zanbak, C (2010) “Failure mechanism and kinematics of Ajka tailings pond incident,” Magyar Aluminum ZRt, Ajka – Hungary. Available from web http://www.redmud.org/Files/2010-ZANBAK_Ajka%20Pond%20Failure-10%20Dec.pdf [cited 5 March 2011].

Paper III

STATIC LIQUEFACTION OF TAILINGS: A REVIEW OF CONSTITUTIVE MODELS

M.A. Zardari, H. Mattsson, and S. Knutsson

Manuscript

Static liquefaction of Tailings: A review of constitutive models

Muhammad Auchar Zardari, Hans Mattsson,[1] and Sven Knutsson

Department of Civil, Environmental and Natural Resources Engineering, Luleå University of Technology, SE-971 87 Luleå, Sweden

[1]Corresponding author

e-mail: hans.mattsson@ltu.se, Tel.: +46-920-492147, Fax: +46-920-492075

Abstract

The catastrophic flow failures due to static liquefaction of tailings dams have lead to loss of human life and pollution of the environment. This paper reviews (*i*) factors that affect the static liquefaction process, (*ii*) strain softening behaviour of tailings, and (*iii*) constitutive models for static liquefaction behaviour of the loose sand. It is deduced that the tailings dams may liquefy due to rapid raising, increase in pore pressures, insufficient drainage, high phreatic level, overtopping and erosion of an outer embankment. It is inferred that the factors that may contribute to the static liquefaction of tailings are: low relative density, low confining pressure, high shear stress, and fines content. Some of the available constitutive models that can simulate static liquefaction behaviour of loose sands are mentioned. It is believed that with numerical modelling using such constitutive model(s), the flow failure due to static liquefaction can be predicted in advance and it might be possible to take remedies to prevent its occurrence.

Key words tailings dams, finite element method, constitutive modelling, static liquefaction, flow failure.

1 Introduction

1.1 Static liquefaction of tailings

A tailings impoundment, consisting of loose sand or silt, can be stable under drained conditions but may be susceptible to failure under undrained loading conditions (Lade 1993; Kramer 1996). These loading conditions may occur due to quick rate of raising, increase in phreatic level (improper drainage, excessive rainfall and snowmelt), and reduction of confinement due to erosion of an embankment.

Because of high degree of saturation and loose densities, the tailings are sensitive to liquefaction. Loose uncompacted saturated sands at relative densities of 30-50% are vulnerable to liquefaction (Vick 1990). Static liquefaction is the most common cause of failure of tailings dams (Davies et al. 2002). Due to static liquefaction, a huge volume of the stored tailings may flow as a viscous liquid and can travel large distances. Thus, the flow failures can cause loss of human life and pollution of the environment. Some examples of tailings dams' failures due to static liquefaction are: Stava (ICOLD 2001; Sammarco 2004), Sullivan Mine (WISE 2010; Davies et al. 1998), Merriespruit (Fourie et al. 2001), and Aznalcóllar (Davies et al. 2002). More records of flow failures in tailings dams can be studied, e.g. in Blight and Fourie (2005).

When a loose saturated sand is sheared under partially drained or undrained conditions, applied load is transferred first to the water present in the soil pores. In this condition, the loose sand can contract and may result in increase of pore pressure and decrease of effective stress. Hence, shear strength of the sand can reduce and extreme deformations can occur. The term liquefaction refers to the deformations of loose saturated sand due to monotonic or cyclic loading under undrained conditions (Kramer 1996). Flow liquefaction can occur when the static shear stress is larger than the shear strength of the soil in its liquefied state (Kramer 1996). In static liquefaction, the mean effective stress reduces due to development of pore pressure under monotonic undrained conditions. The loose sands with high void ratio and low confining pressure are more susceptible to liquefaction (Craig 2004).

Static liquefaction can occur in a tailings dam, if (*i*) the tailings show contractive behaviour during undrained loading, and (*ii*) there is presence of a trigger mechanism (Fourie and Tshabalala 2005). The triggering mechanism can be due to (*i*) overloading (rapid rate of raising, construction activities at crest), (*ii*) changes in pore pressure (quick rate of construction, intense rain storms, and high pond levels), and (*iii*) overtopping (Martin and McRoberts 1999). Static liquefaction can also occur due to reduction in lateral confinement (due to erosion) of an outer embankment. Generally, tailings dams have varying material properties, there can be some contractive layers (susceptible to liquefaction) sandwiched within the dilative layers. When the liquefaction initiates, the reduction in shear strength of contractive layers may also reduce the shear strength of dilative layers (Blight and Fourie 2005).

The occurrence of flow failures in tailings dams can be predicted (and remedial measures can be taken in advance to prevent such flow failures) by performing numerical analyses with the finite element method. A constitutive model is a key component in any finite element program. Therefore, the choice of a proper constitutive model is very essential in performing such analyses. This paper reviews (*i*) the factors that influence static liquefaction, (*ii*) strain softening behaviour of tailings, and (*iii*) available constitutive models that can simulate static liquefaction behaviour. Emphasis is given on those constitutive models that are implemented in commercial finite element programs.

1.2 Examples of flow failures of tailings dams due to static liquefaction

(*a*) Stava, Italy – 1985

Two upstream tailings dams, built one above the other on sloping ground located near Stava in Italy failed in 1985. The lower embankment failed due to overtopping caused by failure of the upper embankment. The slurry flowed at a speed of 60 km/hour and caused 269 deaths (ICOLD 2001). Factors such as high phreatic level, inadequate drainage, unconsolidated state of the tailings might have caused the static liquefaction failure of Stava tailings dam (Sammarco 2004).

(*b*) Sullivan Mine, Canada – 1991

During construction of the incremental raisings, the failure of the Sullivan upstream tailings dam occurred due to static liquefaction in foundation tailings (WISE 2010). The tailings were loose (fine-grained silty sand to sandy silt). The increase in pore pressures due to placement of raisings caused the tailings to liquefy (Davies et al. 1998).

(*c*) Merriespruit, South Africa – 1994

The Merriespruit tailings dam failed a few hours after a rainfall of 50 mm, and 17 people died in this incident. About 600,000 m^3 of liquid tailings flowed a distance of 3 km downstream of the dam, and inundated the village of Merriespruit (Fourie et al. 2001). The failure of Merriespruit tailings impoundment occurred due to overtopping and erosion (caused by heavy rainfall) of the outer dike (Wagener et al. 1997). Static liquefaction is considered as the possible cause of the Merriespruit tailings impoundment failure (Fourie et al. 2001).

(*d*) Aznalcóllar, Spain – 1998

The dam was built on 4 m thick alluvial sand and gravel overlying 60 m marl (heavily overconsolidated marine clay). The shear strains, developed due to shallow foundation failure, triggered static liquefaction of tailings resulting in release of 3 x 10^6 m^3 of liquid tailings (Davies et al. 2002).

2 Effect of relative density, confining pressure, and initial shear stress on static liquefaction resistance

Ishihara (1996) has described the stress-strain behaviour of saturated sand in undrained shear tests (Fig. 1).

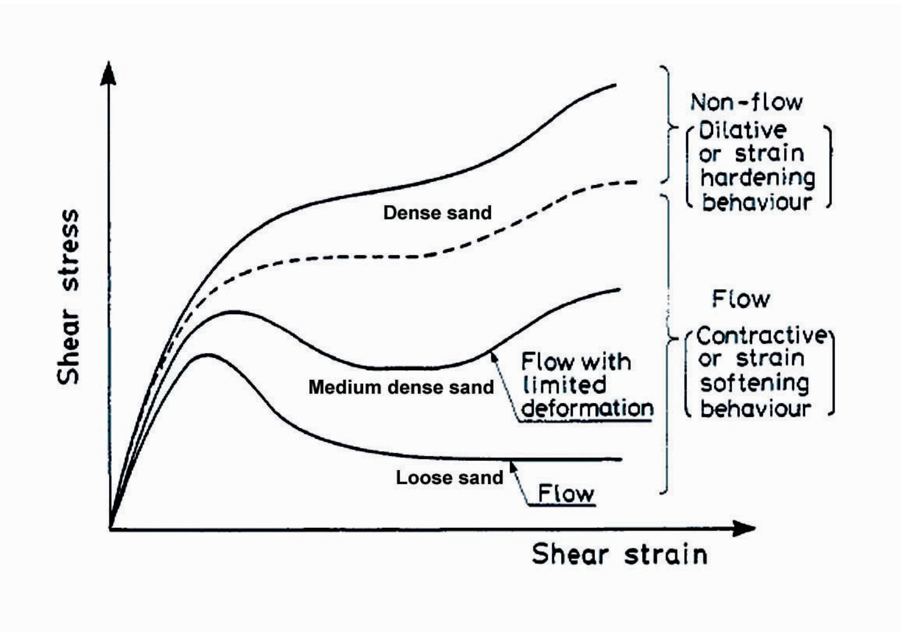

Fig. 1 Behaviour of saturated sand in undrained shear test (Ishihara 1996).

The dense sand shows strain hardening behaviour (the shear stress increases with increase of shear strain). The loose sand exhibits strain-softening behaviour (the shear stress reaches a peak value and then reduces). The medium dense sand initially shows strain softening and then strain hardening behaviour. Davies et al. (2002) assume similar stress-strain behaviour (Fig. 1) for tailings.

Taking advantage of the vast literature on saturated sands, the effect of factors such as: relative density, confining pressure, and initial shear stress on undrained behaviour of loose saturated sand is reviewed. It is believed that the above-mentioned factors can have the similar effect on undrained behaviour of tailings.

Kramer and Seed (1988) described the influence of the factors (*i*) relative density, (*ii*) confining pressure and (*iii*) initial shear stress on the static liquefaction behaviour of Sacramento River Fine Sand (SRFS). The stress-strain and pore pressure behaviour of four isotropically consolidated undrained tests (ICU) on SRFS at different relative densities is shown in Fig. 2 (Kramer and Seed 1988).

The loose samples (having relative densities of 32 and 37 %) showed compressibility and liquefied. The medium dense sample (with relative density of 44 %) initially liquefied at 10 % axial strain and then dilated at higher strains. Dilatant behaviour is observed in the sample with relative density of 47 %. The results indicate that the liquefaction resistance of a soil increases with increasing relative density (Kramer and Seed 1988).

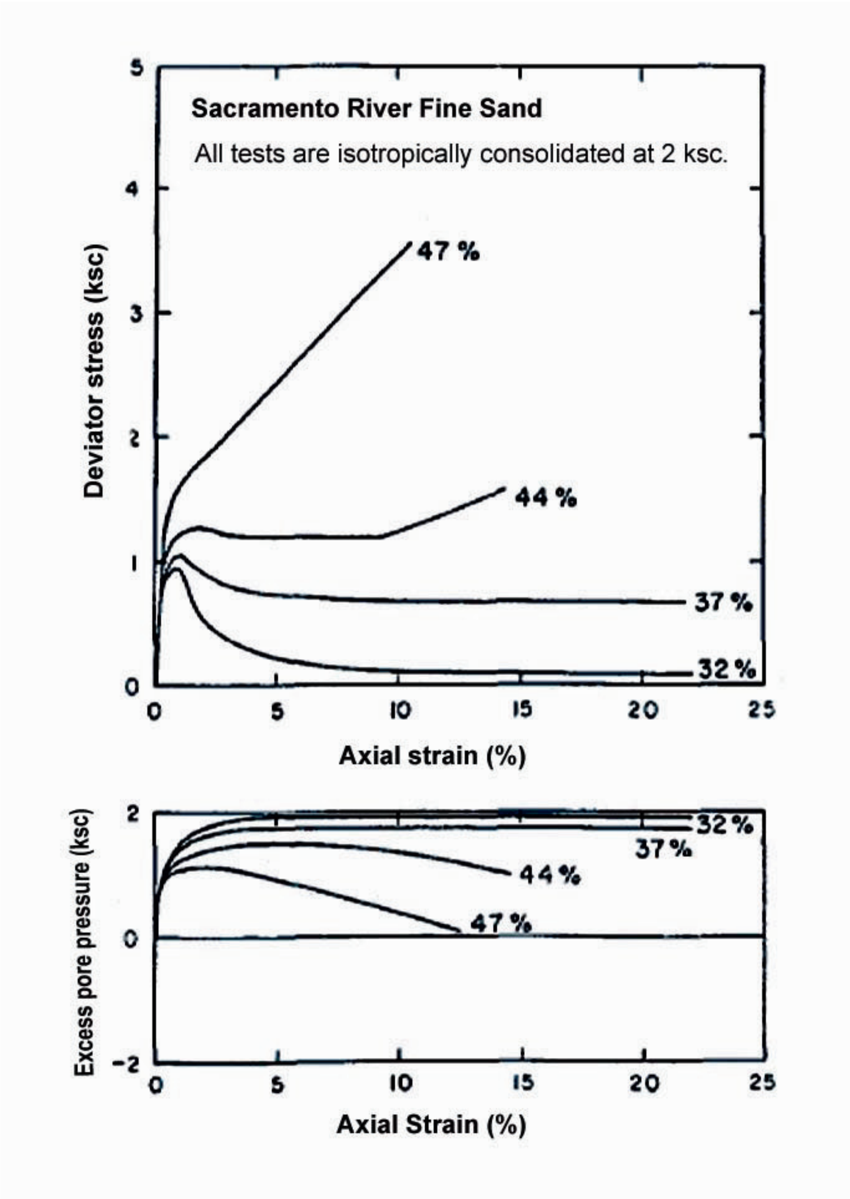

Fig. 2 Effect of relative density on stress-strain and pore water pressure response (Kramer and Seed 1988). The deviatoric stress and the excess pore pressure are expressed in kg/cm^2 (ksc).

The stress-strain and pore pressure behaviour of ICU tests on SRFS samples consolidated to relative density of 31 % at different confining pressures (from 1.0 - 5.0 kg/cm^2) is shown in Fig. 3 (Kramer and Seed 1988). The results show that static liquefaction resistance increases with increasing confining pressure (Kramer and Seed 1988).

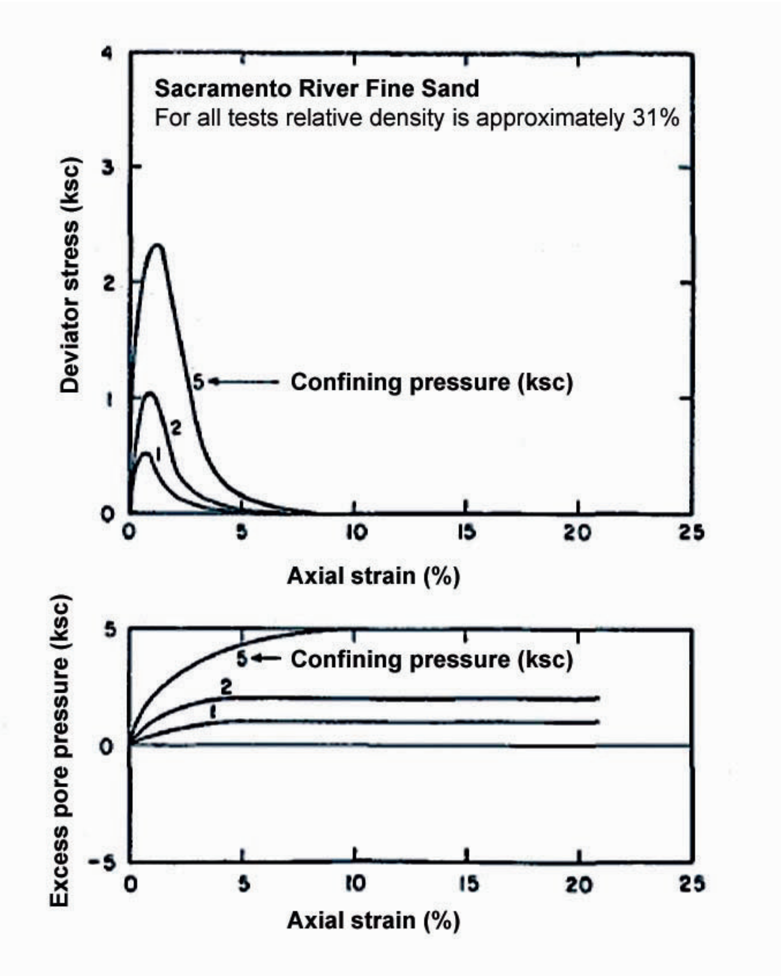

Fig. 3 Effect of confining pressure on stress-strain and pore water pressure response (Kramer and Seed 1988).

Anisotropically consolidated undrained triaxial tests on SRFS are shown in Fig. 4 (Kramer and Seed 1988). Initial shear stresses are induced due to anisotropic consolidation $\left(K_c = \sigma_1'/\sigma_3'\right)$, where σ_1' is the major principal effective stress and σ_3' is the minor principal effective stress. It is evident from the figure that strain softening and thereby the risk of static liquefaction increases with the increase in initial shear stress (Kramer and Seed 1988).

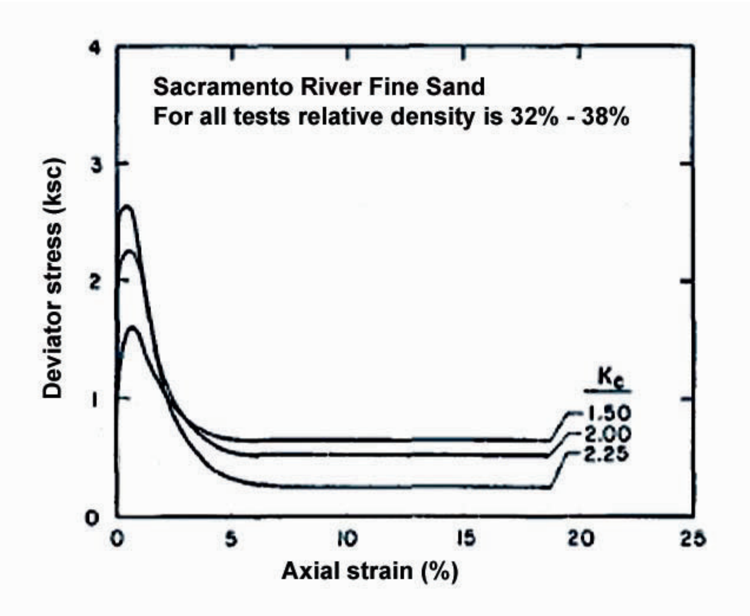

Fig. 4 Effect of initial shear stress on stress-strain response (Kramer and Seed 1988).

Other factors that can influence the static liquefaction behaviour of sand (Kramer and Seed 1988) are: particle angularity, overconsolidation ratio, previous strain history, length of time under sustained pressure, and grain structure.

2.1 Effect of presence of fines on static liquefaction resistance

The liquefaction potential of a sand increases with increase in the fines content (particles smaller than 0.074 mm in diameter), this behaviour of silty sands is due to the creation of a particle structure described below (Yamamuro and Lade 1997; Lade and Yamamuro, 1997).

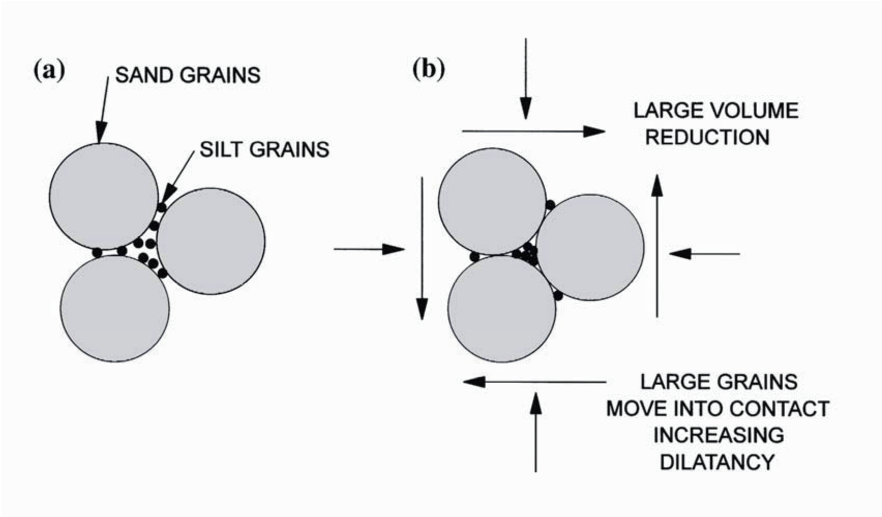

Fig. 5 (*a*) Silty sand deposited in loose state. (*b*) Silty sand compressed and sheared (Yamamuro and Lade 1997).

Figure 5*a* shows that the fine silt particles fill the void spaces between the sand particles. The presence of these fine particles can increase the density but may have a little effect on resistance to liquefaction. Some of the fine particles fill the spaces between the contact points of sand grains. These fine particles can cause slight separation between the sand particles. When the silty sands are compressed and sheared, the fine particles (located at the contact points of sand grains) slide into the void spaces (Fig. 5*b*). Hence, the silty sands become more compressible and thus liable to liquefaction.

As the particle size of tailings may vary from clay to sand size, the particle structure of tailings can resemble to the silty sands described above. It can be inferred that like silty sands, if the fines content of tailings increases, the tailings can be more compressible and sensitive to static liquefaction.

3 Triaxial tests on samples from Merriespruit tailings dam

Fourie and Papageorgiou (2001) carried out triaxial tests on Merriespruit tailings for investigation of the Merriespruit tailings dam failure in 1994. Some of the triaxial test results are presented below that show the static liquefaction behaviour of the tailings.

The deviatoric stress vs. axial strain for undrained triaxial compression tests on Merriespruit tailings (with 0% fines) are shown in Fig. 6 (Fourie and Papageorgiou 2001). The deviatoric stress *q* reaches a peak value before 5 % axial strain, and then strain softening occurs.

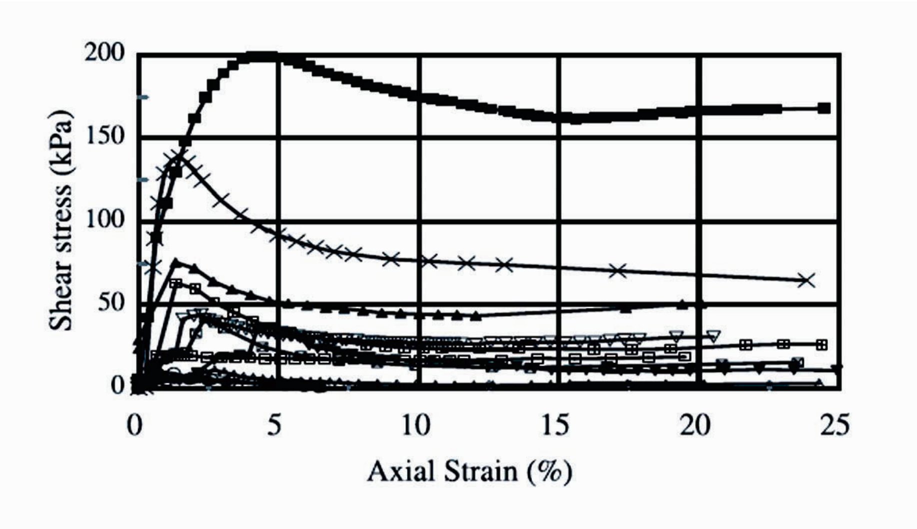

Fig. 6 Deviator stress versus axial strain for undrained triaxial compression tests on Merriespruit tailings (Fourie and Papageorgiou 2001).

The excess pore water pressure vs. axial strain for undrained triaxial compression tests on Merriespruit tailings are illustrated in Fig. 7 (Fourie and Papageorgiou 2001). The pore pressure remains constant after reaching a maximum value. The stress-strain and pore pressure-strain response shows the contractive behaviour of tailings.

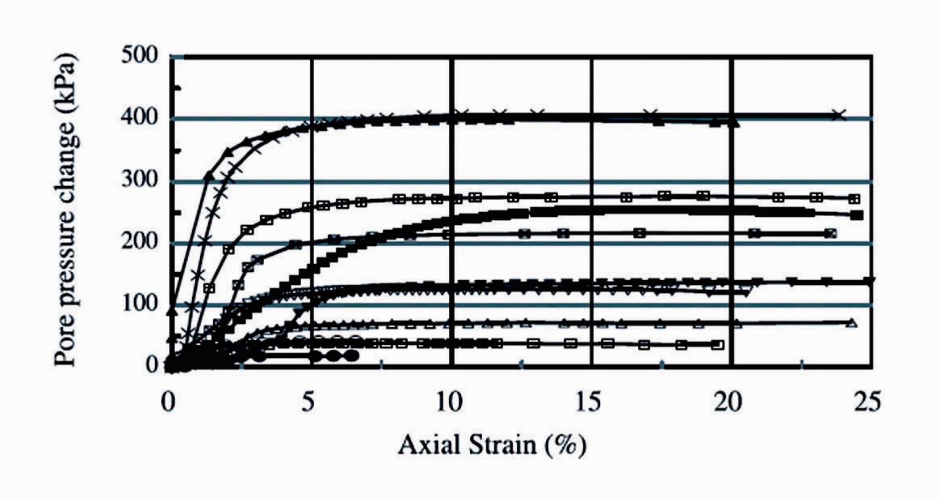

Fig. 7 Excess pore-water pressure versus axial strain for undrained triaxial compression tests on Merriespruit tailings (Fourie and Papageorgiou 2001).

The effective stress paths for undrained triaxial compression tests on Merriespruit tailings are described in Fig. 8 (Fourie and Papageorgiou 2001). The undrained effective stress paths initially reach a peak value of deviator stress *q* and then decrease continuously. Figure 8 indicates that static liquefaction occurs at low confining pressures (Fourie and Papageorgiou 2001).

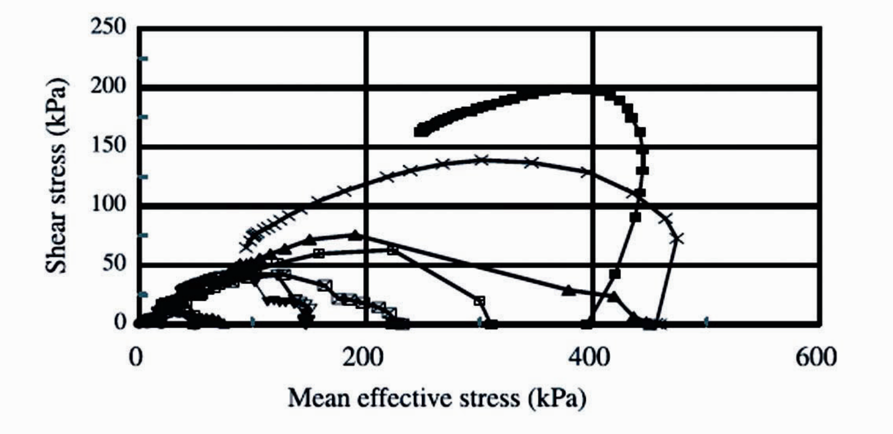

Fig. 8 Stress path plots for undrained triaxial compression tests on Merriespruit tailings (Fourie and Papageorgiou 2001).

4 Numerical Modelling

Numerical modelling is the mathematical simulation of a physical process. The reliable predictions from a numerical model are directly associated with the material properties and boundary conditions of a physical process. The finite element method is widely used in numerical modelling of geotechnical structures, due to its capability to deal with nonlinear stress strain behaviour, irregular geometries and varying material properties. A constitutive model is an integral component of any finite element program. Presently a large number of constitutive models capturing different aspects of soil behaviour are available in the literature. Only a few of these constitutive models are implemented in commercial finite element programs.

4.1 Constitutive modelling of liquefaction

A constitutive model is a mathematical representation of stress – strain relationship of a material. In the past, various constitutive models have been developed which can capture the liquefaction behaviour of sands (Jefferies 1993; Drescher et al. 1995; Byrne et al. 1995; Gudehus 1996; Wolffersdorff 1996; Drescher and Mróz 1997; Puebla et al. 1997; Niemunis and Herle 1997; Beaty and Byrne 1998; Yu 1998; Boukpeti and Drescher 2000; Boukpeti et al. 2002; Jefferies and Shuttle 2002; Mróz et al. 2003; Imam et al. 2005). The practical application of a constitutive model for a geotechnical problem is only possible, when the model is implemented in a finite element/ finite difference program. Therefore, some of the constitutive models that are implemented (as user defined soil models) in commercial finite element/ difference codes are described below.

UBCSAND Model

UBCSAND model was developed at the University of British Columbia (Byrne et al. 1995; Puebla et al. 1997; Beaty and Byrne 1998). It is an elastic–plastic model developed specifically for liquefaction behaviour of sand. The model is implemented in the commercial computer code FLAC (Fast Lagrangian analysis of Continua, ITASCA 2005). The UBCSAND model has also been implemented (Tsegaye 2010) in the finite element program PLAXIS (Brinkgreve et al. 2010). The model response in capturing static liquefaction behaviour of sand is shown in Fig. 9 (Tsegaye 2010).

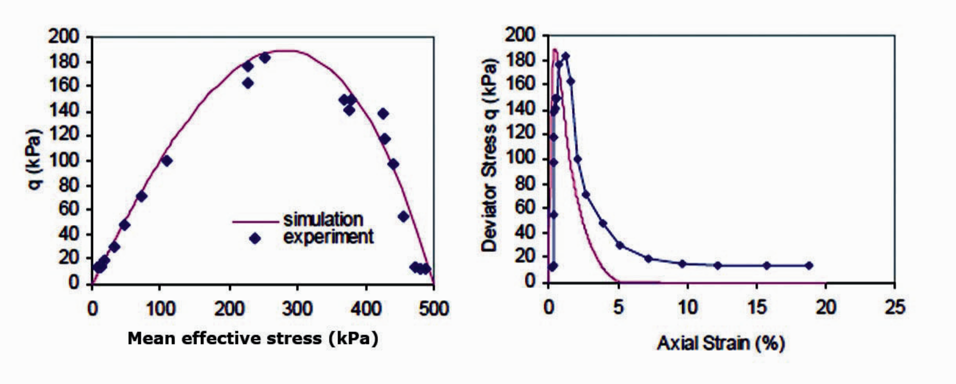

Fig. 9 Undrained triaxial compression test on Nerlerk sand at confining pressure of 500 kPa (Tsegaye 2010).

UBCSAND model has shown satisfactory response (in terms of deformations and pore pressures) for numerical analysis of full-scale field test on CANLEX (Canadian Liquefaction Experiment) embankment (Puebla et al. 1997). In this test, rapid monotonic load (due to disposal of tailings) was applied on the foundation tailings.

The numerical analysis of Mochikoshi tailings dam performed with UBCSAND model also confirmed the seismic liquefaction failure of the dam (Byrne and Seid-Karbasi 2003).

Hypoplastic model for sand

Hypoplasticity is a newly developed framework for constitutive modelling of granular materials. Unlike elasto plasticity, hypoplasticity does not make use of the concepts such as: yield surface and plastic potential (Kolymbas 2000). There are several versions of hypoplasticity available in literature.

The capability of the Hypoplastic model (Wolffersdorff 1996) with intergranular strain extension (Niemunis and Herle 1997) for simulating static liquefaction behaviour of a sand is represented in Fig. 10 (Tsegaye et al. 2010). The Hypoplastic model (Wolffersdorff 1996) have been implemented (Masin 2010) in the finite element program PLAXIS.

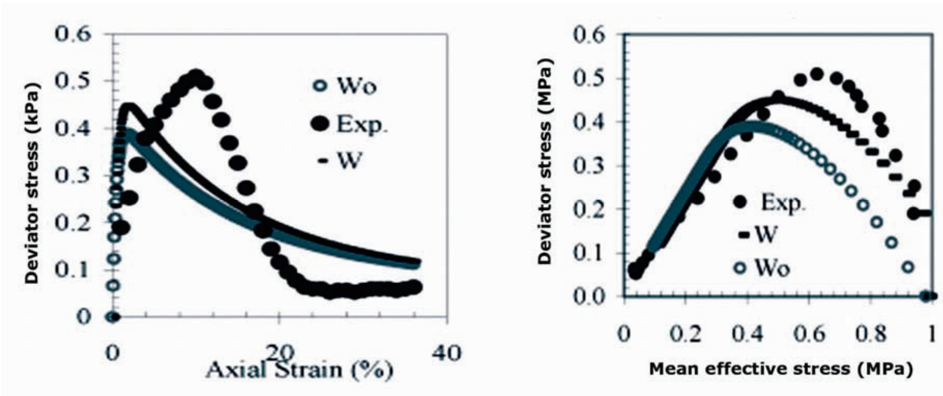

Fig. 10 Undrained triaxial compression simulations on Castro Sand (Exp.= experiment, W = with Intergranular Strain, Wo = without Intergranular Strain) (Tsegaye et al. 2010).

NorSand model

NorSand is a critical state elastic-plastic constitutive model (Jefferies 1993; Jefferies and Shuttle 2002). NorSand has been used for modelling a range of soils from clayey silt to sand (Shuttle and Jefferies 2010). This model is capable to capture liquefaction behaviour of sands. Figure 11 shows comparison of test data (liquefaction) with the model prediction (Jefferies and Shuttle 2005).

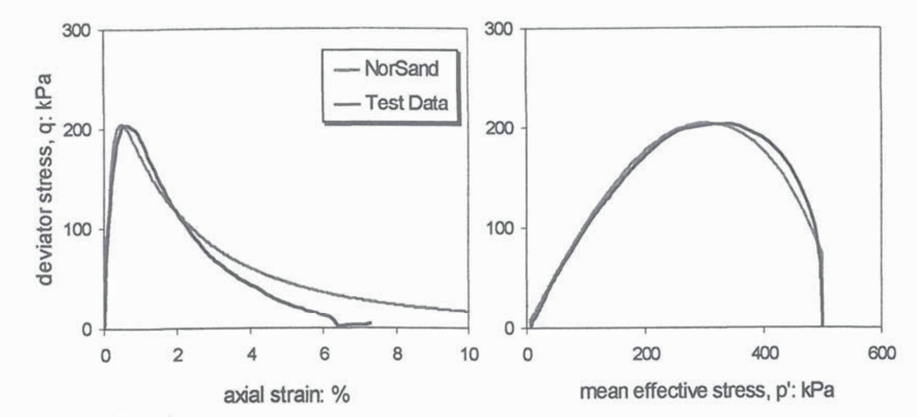

Fig. 11 NorSand predictions for liquefaction in undrained triaxial compression test of Erksak sand (Jefferies and Shuttle 2005).

CASM - A unified state parameter model for clay and sand

CASM (Clay And Sand Model) is a critical state elastic-plastic model developed by Yu (1998) and further extended by Yu et al. (2006). CASM is capable of predicting the behaviour of clay and sand under both drained and undrained loading conditions. The ability of CASM to simulate the liquefaction behaviour of very loose sand is shown in Fig. 12 (Yu 1998). CASM has been implemented (Khong 2004) into the finite element program CRISP (CRItical State soil mechanics Program).

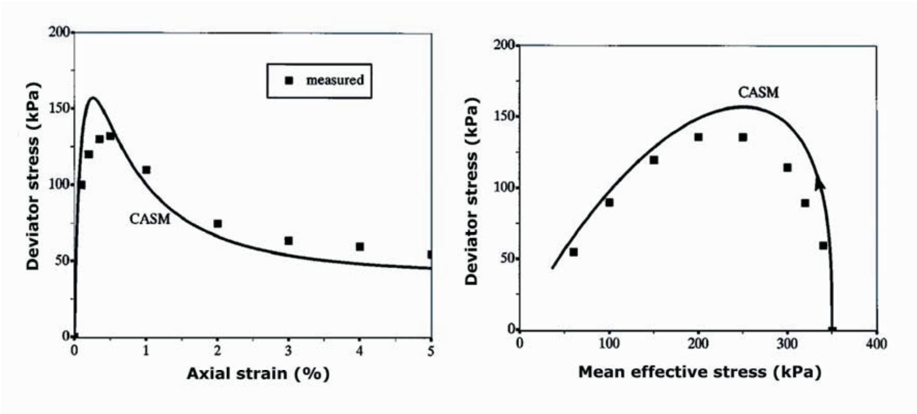

Fig. 12 CASM prediction for undrained compression of very loose Ottawa sand (Yu 1998).

5 Concluding remarks

In this paper, the static liquefaction process, and constitutive models related to the static liquefaction behaviour were reviewed in the context of loose saturated sands and tailings material. It is concluded that the static liquefaction of a tailings dam may occur due to factors such as: contractive behaviour of tailings material, overloading, changes in pore pressures, high phreatic level, inadequate drainage, overtopping and erosion of an outer embankment. It is deduced that like saturated sands, the static liquefaction resistance of tailings may (*i*) increase with increase of relative density and confining pressure, and (*ii*) decrease with increase of shear stress. Due to resemblance between particle structure of silty sands and tailings, it is inferred that the risk for static liquefaction of tailings may increase with increase in fines content.

The complex behaviour of tailings material – in aspects like high compressibility, low hydraulic conductivity, and heterogeneity of material zones - necessitates that the stability analyses of tailings dams be performed with an advanced software based on e.g. the finite element method. A constitutive model is a key element in any finite element program. Therefore, it is very essential to choose a suitable constitutive model that can simulate the static liquefaction behaviour of tailings material. A huge number of such types of constitutive models are available in the literature. Presently, some of these constitutive models, e.g. UBCSAND, Hypoplastic model, NorSand, and CASM have been implemented in commercial finite element programs.

With the availability of these constitutive models in the finite element programs, the next step is to use such models in numerical analyses of tailings dams in order to know the capability of each constitutive model in predicting the static liquefaction related flow failures of tailings dams. If a flow failure of a tailings dam is predicted in advance, it might be possible to prevent it by taking some remedial measures. It is believed that such reliable predictions can be made regarding flow failures of tailings dams with proper numerical modelling using appropriate constitutive model(s).

References

Beaty M, Byrne PM (1998) An effective stress model for predicting liquefaction behaviour of sand. Geotechnical Earthquake Engineering and Soil Dynamics III. Edited by P. Dakoulas, M. Yegian, and R Holtz (eds.), ASCE, Geo-technical Special Publication 75 (1):766-777

Blight GE, Fourie AB (2005) Catastrophe revisited – disastrous flow failures of mine and municipal solid waste. Geotechnical and Geological Engineering 23(3):219-248

Boukpeti N, Drescher A (2000) Triaxial behavior of refined Superior sand model. Comput. Geotech. 26(1): 65–81

Boukpeti N, Mro´z Z, Drescher A (2002) A model for static liquefaction in triaxial compression and extension. Can. Geotech. J. 39(6):1243–1253

Brinkgreve RBJ, Swolfs WM, Engin E (2010). PLAXIS user’s manual – version 10. PLAXIS bv, the Netherlands.

Byrne PM, Roy D, Campanella RG, Hughes J (1995). Predicting liquefaction response of granular soils from pressuremeter tests. ASCE National Convention, San Diego, Oct. 23-27, ASCE, Geotechnical Special Publication 56:122-135

Byrne PM, Seid-Karbasi M (2003) Seismic stability of impoundments. In Proceedings of 17th VGS Symposium on Geotechnical Engineering for Geoenvironmental Applications, Vancouver, British Columbia, pp 77-84. Web http://www.civil.ubc.ca/liquefaction/Publications/VGS12R.pdf. Accessed 15 January 2011

Craig RF (2004) Craig's Soil Mechanics. Spon Press, Taylor and Francis Group, London and New York

Drescher A, Birgisson B, Shah K (1995) A model for water saturated loose sand. Numerical models in geomechanics NUMOG V, GN Pande and S Pietruszczak, eds., Balkema, Rotterdam, The Netherlands, pp 109–112

Drescher A, Mróz Z (1997) A refined Superior sand model. Numerical models in geomechanics NUMOG VI , S. Pietruszczak and GN Pande, eds., Balkema, Rotterdam, The Netherlands, pp 21–26.

Davies MP, Dawson BB, Chin BG (1998) Static Liquefaction Slump of Mine Tailings – A Case History. 51st Canadian Geotechnical Conference, Edmonton, Alberta, October 4-7, 1998

Davies M, McRoberts E, Martin T (2002) Static liquefaction of tailings – fundamentals and case histories. In Proceedings of Tailings Dams 2002, ASDSO/USCOLD, Las Vegas

Fourie AB, Papageorgiou G (2001) Defining an appropriate steady state line for Merriespruit gold tailings. Canadian Geotechnical Journal 38(4):695-706

Fourie AB, Blight GE, Papageorgiou G (2001) Static liquefaction as a possible explanation for the Merriespruit tailings dam failure. Canadian Geotechnical Journal 38(4):707–719

Fourie AB, Tshabalala L (2005) Initiation of static liquefaction and the role of K_0 consolidation. Canadian Geotechnical Journal 42(3): 892-906

Gudehus G (1996) A comprehensive constitutive equation for granular materials. Soils and Foundations, 36(1):1-12

ICOLD (2001) Tailings dams - Risk of dangerous occurrences. Bulletin 121. Commission Internationale des Grands Barrages – 151, bd Haussmann, 75008 Paris

Imam SMR, Morgenstern NR, Robertson PK, Chan DH (2005) A critical-state constitutive model for liquefiable sand. Can.Geotech.J. 42(3): 830-855

Ishihara, K (1996) Soil Behaviour in Earthquake Geotechnics. Oxford University Press

ITASCA (2005) FLAC - Fast langrangian analysis of continua, Version 5.0 ITASCA Consulting Group Inc., Minneapolis, Minnesota.

Jefferies MG (1993) NorSand: a simple critical state model for sand. Geotechnique 43(1):91-103

Jefferies MG, Shuttle DA (2002) Dilatancy In General Cambridge-Type Models. Geotechnique 52(9):625-638

Jefferies MG, Shuttle DA (2005) NorSand: Features, Calibration and Use. Invited paper for the ASCE Geo-Institute Geo-Frontiers Conference, Austin, Texas, January 24−26, 2005. Published as Geotechnical Special Publication No. 128, Soil Constitutive Models: Evaluation, Selection, and Calibration, pp 204-236, editors Jerry A. Yamamuro and Victor N. Kaliakin

Lade PV (1993) Initiation of static instability in the submarine Nerlerk berm. Canadian Geotechnical Journal. 30(6):895-904

Lade, PV, Yamamuro, JA (1997) Effects of nonplastic fines on static liquefaction of sands. Canadian Geotechnical Journal. 34(6):918–928

Khong CD (2004) Development and numerical evaluation of unified critical state models. Ph.D. thesis, University of Nottingham, UK

Kolymbas D (2000) Introduction to Hypoplasticity. A.A. Balkema, Rotterdam, Netherlands.

Kramer SL (1996) Geotechnical Earthquake Engineering. Prentice-Hall, Inc

Kramer SL, Seed HB (1988) Initiation of soil liquefaction under static loading conditions. Journal of Geotechnical Engineering. 114(4):412-430

Martin TE, McRoberts EC (1999) Some considerations in the stability analysis of upstream tailings dams. In proceedings of sixth International Conference on Tailings and Mine Waste ’99, Fort Collins, Colorado, 24-27 January 1999. A.A Balkema Rotterdam, pp 1-17

Masin D (2010) PLAXIS implementation of hypoplasticty. PLAXIS bv, Delft, The Netherlands

Mróz Z, Boukpeti N, Drescher A (2003) Constitutive model for static liquefaction. International Journal of Geomechanics. 3(2):143-144

Niemunis A, Herle I (1997) Hypoplastic model for cohesionless soils with elastic strain range. Mechanics of Cohesive-Frictional Materials. 2(4):279-299

Puebla H, Byrne PM, Phillips R (1997) Analysis of CANLEX liquefaction embankments: prototype and centrifuge models. Can. Geotech. Journal. 34(5):641-657

Sammarco O (2004) A tragic disaster caused by the failure of tailings dams leads to the formation of the Stava 1985 foundation. Mine Water and the Environment. 23(2):91–95

Shuttle D, Jefferies M (2010) Norsand: Description, calibration, validation and applications. Web http://www.itasca-udm.com/media/download/norsandm/NorSand_M.pdf Accessed 18 February 2010

Tsegaye AB (2010) PLAXIS liquefaction model (UBC3D). Report No.1. Plaxis, b.v, Delft, The Netherlands

Tsegaye AB, Molenkamp F, Brinkgreve RBJ, Bonnier PG, Jager RD, Galavi V (2010) Modeling liquefaction behaviour of sands by means of hypoplastic model. In proceedings of seventh European Conference on Numerical Methods in Geotechnical Engineering, Trondheim, Norway, 2nd - 4th June 2010. Taylor and Francis Group London, pp 81-87

Vick SG (1990) Planning, design, and analysis of tailings dams. BiTech Publishers Ltd, Canada

Wagener F, Strydom K, Craig H, Blight G (1997) The tailings dam flow failure at Merriespruit, South Africa, causes and consequences. In Proceedings of the fourth International Conference on Tailings and Mine Waste '97, Fort Collins, Colorado, 13–17 January 1997. A.A. Balkema, Rotterdam, The Netherlands, pp 657–666

WISE (2010) Chronology of major tailings dam failures. Web http://www.wise-uranium.org/mdaf.html. Accessed 15 January 2010

Wolffersdorff VP-A (1996) A hypoplastic relation for granular materials with a pre-defined limit state surface. Mechanics of Cohesive-Frictional Materials 1(4):251-271

Yamamuro JA, Lade PV (1997) Static liquefaction of very loose sands. Canadian Geotechnical Journal. 34(6):905-917

Yu HS (1998) CASM - A unified state parameter model for clay and sand. Int.J.Numer.Anal.Meth.Geomech. 22(8):621-653

Yu HS, Khong C, Wang J (2006) A unified plasticity model for cyclic behaviour of clay and sand. Mechanics Research communications. 34(2): 97-114